THE REGULATION OF ERYTHROID PROGENITORS AND T CELLS BY CD45

by

Yaein Amy Shim

B.Sc., The University of British Columbia, 2012

A THESIS SUBMITTED IN PARTIAL FULFILLMENT OF

THE REQUIREMENTS FOR THE DEGREE OF

DOCTOR OF PHILOSOPHY

in

THE FACULTY OF GRADUATE AND POSTDOCTORAL STUDIES

(Microbiology and Immunology)

THE UNIVERSITY OF BRITISH COLUMBIA

(Vancouver)

April 2020

The following individuals certify that they have read, and recommend to the Faculty of Graduate and Postdoctoral Studies for acceptance, the dissertation entitled:

The Regulation of Erythroid Progenitors and T cells by CD45

submitted by Yaein Amy Shim in partial fulfillment of the requirements for

the degree of Doctor of Philosophy

in Science

Examining Committee:

Pauline Johnson, Microbiology and Immunology
Supervisor

Kenneth Harder, Microbiology and Immunology
Supervisory Committee Member

Ninan Abraham, Microbiology and Immunology
Supervisory Committee Member

Bruce A. Vallance, Experimental Medicine
University Examiner

John Priatel, Pathology and Laboratory Medicine
University Examiner

Additional Supervisory Committee Members:

Lisa Osborne, Microbiology and Immunology
Supervisory Committee Member

Abstract

The immune system plays a crucial role in the protection of the host against infection and the maintenance of homeostasis under normal conditions. This is achieved by cooperative work amongst a diverse population of immune cells. The pan-leukocyte marker CD45 is a receptor-type tyrosine phosphatase expressed on all nucleated hematopoietic cells. While the function of CD45 on adaptive immune cells has been well described, the role of CD45 on innate immune cells and erythroid progenitors is less understood.

$CD71^{+}TER119^{+}$ erythroid progenitors are prevalent in neonates; in addition to generating mature erythrocytes, they create an immunosuppressive environment. Here, I show that CD45 regulates late erythroid development as CD45-deficient mice maintained a high level of $CD71^{+}TER119^{+}$ progenitor cells in the spleen into adulthood. Despite the increase, CD45-deficient mice had normal numbers of mature red blood cells (RBCs) due to increased sensitivity of erythroid progenitors to erythropoietin (EPO) and an increased number of EPO-producing red pulp macrophages (RPMs). Increased $CD71^{+}TER119^{+}$ cells in CD45-deficient RAGKO mice (CD45RAGKO) had an impact on the outcome of T cell transfer colitis. CD45RAGKO had delayed systemic wasting and reduced TNFα production by splenic myeloid cells despite having an equal level of inflammation in the colon. Adoptive transfer of erythroid progenitors from CD45RAGKO donor into RAGKO attenuated the weight loss and reduced TNFα expression by RPMs. Co-culturing of erythroid cells suppressed TNFα expression from RPMs in a phagocytosis-dependent manner. These findings implicate CD45 as a positive regulator of systemic inflammation and suggest erythroid progenitors are an anti-inflammatory agent in colitis.

Using a model of lymphopenia-induced proliferation (LIP), CD45 expression on innate cells was found to positively regulate homeostatic proliferation of T cells. Both the expression of CD45 on $CD11c^+$ cells and the presence of intestinal microbiota promoted faster LIP. Furthermore, CD45 on hematopoietic cells indirectly regulated stromal cell maturation and production of IL-7, which is a critical cytokine that drives slow LIP. Overall, this study identifies a novel role for CD45 in regulating erythroid and myeloid cells and their interaction with other cells which impacts the inflammatory response in colitis and T cell maintenance in homeostasis.

Lay Summary

The immune system protects our body against infection through cooperative work between immune cells, but sometimes it can also cause disease, such as inflammatory bowel disease (IBD). Immune cells and erythroid progenitor cells, which give rise to red blood cells, are both derived from hematopoietic stem cells and express a protein called CD45, which regulates cellular interactions. This thesis aims to understand the role of CD45 in the interactions of different cells in health and in IBD. I describe that CD45 regulates the number of erythroid progenitors in the spleen and during IBD, and these cells can interact with immune cells to reduce wasting. CD45 also regulates the maintenance of T cells, which play a critical role in the development of IBD but also protect us from infections by clearing pathogens. This work demonstrates the importance of CD45 in cellular interactions and the protective role of erythroid progenitors in IBD.

Preface

I have designed and conducted all the experiments and analyses presented in this thesis, with the following exceptions:

- Manisha Dosanjh helped with preparing single cell suspensions from spleen and lymph nodes.
- Sally Lee-Sayer helped with monitoring experimental mice.
- Teresa Campbell, an undergraduate student, performed and analyzed the data for Figure 3.2 C-D and 3.4
- A past lab member, Dr. Asanga Weliwitigoda (Samarakoon), generated the initial preliminary data concerning erythroid development and conducted the experiments to collect data for Figure 3.1, 3.2A, 3.3. The analysis and presentation of the data was done by me.
- Dr. Asanga Weliwitigoda (Samarakoon) first characterized the T cell transfer model of colitis and her experiments and analysis are presented as part of figure 4.1 and 4.2.

A version of chapter 3 has been submitted as a research article for publication and a version of chapter 4 is in preparation for manuscript submission.

In addition, I contributed to the following publications:

- Saunders, A.E., Shim, Y.A. and Johnson, P. (2014), Innate immune cell CD45 regulates lymphopenia-induced T cell proliferation. J. Immunol., 913:2841-2842.

I conducted experiments to address comments from the reviewers after submission of the manuscript.

- Samarakoon, A., Shim, Y.A., Dosanjh, M., Labonte-Raymond, C., Arif, A.A. and Johnson, P. (2016), CD45 regulates GM-CSF, retinoic acid and T-cell homing in intestinal inflammation. Mucosal Immunol. 9:1514-1527.

  I performed experiments for Figures 1C, 2A-B, 3C, 5B and Supplemental figure 2, 3 and 6 in the paper.

Animal studies were conducted in accordance with protocols approved by the University of British Columbia Animal Care Committee and Canadian Council of Animal Care guidelines. The following are project titles and their corresponding certificate numbers applicable to this thesis:

- CD44 and CD45 breeding protocol number: A13-0015
- Regulation of Signaling and Dendritic Cell Functions by CD45, A11-0292
- Regulation of Signaling and Dendritic Cell Functions by CD45, A15-1598

Table of Contents

List of Tables

List of Figures

List of Symbols

α alpha

β beta

δ delta

γ gamma

μ micro

ζ zeta

List of Abbreviations

ACD anemia of chronic diseases

BCL-2 B-cell lymphoma 2

BCL-xL B-cell lymphoma-extra large

BM bone marrow

CCL C-C chemokine ligand

CCR C-C chemokine receptor

CD cluster of differentiation

CD45KO CD45-deficient mouse

CD45RAGKO CD45 and recombination activation gene double-deficient mouse

CFSE Carboxyfluorescein succinimidyl ester

DC dendritic cell

DSS dextran sodium sulphate

EDTA Ethylenediaminetetraacetic acid

ELISA enzyme-linked immunosorbent assay

EPO erythropoietin

FACS fluorescence activated cell sorting

FCS fetal calf serum

FSC forward scatter

GM-CSF granulocyte and macrophage colony stimulating factor

HSC hematopoietic stem cell

IBD inflammatory bowel disease

H hour

Ig immunoglobulin

IL interleukin

ILC innate lymphoid cell

ICAM intercellular adhesion molecule 1

IFNγ interferon gamma

JAK janus kinase

kDa kilodalton

KO knockout

LP lamina propria

LPS lipopolysaccharide

Ly6c lymphocyte antigen 6c

Ly6g lymphocyte antigen 6g

MHCI major histocompatibility complex I

MHCII major histocompatibility complex II

Min minute

MyD88 myeloid differentiation primary response gene 88

NK natural killer

PBS phosphate-buffered saline

Pro E proerythroblast

PRR pattern recognition receptor

pLN peripheral lymph node

PMA phorbol 12-myristate 13-acetate

RAGKO recombination activating gene deficient mice

RBC red blood cell (mature erythrocyte)

RORγt retinoic acid related orphan receptor gamma t

ROS reactive oxygen species

RPM red pulp macrophage

SCID severe combined immunodeficiency

SFK Src family kinase

SLO secondary lymphoid organ

SSC side scatter

STAT signal transducer and activator of transcription

TCR T cell receptor

TNFα tumor necrosis factor alpha

Th1 T helper 1

Th17 T helper 17

TLR Toll-like receptor

TNFα tumor necrosis factor alpha

T_{Reg} regulatory T cell

VCAM1 vascular cell adhesion molecule 1

WT wildtype

Acknowledgements

I would like to express sincere gratitude to my supervisor Dr. Pauline Johnson for her supervision and patience. Pauline has been an excellent mentor and a role model, and as her student I have both witnessed and benefitted from her genuine care. She has been supportive both in and out of the lab and I hope I can be a figure like her to my peers. I will always remember Pauline for her passion for research, macrophages and wine.

I thank my graduate committee of Dr. L Osborne, Dr. K Harder and Dr. N Abraham for their support and guidance throughout my graduate program. They taught me to think critically about my project.

I also thank the past and current members of Dr. Johnson lab for their moral and intellectual support. They have been the source of my wisdom, consolation and adventure. I would like to especially thank Manisha Dosanjh, for helping me with experiments and for keeping the lab in order. I also offer gratitude to fellow students of Microbiology and Immunology department for their friendship.

I offer my deepest gratitude to my family, Howard Shim, Sanghee Shim and Brian Shim, and my friends, YJ Lee, SY Kim and JY Hwang. Without them, I would not have been able to become who I am today, and this journey would not have been possible.

This work was supported by scholarship from Natural Sciences and Engineering Research Council of Canada and University of British Columbia.

Chapter 1: Introduction

1.1 Overview of the Immune System

The immune system comprises a diverse group of cells which arise from hematopoietic stem cells (HSC), and they work together in a complex network throughout life. While the immune system is most appreciated for defending our body against pathogenic conditions, such as bacterial and viral infections, its role extends beyond fighting infection to also include the development of tissue structure as well as the maintenance and restoration of homeostasis. Any issues regarding the ability to tolerate commensal microflora or self, to detect and clear infection and to heal injury can have a detrimental impact on the host.

The immune system consists of innate and adaptive immunity. When pathogens breach a barrier system, the innate immune system is activated as a first response. Innate immune cells, such as dendritic cells (DC) and macrophages, detect pathogen-associate molecular patterns (PAMP) and damage-associated molecular patterns (DAMP). As a result, inflammation begins, which involves recruitment of other immune cells to the site. The activated immune cells kill and clear infections through various ways, such as phagocytosis of the pathogen, degranulation of cytotoxic substances or the release of reactive oxidative species (ROS). Once the pathogens are removed from the system, the inflammation gets resolved and the processes of clearing the aftermath, regenerating the tissue, and remodeling the extracellular matrix occur. However, inflammation may persist if the innate immune system cannot clear the pathogens, in which case the adaptive immune system is required.

The adaptive immune system comprises T cells and B cells. Through somatic recombination, each adaptive immune cell has a T cell receptor (TCR) or B cell receptor (BCR)

with a unique specificity. During inflammation, a subset of DC at the site of infection processes the pathogen it phagocytosed and migrates to the secondary lymphoid organs (SLO). In the SLO, DCs present the processed antigen on major histocompatibility complex (MHC) molecules to T cells. Any T cell that has a specific receptor to the antigen gets activated, which results in differentiation and proliferation into effector cells and memory cells. The effector cells mount a powerful immune response against the specific pathogen and the memory cells remain even after the clearance of an infection, allowing a faster and stronger immune response when re-infected by the same pathogen.

In any type of immune response, immune cells must interact with other cells and this can occur through various means, such as TCR, PRR, cytokine receptors and adhesion molecules. Interactions as such activate signaling pathways within the immune cells through series of phosphorylation and dephosphorylation of signaling molecules to elicit responses to the initial stimuli. CD45 is a protein tyrosine phosphatase commonly expressed on all leukocytes and it is implicated in the regulation of cell signaling associated with cellular interactions mentioned above.

1.2 CD45

1.2.1 Structure of CD45

CD45 is a receptor-like tyrosine phosphatase. It is expressed on all nucleated cells derived from HSCs, which excludes mature RBCs (Scheid and Triglia, 1979). It is a large protein ranging from 180 kDa to 240 kDa in size with a well conserved cytoplasmic region with 95% homology in amino acid sequence in the cytoplasmic domain among different mammalian

species (Thomas, 1989). Its receptor-like domain comprises three alternatively spliced regions designated as A, B and C, a cysteine rich region, and three fibronectin type III repeats (Figure 1.1) (Saunders and Johnson, 2010). After a transmembrane domain, it has a wedge domain and two phosphatase domains, of which the one closer to the membrane is catalytic.

The extracellular region of CD45 is heavily glycosylated with N- and O-linked carbohydrates, with the carbohydrates constituting 25% of the weight (Brown et al., 1981), thus allowing other lectin molecules, such as galectin-1, to interact with carbohydrates on CD45 (Walzel et al., 1999). However, CD45-specific ligands have yet to be found.

1.2.2 Substrates of CD45

One of the best-known targets of CD45 are Src family kinases (SFKs), such as Lck and Lyn, which have two tyrosine residues that regulate their activity (Saunders and Johnson, 2010): for instance, Lck in T cells has both a negative regulatory tyrosine (Y505) and a positive regulatory tyrosine (Y394) (Figure 1.2). When the negative regulatory tyrosine is phosphorylated, Lck is in an inactive state. Upon dephosphorylation of the negative regulatory tyrosine, Lck becomes primed for activation by adapting an open conformation, which allows another Lck to access and phosphorylate the positive regulatory tyrosine site to fully activate Lck (Hermiston et al., 2003). CD45 can dephosphorylate tyrosine from either the negative or positive regulatory site, thus favoring maintenance of Lck in a so-called “primed” state (Hermiston et al., 2003). CD45 is also implicated in many cytokine-mediated signaling pathways by acting on Janus kinase (JAK), which is a family of intracellular tyrosine kinases, JAK1, JAK2, JAK3 and tyrosine kinase 2 (TYK2). Mast cells, B cells and thymocytes isolated from CD45-deficient mice have hyperphosphorylated JAK when stimulated with IL-3 or IFNα (Irie-Sasaki et al., 2001).

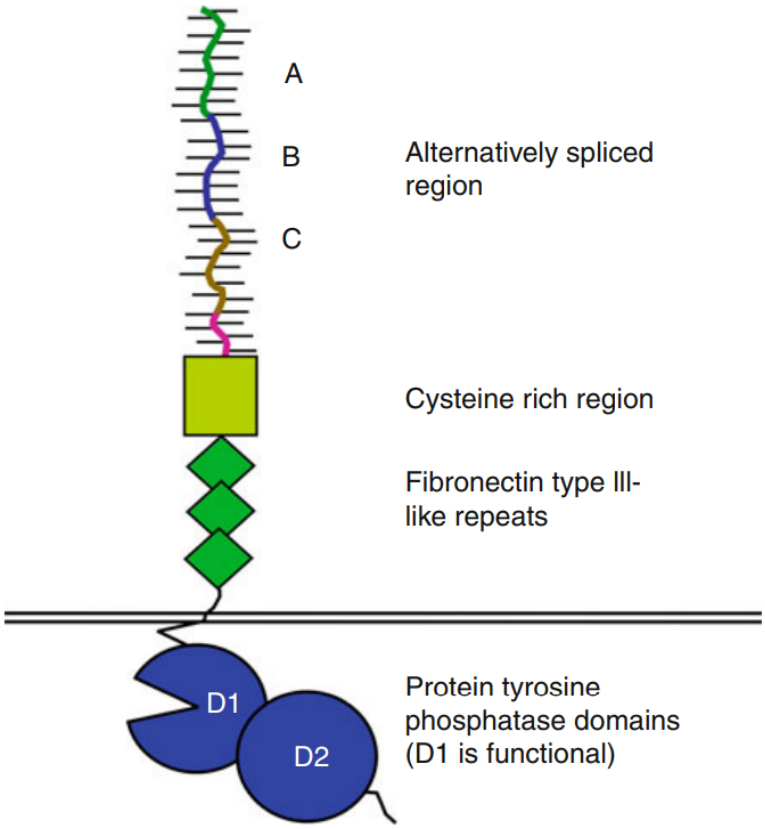

Figure 1.1 Structure of CD45

CD45 is a relatively a large transmembrane protein of 180-220 kDa. It is a receptor type protein phosphatase with a heavily glycosylated extracellular domain that includes three alternatively spliced regions (A, B and C), a cysteine rich region and fibronectin type III-like repeats. The intracellular domain includes two phosphatase domains (D1 and D2), of which D1 is catalytically active. (Johnson et al., 2012)

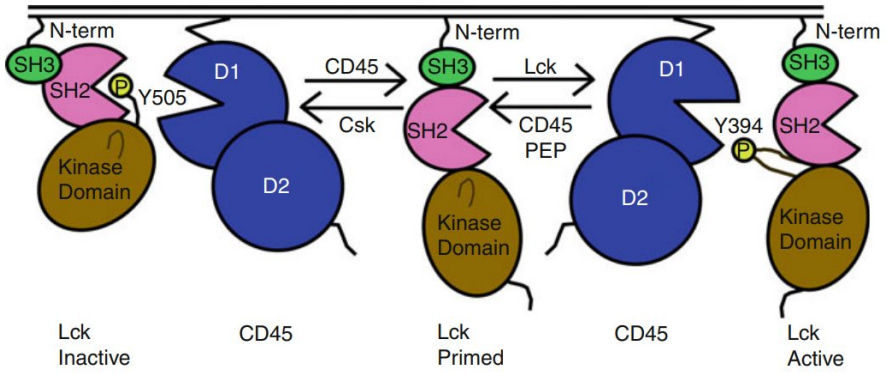

Figure 1.2 Catalytic Activity of CD45 on Lck

CD45 targets Src family kinases, such as Lck, as shown in the diagram. Lck has two tyrosine residues that can be dephosphorylated by CD45: a negative regulatory site, Y505, and a positive regulatory site, Y394. Dephosphorylation of the negative regulatory site, Y505, on inactive Lck opens the inactive Lck into a primed state. Dephosphorylation of the positive regulatory site, Y394, turns active Lck back into the primed state. (Johnson et al., 2012)

Using SFK inhibitors and recombinant CD45, Irie-Sasaki *et al.* further showed that CD45 can directly dephosphorylate JAK1, JAK2 and TYK2 *in vitro* (Irie-Sasaki et al., 2001). While these results show that CD45 can act on JAK and is implicated in down-regulating the activity of JAK, it is important to note that Src kinases can also impact JAK/STAT pathways as well (Ingley and Klinken, 2006) as SFK have been shown to phosphorylate STAT3 and 5 independent of JAK in other systems (Kazansky and Rosen, 2001; Qing and Stark, 2004).

1.2.3 CD45 on Adaptive Immune Cells

T cells express different isoforms of CD45 at different stages of development and activation, which arise from alternative splicing of exon 4, 5 and 6, the A, B and C regions of the extracellular domain. Transfection of thymocytes with different spliced variants of CD45 provided some evidence for different CD45 isoforms affecting T cell migration to distinct peripheral organs (Kozieradzki et al., 1997). However, the effect of different CD45 isoforms on T cell function is largely unknown.

Three different CD45KO mouse strains targeting exon 6, 9 and 12 were generated (Byth et al., 1996; Kishihara et al., 1993; Mee et al., 1999). In these mice, the number of mature T cells in the periphery is reduced to 5-10 % of the number in the wild type, establishing an effect of CD45 on T cell development. Further investigation of thymocytes revealed that the major defect happens during transition from the $CD4^+CD8^+$ double-positive stage into the $CD4^+$ or $CD8^+$ single-positive stage with the observation of 20-fold reduction in $CD4^+$ and 60-fold reduction in $CD8^+$ populations in numbers attributed to insufficient TCR signaling and subsequent failure to undergo positive selection (Byth et al., 1996; Johnson et al., 2012).

The few mature T cells in the periphery of CD45-deficient mice show reduced proliferation in response to TCR/CD3 cross linking (Kishihara et al., 1993), suggesting that CD45 is required for optimal T cell activation. To activate a T cell, an immunological synapse needs be formed between the T cell and the antigen-presenting cell at the point of contact with supramolecular activation clusters (SMACs) in the center, which comrise the TCR and MHC complex. Due to the large and rigid extracellular domain of CD45, exclusion of CD45 was observed from supramolecular activation clusters (SMACs) in immunological synapses formed between TCRs on T cells and MHCs on antigen-presenting cells (Varma et al., 2006). Using high-resolution microscopy and fluorescently tagged CD45 and Lck, Chang *et al.* showed that CD45 gets pushed out of the SMACs during the early stage of immunological synapse formation due to its rigid and large extracellular domain that extends the span of distance between the TCR and ligand complex (Chang et al., 2016). Through this process, CD45 becomes segregated from Lck, facilitating colocalization of Lck with TCR along with other proteins such as Zap70 to activate the downstream TCR signaling pathways. The proximity between CD45 and Lck before a formation of an immunological synapse is likely to maintain Lck in a primed state, while the segregation of CD45 from SMACS prevents CD45 from dephosphorylating Lck at the positive regulatory tyrosine to allow sustained activation.

CD45 is implicated in negative regulation of T cell adhesion. Cells can adhere to other cells or extracellular matrix through the integrin-receptor family. One study has shown that CD45-deficient cell lines have increased adhesion to fibronectins through α5β1 (VLA5), but not α4β1 (VLA4) (Shenoi et al., 1999). In different studies, CD45 was shown to negatively regulate signaling mediated by CD44, an adhesion receptor that binds to hyaluronan in the extracellular matrix (Li et al., 2001). When incubated with immobilized CD44 antibodies, CD45-deficient

cells spread in an elongated shape, instead of a round one, with overly sustained phosphorylation of Lck at the positive regulatory tyrosine site and increased recruitment of other signaling molecules, including Fyn and Pyk2 (Wong et al., 2008).

The impact of CD45 on T cell function *in vivo*, is largely unknown. However, we have previously reported that in a DSS-induced model of colitis, two different strains of CD45KO mouse models, one targeting exon 6 and another targeting exon 9, showed increased pathology (Samarakoon et al., 2016). Lack of CD45 increased T cell homing to the gut and the expression of α4β7 by the T cells (Samarakoon et al., 2016). In the same model, CD45KO T cells in the colon were more proinflammatory, with increased production of IFNγ and IL-17 upon colitis.

1.2.4 CD45 on Innate Immune Cells

A role for CD45 in the regulation of TLR-mediating signaling pathways has been shown in bone marrow-derived dendritic cells (BMDC) generated by culturing bone marrow cells in GM-CSF. While CD45 does not affect the upregulation of CD80 and CD86 on DCs upon TLR stimulation, CD45 deficiency affects production of proinflammatory cytokines both negatively and positively depending on the TLR targeted (Cross et al., 2008; Piercy et al., 2006). CD45-deficient BMDC show increased production of IL-12, IL-6 and TNFα in response to TLR-2/9 and TLR-4 stimulation, suggesting that CD45 positively regulates MyD88-dependent pathways (Cross et al., 2008). On the other hand, IFNβ production in response to TLR-3 stimulation, which signals through TRIF, is reduced by CD45 deficiency (Cross et al., 2008). $CD11c^+$ cells isolated from spleens of CD45KO mice were able to activate OT-I and OT-II T cells when loaded with OVA peptide in the presence of CpG or poly(I:C), indicating the CD45 has little or no impact on inducing classical activation of T cells (Saunders et al., 2014). However, CD45-

deficient $CD11c^+$ cells were less able to induce T cell proliferation in response to lymphopenia which occurs in the absence of cognate antigen signal or co-stimulatory molecule (Saunders et al., 2014); this suggests that the impact of CD45 is restricted to immature DCs, or that its effect is overridden by the strength of antigenic signals or the presence of costimulatory signals in classical T cell activation.

CD45 has also been shown to affect other innate immune cells: for instance, CD45-deficient mast cells generated from bone marrow show reduced IgE triggered degranulation and CD45KO mice are unable to mount an anaphylactic response (Berger et al., 1994; Grochowy et al., 2009). In NK cells, CD45 is required for production of IFNγ in response to ITAM-dependent signaling from NKG2D or NK1.1 receptor stimulation (Hesslein et al., 2006). Furthermore, CD45KO mice have a lower survival rate to mouse cytomegalovirus (MCMV) infections, which was attributed to defective NK cell responses, including IFNγ production, cell expansion and degranulation (Hesslein et al., 2011). While these data show involvement of CD45 in innate signaling pathways in NK cells, DCs and mast cells, the role of CD45 in macrophages are less well known. Also, a comprehensive understanding of the role of CD45 in the interactions between different group of cells during steady state or during inflammation is lacking.

1.2.5 CD45 in Human Disorders

Deletion of CD45 has been reported in patients with severe combined immunodeficiency (SCID) (Kung et al., 2000; Tchilian et al., 2001): in one male patient, the T cell frequency in peripheral blood was as low as 8.9% compared to the 64% in a healthy individual, similar to the reduced T cell frequency in CD45KO mouse models (Byth et al., 1996; Kung et al., 2000). Certain variants of CD45 have been associated with autoimmunity. For instance, the C77G

single nucleotide polymorphism, which occurs in exon 4 and results in the expression of CD45RA isoform by all cells, is associated with an increased risk of systemic sclerosis and autoimmune hepatitis (Schwinzer et al., 2003; Vogel et al., 2003). On the other hand, A138G in exon 6, which promotes the expression of CD45 isoforms with lower molecular weights, CD45RO, results in increased expression levels of CD45 on peripheral blood mononuclear cells (PBMCs). An increased frequency of IFNγ expressing CD4 and CD8 T cells was observed when PBMCs from individual with the A138G variant were stimulated by PMA and ionomycin in culture, and the A138G allele was associated with reduced frequency of Hepatitis B and Graves thyroiditis from a cohort study done with ~150 people in each comparison group (Boxall et al., 2004). These effects of the loss or polymorphism of CD45 suggest an important role of CD45 in the development of immune disorders.

1.3 Erythropoiesis

Erythrocytes are one of the most abundant cells in the body that play a vital role in the transport of oxygen in the circulatory system. While mature erythrocytes (RBCs) do not express CD45 (Scheid and Triglia, 1979), they are generated from $CD45^+$ HSC and downstream erythroid progenitors through cytokine signaling, such as by stem cell factor (SCF) and EPO (Wang et al., 2008). Due to their limited life span of approximately 120 days in humans and 40 days in mice, erythrocytes need to be replenished daily (Franco, 2012). Healthy adults have been reported to produce over 2 million erythrocytes each second (Franco, 2012). During steady state, humans produce erythrocytes from the BM and mice produce them from the BM and spleen (Dzierzak and Philipsen, 2013; Wolber et al., 2002). Upon stress, such as hypoxia or

inflammation, the spleen plays an important role in extramedullary erythropoiesis to augment the production of erythrocytes (Hara and Ogawa, 1976; Paulson et al., 2011; Socolovsky, 2007).

1.3.1 Fetal and Neonatal Erythropoiesis

Neonatal mice have a higher rate of erythropoiesis than adult mice to meet the increasing demands for oxygen elicited by the rapid growth of the body (Finne and Halvorsen, 1972). This is substantiated by the elevated capacity of erythroid progenitor cells to generate mature erythrocytes and the increased frequency of erythroid progenitor populations (Finne and Halvorsen, 1972; Yan et al., 2018). The earliest generation of primitive erythrocytes are derived from yolk sac, followed by more definitive erythrocytes from HSC in fetal liver (Dzierzak and Philipsen, 2013; Ema and Nakauchi, 2000; Medvinsky and Dzierzak, 1996). Around the time of birth, erythrocytes are derived from HSCs in the BM and spleen, which remain the sites of hematopoiesis throughout adult life during steady state or under stress (Dzierzak and Philipsen, 2013).

1.3.2 Developmental Stages

Cells proliferating and differentiating from HSCs into erythrocytes undergo many stages of development (Figure 1.3A). One of the earliest progenitors which commit to become erythrocytes or thrombocytes are called megakaryocyte-erythroid progenitors (MEP), which express KIT, a receptor for SCF (Sanchez et al., 2006). Early studies identified erythroid progenitors by determining how many hemoglobinized cells they can produce in colony forming assays in methylcellulose. For mice, the progenitors are characterized as burst-forming, BFU-E, if they produce 1000 hemoglobinized cells in 5-9 days, or colony-forming, CFU-E, if they

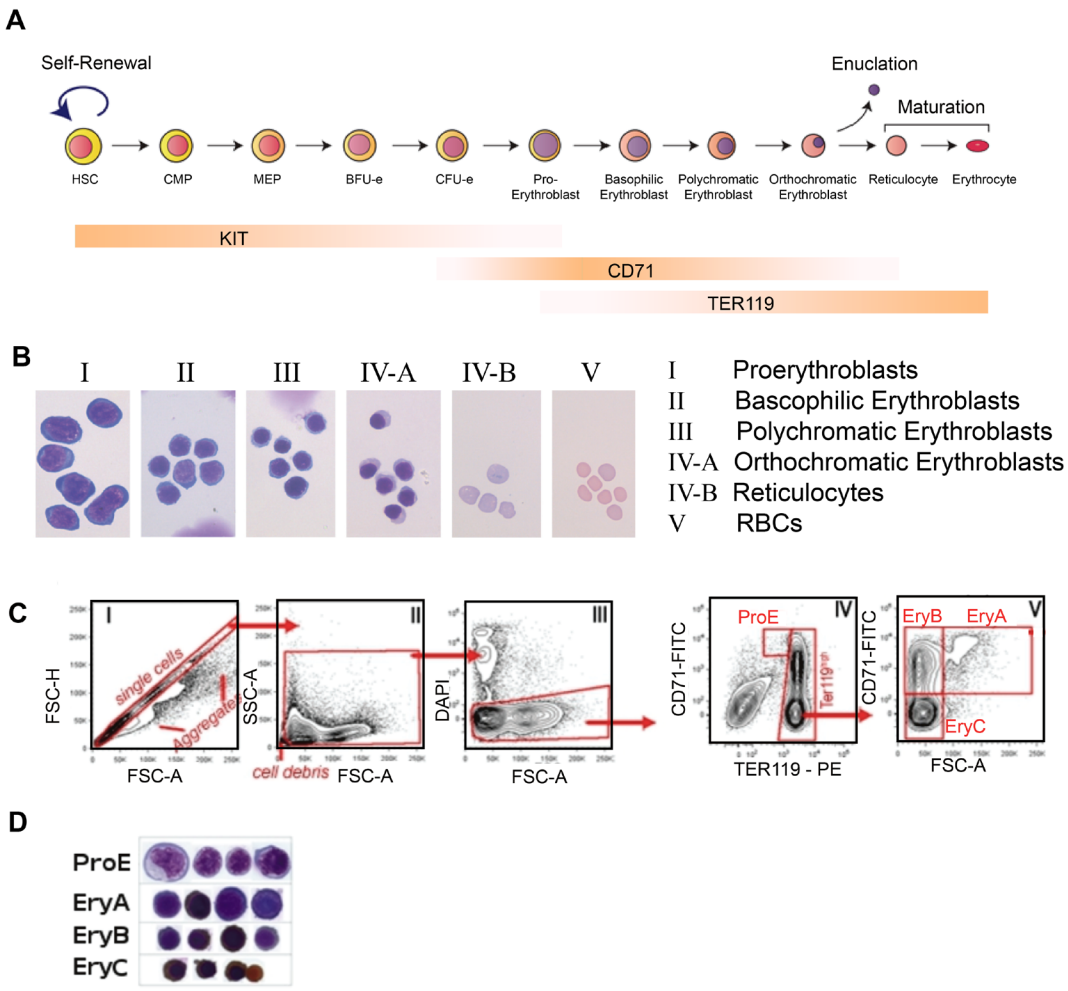

Figure 1.3 Erythropoiesis

(A) HSCs proliferate and generate downstream progenitor cells which progressively become more committed to becoming mature erythrocytes. The earlier populations express Kit, which is gradually lost. Downstream progenitors gain expression of CD71 transiently from Pro E cells to Polychromatic erythroblasts, while TER119 begins to be expressed and remains high from Pro E cells to mature RBCs. Adapted from (Dzierzak and Philipsen, 2013). (B) Erythroid progenitors downstream of Pro E can be distinguished by morphological features observed under the microscope. Adapted from (Chen et al., 2009) (C-D) Flow cytometric gating strategy used to distinguish erythroid progenitors downstream of Pro E using differential patterns of CD71 and TER119 expression. Adapted from (Sanchez et al., 2006).

produced 16-125 hemoglobinized cells in 2-3 days (Palis and Koniski, 2018). These cells give rise to Proerythroblasts (Pro E), and to mature RBCs through multiple stages of proliferation and maturation, which involve reduction in size, loss of organelles such as endoplasmic reticulum and mitochondria, expulsion of the nucleus, as well as adaptation of a biconcave shape to increase surface area for efficient oxygen transport (Dzierzak and Philipsen, 2013). Based on microscopic features, the erythroid cells from the Pro E stage and onwards can be further identified as basophilic erythroblasts, polychromatic erythroblasts, orthochromatic erythroblasts, reticulocytes and finally RBCs (Figure 1.3B).

A specific pattern of protein expression on cell surface changes during erythroid maturation, which allows adoption of flow cytometric analysis to identify different stages of maturation from Pro E to Ery A, Ery B and finally to the mature erythrocytes, Ery C (Figure 1.3C-D). The distinction is based on changes in the expression of the key erythroid marker, TER119, and of transferrin receptor, also known as CD71 (Chen et al., 2009). Briefly, TER119 expression begins at the Pro E stage, and the level of expression increases and remains increased until the cells complete maturation. Cell size, which is detected by forward scatter (FSC), decreases from Ery A to Ery B. Finally, CD71 expression, which is highly expressed from Pro E to Ery B cells, is lost, as the cells transition to Ery C (Chen et al., 2009; Koulnis et al., 2011).

1.3.3 Erythropoietin

As Pro E lose the expression of KIT and begin to express EPO receptor, EPO becomes the main driver of later erythroid development (Kosmider et al., 2009; Wu et al., 1995). EPO is a hormone mainly produced by peritubular fibroblasts in the kidney (Bachmann et al., 1993). However, extrarenal production of EPO was found to account for approximately 10% of the

basal EPO level in rat serum at steady state (Erslev et al., 1980). Macrophages have been also reported to express both EPO and the receptor for EPO in response to sphingosine-1-phosphate (S1P), which is exceptionally high in circulation as the major source of S1P is erythrocytes (Bode et al., 2010; Luo et al., 2016).

The receptor for EPO does not have a kinase domain, instead it associates with JAK2 for trans-phophorylation. Activation of JAK2 through binding of EPO to its receptor leads to phosphorylation of the transcription factor STAT5 which then translocates to the nucleus and drives the expression of genes for survival, proliferation and differentiation of erythroid cells (Dzierzak and Philipsen, 2013; Gillinder et al., 2017; Witthuhn et al., 1993). EPO also signals through PI3K/Akt and ERK/MAPK pathways to inhibit apoptosis and to induce proliferation (Bouscary et al., 2003; Devemy et al., 1997; Klingmuller et al., 1997; Uddin et al., 2000).

Lyn, which is a SFK member, is also involved in EPO signal transduction as a modulator of erythropoiesis. Lyn null mice exhibit age-dependent splenomegaly with accumulation of KIT^+ erythroid progenitors with increased pAkt, however the cells are more apoptotic with reduced expression of Bcl-xL (Harder et al., 2004; Ingley et al., 2005). Interestingly, dominant active mutation of Lyn in $Lyn^{up/up}$ mice also exhibit an accumulation of erythroid progenitors when induced by phenylhydrazine with increased Bcl-xL and pSTAT5 in the progenitors (Slavova-Azmanova et al., 2013). The number of mature RBC in $Lyn^{up/up}$ mice are equal to the wildtype but with perturbations in morphology and function. Together, these reports suggest that Lyn supports EPO signaling pathways, however further investigation revealed that while Lyn can relay pro-survival signals through Akt pathways, it can also inhibit JAK2/STAT5 pathways as a part of negative feedback through SHP-1 (Slavova-Azmanova et al., 2014).

CD45, which targets JAK and Lyn, has been implicated in the negative regulation of erythropoiesis through work done *in vitro*. The BM of CD45KO mice generates increased numbers of erythroid colonies in response to EPO stimulation (Irie-Sasaki et al., 2001), while the $CD34^+$ cells isolated from human umbilical cord generate increased number of erythroid cells when CD45 signaling is interrupted (Harashima et al., 2002). However, little is known about the role of CD45 in the regulation of erythropoiesis *in vivo*, as well as its impact on specific erythroid progenitors.

1.3.4 Role of Macrophages in Erythropoiesis

Other than soluble factors, erythrocyte-nursing macrophages also play a crucial role in the final maturation of the RBC downstream of Pro E, both in the BM and red pulp of the spleen. Erythroblasts are found in erythroblastic islands which surround the erythrocyte-nursing macrophages in the center. In this form, the macrophage supports the enucleation process by phagocytosing the extruded nucleus (Klei et al., 2017; Manwani and Bieker, 2008). In the spleen, these are red pulp macrophages (RPM) (Toda et al., 2014), as splenectomy or depletion of the RPMs with clodronate inhibits erythroid maturation (Rhodes et al., 2016). RPMs also regulate erythroid turnover by recycling iron and clearing senescent RBCs through phagocytosis, which are recognized by phosphatidylserine on the cell surface or naturally occurring antibodies against modified band 3 (Lutz, 2012; Schroit et al., 1985).

RPMs are characterized by high expression of F4/80 and low expression of CD11b on the cell surface, and express heme oxygenase1 (Hmox-1) and SPI-C (Haldar et al., 2014; Kohyama et al., 2009; Kurotaki et al., 2015), as well as adhesion molecule, such as VCAM-1 (Kurotaki et al., 2011). In steady state, Hashimoto's group has shown that RPMs have a long-life span with a

low proliferation rate through long-term parabiosis and BrdU uptake experiments (Hashimoto et al., 2013). However, when depleted by clodronate or radiation, monocytes replenish the RPMs. Phagocytosis of erythrocytes is a key step in this process, as intracellular heme triggers the expression of SPI-C and degradation of BACH1, thus promoting the development of monocytes into RPMs over F4/80$^+$ BM-derived macrophages (Haldar et al., 2014; Kohyama et al., 2009). RPMs can also interact with other immune cells and partake in immune responses. For example, RPMs have been reported to constitutively express IL-10 and TGFβ and help induce Foxp3 expression in CD4$^+$ T cells to generate T_{Reg} cells (Dillon et al., 2006; Kurotaki et al., 2011). However, proinflammatory roles for RPMs has been observed in different models. Macrophages in red pulp have been reported to produce TNFα during endotoxemia induced by i.p. injection of LPS, and RPMs also have been reported to produce type I IFN in *Plasmodium chabaudi* infection (Inoue et al., 2014; Yadava et al., 1996).

1.3.5 Immunomodulation by Erythroid Progenitors

In addition to generating mature RBCs, CD71$^+$TER119$^+$ cells, which comprise heterogenous population of erythroid progenitor cells, have been shown to possess immunosuppressive properties (Elahi, 2019). Neonatal erythroid cells which are enriched with erythroid progenitors reduce proinflammatory cytokine production by splenic innate immune cells when cocultured *in vitro*, while the depletion of the erythroid progenitors in neonates *in vivo* not only increases cytokine production in response to *Listeria monocytogenes* infection but also allows better pathogen clearance (Elahi et al., 2013). Erythroid progenitors have also been shown to modulate adaptive immune responses to *Bordetella pertussis* infection by reducing IL-17 and IFNγ production by T cells and antibody production by B cells (Namdar et al., 2017). In

these studies, the immunosuppressive activities were attributed to the expression of arginase-2 by the erythroid cells, thereby depleting arginine from the leukocytes.

Accumulation of immunosuppressive erythroid cells has been described from other models as well. Zhao *et al.* reported accumulation of extramedullary erythroid progenitors in mice inoculated with Lewis lung cancer (LLC) cells and a subsequent reduction in antiviral response to lymphocyte choriomeningitis virus (LCMV) with a reduced $CD8^+$ T cell response (Zhao et al., 2018). Use of an anti-transferrin receptor CD71 antibody to deplete erythroid cells fully restored the $CD8^+$ T cell response. They also showed that erythroid cells suppress $CD8^+$ T cell activation and effector function through production of ROS by performing inhibition assays *in vitro* (Zhao et al., 2018).

Expansion of erythroid cells has also been reported during both human and mouse pregnancy (Dunsmore et al., 2018; Fowler and Nash, 1968), suggesting their involvement in the suppression of immune responses that can be elicited between the allogeneic mother and fetus during pregnancy. Human erythroid progenitors isolated from PBMCs of pregnant woman reduce both $CD4^+$ and $CD8^+$ T cell proliferation in response to anti-CD3/CD28 stimulation (Delyea et al., 2018). Also, in mouse allogenic pregnancy model, depletion of erythroid cells results in gestation failure due to immunological rejection of the fetus, reflected in the increased number of $CD4^+$ and $CD8^+$ T cells, leukocyte infiltration and proinflammatory cytokine production in the placenta (Delyea et al., 2018). In this study, they showed that the erythroid progenitors isolated from pregnant mice uniquely express PD-1 and PDL-1, and the immunosuppression by the maternal erythroid progenitors is overridden by PDL-1 blockade (Delyea et al., 2018). Correlation between reduced T_{Reg} cells and increased proinflammatory cytokine production has been reported from pregnant IBD patients who also have reduced

$CD71^+$ erythroid cells compared to healthy pregnant controls (Dunsmore et al., 2018). It is possible that $CD71^+$ erythroid cells promote iTreg development by secreting TGFβ, which have been reported from a subset of erythroid cells present in newborn mice that express a unique inhibitory marker, V-domain Immunoglobulin (Ig) Suppressor of T Cell Activation (VISTA) (Shahbaz et al., 2018). However, whether the $CD71^+$ cells have a general immunosuppressive role in non-pregnant IBD patients has yet to be addressed.

1.4 Inflammatory Bowel Disease

Maintenance of a healthy level of immune tolerance towards self-antigens and innocuous microbiota in the gut is crucial for intestinal homeostasis and it involves complex cross-talk between microbiota, immune cells and non-hematopoietic cells. Development of IBD occurs when tolerance is broken, which is not only restricted to chronic inflammation in the intestine, but can result in a systemic inflammatory response, leading to complications such as cachexia and anemia (Cronin and Shanahan, 2005). In the clinic, IBD is manifested as ulcerative colitis (UC) or Crohn's disease (CD). UC involves mucosal inflammation restricted to the colon, while CD involves inflammation which can extend to the submucosa in any part of the gastrointestinal tract (Abraham and Cho, 2009).

While the exact etiology is unknown, environmental and genetic factors have been implicated in predisposition to the disease. Environmental factors include smoking, diet, geography, social stress and intestinal microbiota (Fiocchi, 1998). Polymorphism in NOD2 and autophagy-related genes such as ATG16L1 and IRGM have been associated with increased susceptibility to CD (Hampe et al., 2007; McCarroll et al., 2008; Ogura et al., 2001).

The prevalence of IBD has become a growing concern, particularly in high-income countries: IBD rates are as high as one in 200 people for UC and one in 300 people for CD in Europe and North America (Ng et al., 2018). Predictive models estimate the prevalence of IBD to further increase to one in 100 by 2030 in Canada (Kaplan et al., 2018).

1.4.1 T cell Transfer Colitis

Originally described by Powrie (Powrie et al., 1994), the T cell transfer model of colitis has been key in identifying the various roles of T cells and their cytokines in the pathogenesis of IBD (Groux et al., 1997; O'Connor et al., 2009; Powrie et al., 1994). In addition to the role of T cells, intestinal myeloid cells and their cytokines have been implicated in perpetuating and regulating inflammation (Coombes and Powrie, 2008; Friedrich et al., 2019). The T cell transfer model of colitis involves the transfer of $CD25^{-}CD45RB^{high}CD4^{+}$ T cells, which are enriched for naïve T cells and depleted of T_{Reg}, into lymphopenic mice such as C.B-17 scid or $RAG1^{-/-}$ (RAGKO) (Powrie et al., 1993). In the absence of T_{Regs}, the T cells proliferate from being exposed to a lymphopenic environment and become activated and colitogenic in response to commensal antigens, demonstrated by the impaired development of colitis in mice treated with antibiotics or in germ free conditions (Feng et al., 2010). Generally, the disease manifests in IFNγ and IL-17A production from T cells and TNFα, IL-1 and IL-6 from myeloid cells (Friedrich et al., 2019). As the development of IBD progresses, leukocyte infiltration leads to severe inflammation and ulceration, loss of architecture of the intestine, along with signs of weakness, dehydration and wasting. Inflammation occurs throughout the gastrointestinal tract and is skewed towards a Th1 response like CD while it appears as contiguous lesions like UC (Strober and Fuss, 2011), recapitulating aspects of both CD and UC.

1.4.2 Systemic Effects of IBD

1.4.2.1 Extra-intestinal Inflammation

Extra-intestinal inflammation can be observed in IBD, which can have a detrimental impact on a patient's quality of life. Examples of extra-intestinal inflammation include arthritis and osteopenia as well as inflammation in skin, spine and oral mucosa (Vavricka et al., 2015). Separate prospective studies with over 400 patients for each have shown that 36.6 to 42.2% of CD patients and 15.0 to 51.5% of UC patients develop extra-intestinal inflammation at one or more sites (Lakatos et al., 2003; Mendoza et al., 2005). There is a higher incidence of extra-intestinal manifestation in pediatric IBD patients, with an occurrence of 80% in CD, and 50% in UC, patients (Stawarski et al., 2006). The exact pathogenesis of extraintestinal inflammation is not well understood. However, it is believed that the loss of immune tolerance towards commensals could also lead to a general loss of tolerance towards self (Snook et al., 1989). For example, Zafar *et al.* have detected presence of autoantibodies generated against specific isoform of microfilament cytoskeletal proteins called tropomyosins, both in colon and other common sites of extraintestinal inflammation, such as gall bladder, esophagus, skin, liver and eyes from UC patient samples (Mirza et al., 2006). This implicates that these autoantibodies may contribute to the inflammatory response in the extraintestinal sites through engagement with effector immune cells. Also, frequency of human leukocyte antigen (HLA) haplotype-B27, which has a known association with ankylosing spondylitis, has been reported to be higher in the IBD patients compared to normal population (Turkcapar et al., 2006). Furthermore, Infiltration of

microbiota from damaged architecture and compromised barrier function may be a possible cause.

1.4.2.2 Anemia

Patients with chronic diseases can develop anemia, known as anemia of chronic diseases (ACD). As many as one-third of IBD patients are reported to develop anemia. ACD may result from iron deficiency due to malabsorption or from ineffective erythropoiesis and shortened RBC survival (Gasche et al., 2004). Excessive production of TNFα, IL-1 and IL-6 in chronic inflammation has also been implicated in ACD (Madu and Ughasoro, 2017). Treating animals with exogenous EPO not only reduces ACD but also reduces the expression of proinflammatory mediators such as IL-12, IL-6 and TNFα in a model of 2,4,6-trinitrobenzene sulfonic acid (TNBS) induced colitis (Christodoulou and Tsianos, 2000; Nairz et al., 2011). In fact, EPO signaling in various macrophages has been shown to promote the clearance of apoptotic cells through the activation of PPARγ (Luo et al., 2016).

1.4.2.3 Systemic Wasting

Systemic wasting syndrome, also referred to as cachexia, is defined as continuous and involuntary weight loss by systemic inflammation (Argiles et al., 2015; Fearon et al., 2011). Common to many diseases such as IBD and cancer, cachexia has a profound effect on a patient's overall health and is associated with increased morbidity (Evans et al., 2008). In the context of IBD, malnutrition due to malfunction of the gut may be a contributing factor to the weight loss, but systemic immunity can also contribute to development of wasting disease through cytokines such as TNFα and IL-1(Fisher, 1999; Langhans and Hrupka, 1999). In fact, TNFα is a potent

cachectin, where a single treatment of TNFα into a healthy rat induces anorexia by reducing the amount of food intake over 24 h (Cerami et al., 1985; Yang et al., 1994), and daily injections of TNFα reduces percentages of both body fat and protein (Tracey et al., 1988). TNFα has also been shown to induce muscle degeneration by increasing proteolysis and inhibiting muscle regeneration (Bossola et al., 2001; Llovera et al., 1996; Moresi et al., 2009). The role of TNFα in wasting is better understood in the context of cancer. Previous studies have shown that $Tnfr1^{-/-}$ mice have less severe muscle loss during cancer and anti-TNFα treatment reduces the expression of muscle ubiquitin genes in tumor-bearing rats (Llovera et al., 1996; Llovera et al., 1998). In contrast, the impact of TNFα on wasting associated with colitis has not been well explored, and whether blocking TNFα production or signaling can reduce wasting in colitis needs to be investigated.

1.5 Homeostatic T cell Proliferation

T cells play an essential role in the pathology of IBD, especially in the T cell transfer model of colitis in mice. T_{Reg} cells contribute to tolerance of commensal and self antigens, and in preventing and suppressing IBD, while effector T cells, such as Th17 cells, contribute to the pathogenesis of IBD (Eri et al., 2012). Thus, it is important to study how T cells are regulated to further understand their contribution to inflammation and autoimmunity.

T cell development occurs in the thymus through a series of positive and negative selection steps. This ensures that each thymocyte, which expresses a unique TCR on its surface, can effectively bind to an MHC and peptide complex on antigen-presenting cells with an appropriate strength of binding that is neither too weak nor too strong. Upon completion of maturation, thymocytes becomes mature T cells and leave the thymus through blood vessels to

enter the circulation and the SLOs (Jin et al., 2008), where they await the appearance of cognate antigen. Keeping a large library of T cells ensures a diverse TCR repertoire to protect the body from infections which may occur. However, the thymus deteriorates by the time of puberty, after which the maintenance of the T cells already generated becomes critical. As the amount of space and resource for the T cells is limited, the size of the T cell repertoire in the periphery is homeostatically regulated within a narrow range (Takada and Jameson, 2009). This occurs through homeostatic proliferation, which refers to T cell proliferation in response to reduced T cell numbers in the vicinity. It contrasts with proliferation induced by T cell activation, as it occurs in the absence of robust cognate antigen and costimulatory signals from DCs. As an example, active homeostatic proliferation has been observed from neonates or lymphocyte-deficient patients who are functionally lymphopenic (Chomont et al., 2009; Min et al., 2003). Defective homeostatic proliferation may lead to detrimental outcomes, such as immunodeficiency or autoimmunity, such as expansion of autoreactive T cells in patients who have undergone an organ transplant.

1.5.1 Experimental Model of Homeostatic Proliferation

In the lab setting, homeostatic proliferation has often been studied using lymphopenia induced proliferation (LIP). To induce LIP, polyclonal T cells that are pre-labeled with a cell proliferation dye are injected into a lymphocyte deficient host, such as RAGKO mice. Generally, the proliferation of the T cells from the SLO can be observed in a week (Martin et al., 2013). T cells undergo both slow and fast LIP.

1.5.2 Slow Proliferation

Slow proliferation is driven by common-γ chain cytokine signaling, such as IL-7 and IL-15 (Martin et al., 2013; Takada and Jameson, 2009). For instance, significant loss of slow proliferation is observed when T cells are injected into IL-7 deficient mice (Tan et al., 2001). IL-7 is the most effective cytokine as it can induce proliferation of both naïve and memory T cells (Lenz et al., 2004; Schluns et al., 2000). IL-15 which shares the common- γ chain receptor can also induce proliferation, but primarily of memory CD8 T cells (Tan et al., 2002). Both of these cytokines signal through JAK/STAT pathways, where STAT3 and STAT5 phosphorylated by JAK enter the nucleus and activate genes for proliferation and survival of T cells (Spolski et al., 2017).

1.5.3 Fast Proliferation

Fast LIP is also known as spontaneous proliferation, and the main driving signal is MHC-antigen complex-driven stimulation. This was demonstrated by the lack of fast LIP in TAPKO, β2MKO and MHCIIKO mice, as these hosts are unable to provide, or sufficiently provide, MHCI or II-derived stimulation to the T cells (Ge et al., 2001; Martin et al., 2003). Likewise, depletion of $CD11c^{high}$ cells, which is a DC-enriched population, using CD11c-diptheria toxin receptor transgenic mice, severely reduces fast proliferation when LIP is induced (Zaft et al., 2005). Unlike slow LIP, the T cells that have expanded through fast LIP upregulate CD44 and downregulate CD62L expression, resembling the phenotype of a memory T cell, but without the expression of the early activation markers, CD69 and CD25 (Min et al., 2005). Overall, the current thinking is that fast proliferation is driven by antigenic stimulation and slow proliferation is driven by cytokine signaling.

1.5.4 Microbiota

Other than MHC and cytokines, the presence of the gut microbiota has been implicated in LIP. This was demonstrated by observing either significant or complete loss of fast proliferation from antibiotic treated or germ free (GF) mice and observing restoration of fast proliferation upon reconstitution of the microbiota in the gut (Feng et al., 2010; Kieper et al., 2005). A study reported that depleting the microbiota through antibiotic treatment leads to a lower level of IL-7 in the gut (Vonarbourg et al., 2010); therefore, whether or not microbiota induce fast proliferation directly, as a source of antigen for TCRβ stimulation, or indirectly, through inducing IL-7, still remains unclear. Interestingly, LIP is most pronounced in neonates or in patients suffering from IBD (Feng et al., 2010; Min et al., 2003), who also have increased gut permeability, which may allow for increased interaction between the host and the gut microbiota.

1.5.5 Role of CD45 in LIP

In our lab, we previously showed that CD45 expression on innate immune cells supports LIP by demonstrating that both fast and slow proliferation of WT T cells are reduced when they are adoptively transferred into CD45RAGKO mice compared to RAGKO mice (Saunders et al., 2014). CD45 expression on $CD11c^+$ cells played an important role as the defective T cell LIP in CD45RAGKO host was partially rescued when $CD45^+CD11c^+$ cells were co-adoptively transferred with the T cells (Saunders et al., 2014). It is still unclear whether the restoration by CD11c+ cells is a dose-dependent effect. If not, then the partial restoration observed would suggest an additional mechanism where CD45 plays a role in the regulation of fast proliferation, possibly by promoting intestinal microbial composition that may provide stronger antigenic stimulation for fast LIP. Also, some evidence was found for an indirect role of CD45 in

regulating stromal cell function, as the lineage$^-$PDPN(podoplanin)$^+$ stromal cells from the CD45RAGKO pLN expressed lower levels of IL-7 mRNA (Saunders et al., 2014). Since CD45 is not expressed on stromal cells, this suggests that innate immune cells indirectly regulate IL-7 production by the stromal cells. However, the mechanism of this interaction is still unknown.

1.6 Secondary Lymphoid Organs

Cell-to-cell interactions occur practically everywhere within our body but the SLO is the site where adaptive immune cells encounter innate immune cells and get activated to mount an adaptive immune response against disease-causing agents. Immune cells are strategically located in SLO to maximize the efficiency of antigen sampling by lymphocytes. In LN for instance, T cells can be found in the paracortex area and B cells in primary follicles located in the cortex (Figure 1.4) (Drayton et al., 2006). SLOs are vascularized with high endothelial venules (HEV) and lymphatic vessels.

Non-immune cells are also found in SLO, such as blood or lymphatic endothelial cells, fibroblastic reticular cells (FRC) and follicular dendritic cells (FDC), collectively called stromal cells. These cells form the architecture while actively interacting with immune cells: for instance, during homeostasis, FRCs maintain the T cell zone by producing IL-7 for T cell survival and CCL19 and 21 for recruitment (Link et al., 2007; Roozendaal and Mebius, 2011). Likewise, FDCs provide BAFF and CXCL13 to maintain germinal centers for B cells. During inflammation (Park and Choi, 2005), T cell zone FRCs have been demonstrated to drive dendritic cell (DC) migration on FRC scaffolds through PDPN on FRC activating C-type lectin-like receptor-2 (CLEC2) on DCs (Acton et al., 2012). In mesenteric lymph nodes, stromal cells

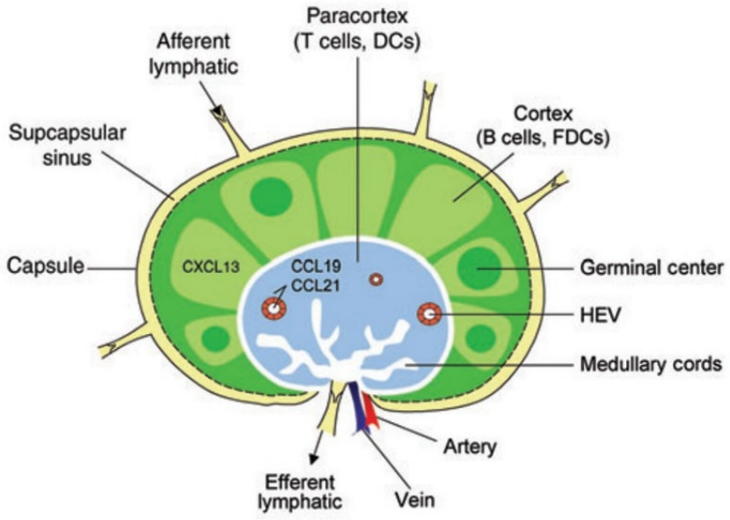

Figure 1.4 Secondary lymphoid organ – peripheral lymph node

Immune cells are strategically located in the secondary lymphoid organs in order to maximize the efficiency of antigen sampling by the lymphocytes. T cells can be found in the paracortex area and B cells in primary follicles located in the cortex. Lymph nodes are vascularized with high endothelial venules (HEV) and lymphatic vessels. Non-immune cells are also found in SLO such as blood or lymphatic endothelial cells, FRC and FDC. (Drayton et al., 2006)

contribute to T cell homing to the gut by providing retinoic acid (RA), which induces expression of gut-homing molecules on activated T cells (Molenaar et al., 2009).

The interaction between stromal cells and HSC-derived cells starts as early as E12 when SLO formation begins, when retinoic acid from neuronal cells activates mesenchymal stromal cells (MSC) to produce the chemokine CXCL13 (van de Pavert et al., 2009). This recruits lymphoid tissue-inducer cells (LTi) that act back on the MSC to induce their maturation and differentiation into lymphoid tissue-organizer cells (LTo) (White et al., 2007). LTo cells give rise to downstream subsets of stromal cells and the stromal cells recruit other cells through production of chemokines. The primary interaction between LTi and stromal cell progenitors is via lymphotoxin (LT) acting on stromal cell LTβR (White et al., 2007). Recent work has shown that without LTβR expression on stromal cell progenitors, mice still develop lymph nodes, but with reduced maturation, defined by lower levels of PDPN, ICAM-1 and VCAM-1 expression, as well as homeostatic cytokines, such as IL-7. This was observed even in mature mice older than six weeks, and was associated with an increased susceptibility to viral infection (Chai et al., 2013).

1.7 Research Objectives

This study aims to understand the role of CD45 in regulating erythroid and myeloid cells during homeostasis and colitis, as well as the role of CD45 in regulating maintenance of T cells in SLO.

While culturing of BM progenitors in EPO implicates CD45 as a positive regulator of erythropoiesis, its function *in vivo* has not been established, and where, when and how it exerts its effect are not known. The first aim of my project is to determine the role of CD45 on

erythroid development *in vivo* using CD45-deficient mouse models. I hypothesize that CD45 negatively regulates erythroid progenitor cell production *in vivo*, by regulating cellular response to EPO. I further hypothesize that CD45 modulates erythropoiesis through regulating EPO production and erythrocyte-nursing macrophage.

The second aim of my thesis is to understand the role of CD45 on myeloid cells in the chronic development of colitis using a T cell transfer colitis in RAGKO and CD45RAGKO mice with $CD45^{+/+}$ T cells. In this model, I compare the intestinal inflammation in colon and extra-intestinal inflammation in the spleen, evaluating the effect of CD45 on inflammation occurring at these different sites and aim to find out the link between the two.

The third aim is to understand how CD45 regulates T cell maintenance by studying LIP in RAGKO and CD45RAGKO mice. One of my specific aims is to understand how CD45 affects fast LIP by comparing how well $CD11c^{+}$ cells and intestinal microbiota from CD45-deficient mice can induce fast LIP compared to the ones from CD45-sufficient mice. The other specific aim is to understand how CD45 affects slow LIP, where I hypothesize that CD45 promotes maturation of stromal cells and their production of IL-7.

Chapter 2: Materials and Methods

2.1 Mice

C57BL/6 (WT), BoyJ (B6.SJL CD45.1), CD45KO (exon 9) and RAGKO mice were obtained from The Jackson Laboratory (Sacramento, CA). The CD45KO mice were backcrossed for ten generations onto the C57BL/6 background. CD45RAGKO mice were generated by crossing the CD45KO mice with RAGKO mice to homozygosity. All animals were bred and maintained in specific pathogen-free (SPF) conditions at the Containment Level 1 of the Centre for Disease Modeling (CDM) or Modified Barrier Facility (MBF) at the University of British Columbia (UBC). Mice were used between 6 and 15 weeks of age and matched for age, sex and strain. All animal experiments were conducted in accordance with the Canadian Council of Animal Care Guidelines using protocols approved by the University Animal Care Committee.

2.2 Cell Isolation

Single cell suspensions of Ter 119^+ cells were obtained from spleens after mincing and passaging through a 70 μm strainer. For analysis of $TER119^+$ cells from the bone marrow, the femurs and tibias were flushed with PBS with 2% fetal bovine serum (FBS) using a 26-gauge needle and syringe. RBC lysis was not performed unless specifically stated. RBC and their progenitors were isolated from RAGKO and CD45RAGKO spleens by negative depletion after labeling cells with biotinylated antibodies against NK1.1, CD4, CD11b, CD11c, Gr1 and F4/80 (UBC Antibody Lab), adding anti-biotin beads (Miltenyi Biotec) and passing through magnetic columns (Miltenyi Biotec) for collection of the unlabeled fraction. For experiments that required further enrichment of erythroid progenitors, the isolated cells were further incubated in 0.84%

ammonium chloride, 2 mM Tris-HCl pH 7.2 buffer at room temperature for 5 min to lyse the mature RBCs to achieve a purity above 90%.

When myeloid cells were harvested from the spleen, a single cell suspension was obtained after incubating the spleen with 1 mg/ml of collagenase IV (Worthington Biochemical Corporation, Lakewood, NJ) for 20 min at room temperature, followed by chopping of the spleens and additional 20 min of incubation in a digestion media before passing it through the 70 µm strainer. The cells were then resuspended in 0.84% ammonium chloride, 2 mM Tris-HCl pH 7.2 buffer at room temperature for 5 min to lyse RBC, then resuspended in RPMI or in PBS. For coculture experiments which require isolation of myeloid cells, the isolated splenocytes were further incubated with biotinylated antibodies for CD11c, CD11b, Gr1, and MHCII, washed with a solution of PBS, 0.5% BSA and 2 mM EDTA and then incubated with anti-biotin antibodies (Miltenyi Biotec) for another 20 min at 4°C. The cells were put through a magnetic column (Miltenyi Biotec) and the positive fraction was collected.

For isolation of cells from the colon, colons were dissected from euthanized mice and opened longitudinally then cut into approximately 0.5 cm pieces. Colon pieces were then incubated for 20-30 min at 37°C in a solution of PBS, 5% FCS and 4 mM EDTA for at least 3 washes to remove epithelial cells. Colon pieces were washed twice with a solution of PBS and 5% FCS and then minced with a scalpel, incubated twice at 37°C for 40 min in a solution of RPMI, 5% FCS and 1mg/ml of Collagenase IV and passed through a 70 µm strainer to obtain the lamina propria cells.

Stromal cell isolation was done as described previously (Fletcher et al., 2011). In brief, inguinal, axillary, and brachial lymph nodes were punctured with a needle and were digested for 20 min at 37˚C with 2 ml digest mix consisting of RPMI 1640 with 0.2 mg/ml Collagenase VIII

(Sigma), 0.8 mg/ml Dispase (Invitrogen), and 0.1 mg/ml DNase I (Roche). The suspension was vigorously mixed and then left for large particles to settle. The supernatant was removed and washed, and the sedimented material was digested with fresh digest mix for an additional 15 min and the debris were gently pipetted up and down to dissociate any remaining tissues into a single cell suspension.

2.3 Induction of T Cell Transfer Colitis

A single cell suspension was obtained by mechanical disruption of C57BL/6 mouse spleen between two frosted slides. RBCs were lysed with 0.84% ammonium chloride, 2mM Tris-HCl pH 7.2 buffer at room temperature for 5 min. The cells were then incubated with biotinylated antibodies for TER119, B220, CD11b and CD8α for 20 min at 4°C, washed with a solution of PBS, 0.5% BSA and 2 mM EDTA and then incubated with anti-biotin antibodies (Miltenyi Biotec) for another 20 min at 4°C. The cells were put through a magnetic column (Miltenyi Biotec) and the negative fraction was collected and labelled with PECy7 conjugated anti-CD4, PE conjugated anti-CD25 and FITC conjugated anti-CD45RB (all from eBioscience) and sorted for the CD4+CD25-CD45RBhigh naïve T cells on a BD AriaTM or InfluxTM. RAGKO or CD45RAGKO mice received 4×10^5 of the sorted cells in 200 uL sterile PBS by intraperitoneal injection.

2.4 Induction of Lymphopenia Induced Proliferation

T cells were purified from spleen along with inguinal, axillary, and brachial lymph nodes. T cells were negatively selected using biotinylated antibodies, obtained from the Biomedical Research Center Antibody lab, against TER119 (TER119), CD11c (N418), CD11b (M1/71),

B220 (RA3-6B2) or CD19 (1D3) (for CD45KO T cells) and CD4 (GK1.5) for OT-I T cells, or CD8α (53-6.7) for OT-II T cells. The labeled cells were separated from unlabeled cells using anti-biotin microbeads and LS MACS columns (Miltenyi Biotec). The purity of the cells was checked by flow cytometry and was around 95% for CD45.1 and OT-I T cells, and around 85% for OT-II T cells and CD45KO T cells. The T cells were labeled with 10 μM CFSE (Invitrogen Cell Probes) in RPMI 1640 at 37˚C for 12 min. For T cell LIP in RAGKO, CD45KO, or 45RAGKO mice, 1–5 × 10^6 CD45.1 T cells in PBS were injected per mouse i.v. into the tail vein and 3–12 × 10^5 T cells were injected when CD45KO and WT T cells were being compared. The cells were allowed to proliferate *in vivo* for 7 days and spleens and pLNs (inguinal, brachial and axillary LNs) were harvested for analysis.

For LIP experiments with adoptive transfer of splenic $CD11c^+$ cells, the donor mice for $CD11c^+$ cells were injected with B16 cells transfected with Flt3L subcutaneously to expand the cells *in vivo.* When the tumor size reached 1 cm^3 in volume, the mice were euthanized to harvest spleens. Single cell suspensions were made according to the method mentioned above by digesting the spleens with Collagenase I, and RBCs were lysed with 0.84% ammonium chloride, 2 mM Tris-HCl pH 7.2 at room temperature for 5 min. Enrichment for $CD11c^+$ cells was performed by using anti-CD11c microbeads and LS magnetic columns (Miltenyi Biotec). The enriched cells were used for the T cell and $CD11c^+$ cell co-injection experiments, where 10 × 10^6 $CD11c^+$ enriched cells were isolated from WT mice and injected with 3 × 10^6 T cells into CD45RAGKO mice.

2.5 *In vivo* Proliferation Assay

Mice received one intra-peritoneal injection of 0.5 mg of Edu (5-ethynyl-2'-deoxyuridine, Thermo Fisher) in 100 µL of sterile PBS (Gibco) at 2 h prior to harvesting spleens, then single cell suspensions were prepared in PBS with 1% bovine serum albumin (BSA) at 4°C. The cells were then stained for surface markers prior to fixation and permeabilization with the ClickIT fixative (Thermo Fisher), then the samples were treated with the Click-IT reaction (Thermo Fisher) to attach the fluorochrome to Edu. Edu uptake was detected by flow cytometry. For gating, samples from mice injected i.p. with PBS were used as a negative control.

2.6 Apoptosis Assay

After creating single cell suspensions from the spleen, 2 million cells from each sample were transferred into round-bottom polypropylene tubes with caps at 10×10^6 cells/mL in PBS and incubated with FLICA660 agent (ImmunoChemistry, Bloomington, MN) for 30 min at 37°C. A negative control was prepared by incubating the sample without the FLICA660 agent. As a positive control for Caspase3/7 activation, apoptosis was induced by incubating cells in 100 nM dexamethasone (Sigma) for 3 h prior to the incubation in FLICA660. Cells were washed twice with 1 mL of apoptosis buffer (ImmunoChemistry) then stained for surface antigens and live and dead staining as mentioned above. Samples were analyzed on a BD FACSCanto or LSRII (BD) with FlowJo software (Tree Star). Fluorescence-minus-one (FMO) controls were prepared from the negative control which was incubated with the FLICA660 to determine gating and exclude non-specific binding.

2.7 Cytokine Measurement by ELISA

Blood was collected by cardiac puncture into anti-coagulant containing tubes, Microvette CB300 (Sarstedt), and centrifuged for 10 min to collect the plasma. The spleen and kidney were harvested and kept on ice until the samples were digested with ice cold protein extraction buffer (100 mM Tris, 150 mM NaCl, 1 mM EDTA, 1% Triton X-100 and 0.5% Sodium deoxycholate) with protease inhibitor cocktail tablet (Roche) added immediately before use. The samples were agitated for 2 h at 4°C and centrifuged for 20 min to collect supernatant. The supernatants and plasma were measured for EPO using the LEGEND MAX^{TM} ELISA kit from BioLegend, according to the manufacturers' instructions.

2.8 Cytokine Measurement Using Bead Array

TNFα cytokine secretion was analyzed by ELISA (eBioscience) or Flowcytomix (eBioscience) bead array according to manufacturer's instructions. Spleen and colon explants were washed with PBS with 5% FCS, weighed to 0.05 g and cultured in serum free RPMI media supplemented with penicillin, streptomycin and gentamycin overnight at 37°C. Serum was obtained by cardiac puncture.

2.9 Histological Grading of Colon Inflammation

Mice were euthanized when physical symptoms of disease (20% weight loss, hunching and diarrhea) were evident in the RAGKO mice, which occurred usually around 4 weeks at the Wesbrook Animal Unit, at 2-3 weeks in pre-Containment Level 1 at the Centre for Disease Modeling and 3 weeks in the Modified Barrier Facility. For colon sections, approximately 0.5 cm of the distal colon was put in 10% formalin. 5 to 7 microns of paraffin-embedded sections

were stained with hematoxylin and eosin by Wax-It Histology Services Inc. (Vancouver). For assessment of disease severity, colon sections were graded blindly on a scale of 0 (none) to 2 (severe) for each of the following parameters: degree of leukocyte infiltration, epithelial cell hyperplasia, mucin depletion, transmural inflammation, and ulceration. All scores were then summed to generate a final score for each sample.

2.10 EPO Stimulation

After the isolation of erythroid cells from the spleens, the cells were resuspended in sterile RPMI and were plated in a 48 well plate at 10×10^6 cells/mL in 500 uL. First, the cells were incubated for 3 h at 37°C to starve the cells from endogenous EPO, then 100 pg/ml of recombinant mouse EPO (BioLegend) was added to each well. Cells were incubated for 0.5, 1 and 2 hrs, after which the cells were harvested in PBS with 2% PFA to label intracellular pSTAT5 for flow cytometric analysis as mentioned above.

2.11 Coculturing of Erythroid Cells and Myeloid Cells

After isolating myeloid cells and $TER119^+$ cells as mentioned above, 5×10^5 myeloid cells were seeded into 48- or 24-well flat bottom tissue-culture treated plates individually or with $CD71^+TER119^+$ cells enriched cells or total $TER119^+$ cells that included both the $CD71^+$ and $CD71^-$ populations at the specified ratio in complete RPMI 1640 medium (10% fetal bovine serum, 20 mM HEPES (Invitrogen), nonessential amino acid (Invitrogen), 55 μM 2-mercaptoethanol (Invitrogen), 50 U/ml penicillin/streptomycin (Invitrogen), 1 mM sodium pyruvate (Invitrogen) and 2 mM L-glutamine (Sigma-Aldrich)). Cells were stimulated with 10 ng/mL LPS with 10 μg/ml brefeldin A overnight at 37°C.

2.12 Phagocytosis Assay

To label cells that phagocytose erythroid cells, cells were labeled with pHrodo (Invitrogen), which is a fluorogenic dye which gains fluorescence in an acidic environment, such as in a lysosome, by following a previously reported protocol (Stijlemans et al., 2015). Briefly, up to 10^9 cells were washed twice with PBS, then incubated with 50 μM pHrodo dye in 1mL of PBS. After 30 min of incubation at 37°C, 14 mL RPMI with 5% FCS was added and cells were incubated for 15 min at 37°C. Cells were washed twice and resuspended in complete RPMI 1640 medium then used in the phagocytosis assay by coculturing them with myeloid cells in complete RPMI 1640 medium. After 4 h of coculture, cells that have phagocytosed the erythroid cells were detected or sorted using flow cytometry.

2.13 Flow Cytometry and Intracellular Staining

Single cell suspensions were blocked for FcR binding with 2.4G2 cell culture supernatant unless the cells were stained with antibody for CD16/32 (Biolegend, clone 93), in which case the cells were first stained first with CD16/32 before labeling for other surface markers. Biotin-conjugated antibodies were detected with fluorescently labeled streptavidin from Thermo Fisher. A detailed list of antibodies used for staining is in Table 2.13.

For gating on megakaryocyte-erythroid progenitor (MEP) cells in WT and CD45KO, lineage specific antibodies included a cocktail of the following: NK1.1 (PK136), CD4 (GK1.5), CD3 (17A2), CD19 (1D3), CD11b (M1/70), CD11c (N418), Gr1 (RB6-8C5) and CD8α (53-6.7) from Thermo Fisher. For gating on MEP in RAGKO and CD45RAGKO, lineage specific antibodies included a cocktail of the following: CD11b (M1/70), CD11c (N418), Gr1 (RB6-8C5), MHCII (M5/114.15.2) and F4/80 (BM8).

Target	Clone	Source
Arginase-2	Ab81505	Abcam
Bcl-2	BCL/10C4	BioLegend
CD3	17A2	Thermo Fisher Scientific
CD4	GK1.5	Thermo Fisher Scientific, UBC Antibody Lab
CD8α	53-6.7	Thermo Fisher Scientific, UBC Antibody Lab
CD11c	N418	Thermo Fisher Scientific, UBC Antibody Lab
CD11b	M1/70	Thermo Fisher Scientific, UBC Antibody Lab
CD16/32	93	Thermo Fisher Scientific
CD19	1D3	Thermo Fisher Scientific
CD25	PC61.5	Thermo Fisher Scientific
CD31	390	Thermo Fisher Scientific
CD34	RAM34	Thermo Fisher Scientific
CD45.1	A20	Thermo Fisher Scientific, UBC Antibody Lab
CD71	R17217	Thermo Fisher Scientific
CD103	2E7	Thermo Fisher Scientific
CCR7	4B12	Thermo Fisher Scientific
c-Kit	2B8	Thermo Fisher Scientific
EPO	10F3	Novus Biologicals
EPO-Receptor	140	Sino Biological
F4/80	BM8	Thermo Fisher Scientific, UBC Antibody Lab
Foxp3	FJK-16s	Thermo Fisher Scientific

PDPN	eBio8.1.1 (8.1.1)	Thermo Fisher Scientific, BioLegend
Gr1	RB6-8C5	Thermo Fisher Scientific
ICAM-1 (CD54)	YN1/1.7.4	BioLegend
IFNγ	XMG1.2	Thermo Fisher Scientific
IL-17A	eBio17b7	Thermo Fisher Scientific
LTβR	Clone3C8	Thermo Fisher Scientific
Ly6C	HK1.4	Thermo Fisher Scientific
Ly6G	1A8	Thermo Fisher Scientific
MHCII	M5/114.15.2	Thermo Fisher Scientific
NK1.1	PK136	Thermo Fisher Scientific, UBC Antibody Lab
pSTAT5	47/Stat5	BD Biosciences
TCRβ	H57-597	Thermo Fisher Scientific
TER119	TER119	Thermo Fisher Scientific, UBC Antibody Lab
Thy1.2	TIB107 (30H12)	UBC Antibody Lab
TNFα	MP6-XT22	Thermo Fisher Scientific
Sca1	D7	Thermo Fisher Scientific
VCAM-1 (CD106)	M/K-2	Thermo Fisher Scientific

Table 2.13 Antibodies Used for Flow Cytometric Analysis

For the assessment of cytokine production, the isolated cells from the spleen and lamina propria were stimulated with PMA (50 ng/ml) and Ionomycin (500 ng/ml) for 4-6 h in the presence of Brefeldin A (10 μg/ml). After labeling surface antigens, the cells were treated with Foxp3 fixation/permeabilization concentrate and associated buffers (Thermo Fisher) then were stained with antibodies against intracellular targets.

For pSTAT5 labeling after EPO stimulation of erythroid cells, the cells were placed in 2% paraformaldehyde (PFA) in PBS on ice, followed by 10 min incubation at room temperature. The cells were washed with PBS with 2% FBS then incubated in ice-cold 90% methanol for permeabilization for 3 h at 4°C. After washing, the cells were labeled with pSTAT5 (pY694; BD) or with isotype matched control (Thermo Fisher).

Samples were analyzed on a FACSCanto or LSRII (BD) with FlowJo software (Tree Star) with isotype controls to determine gating and exclude non-specific binding. All cells were stained with a viability dye, either DAPI or 7-AAD when performing analysis of surface markers or with a fixable/viability dye (Invitrogen, BioLegend) for intracellular staining.

2.14 RNA Isolation and Quantitative PCR

Fecal DNA was isolated using QIAamp DNA stool mini kit (Qiagen) and the manufacturer's protocol was followed. Quantitative PCR (QPCR) reactions were set up using SsoFast EvaGreen Super mix (Bio-Rad) with 400 nM of each primer and were run on a Bio-Rad CFX96 machine. RNA was extracted using TRIzol (Invitrogen) in accordance with the manufacturer's instructions. Cells were isolated as described earlier and were resuspended in 800 ml TRIzol. A 160-ml aliquot of chloroform was added, and the tubes were shaken vigorously. The phases were separated by centrifugation at 12,000 × g, 4˚C for 15 min. The aqueous phase

was transferred to a clean tube, and 400 µL isopropanol was added to precipitate the RNA. The tubes were inverted, incubated at room temperature for 10 min, and then were centrifuged at 12,000 × g, 4˚C for 10 min. The RNA was washed with 75% ethanol and then air-dried. The RNA was resuspended in RNase free
H2O and was treated with DNase I (Invitrogen) following the manufacturers' instructions. The RNA was used to synthesize cDNA using the iScript cDNA synthesis kit (Bio-Rad) following the manufacturers' instructions. For the IL-7 QPCR, the cDNA was purified from any unused primers using the QIAquick PCR purification kit (Qiagen). QPCR reactions were set up using SsoFast EvaGreen Super mix (Bio-Rad) with 400 nM of each primer and were run on a Bio-Rad CFX96 machine. The primers used for analysis are listed in Table 2.14

Data were analyzed using the following formula: Fold change = $2^{-\Delta\Delta CT}$, where CT is the number of cycles at which a threshold quantity of amplicon DNA is generated, $\Delta CT = CT_{IL\text{-}7}$ for sample ΔCT_{GAPDH} for sample and $\Delta\Delta CT = \Delta CT_{\text{ for sample}} - \Delta DCT_{\text{ for reference}}$.

2.15 Antibiotics Treatment

To deplete the intestinal microbiota, antibiotics cocktail was given to mice in drinking water *ad libitum* beginning 2-3 weeks prior to the LIP induction until the experimental endpoint. The antibiotics cocktail consisted of ampicillin (0.5 mg/mL), neomycin (0.5 mg/mL), metronidazole (0.5 mg/mL), vancomycin (0.25 mg/mL) and Splenda (4 mg/mL) dissolved in autoclaved water. The cocktail water was sterile filtered before given to mice.

Target	Sequence (5'- 3')	Reference
GAPDH Forward	ACCACAGTCCATGCCATCAC	(Blaeser et al., 2003)
GAPDH Reverse	CACCACCCTGTTGCTGTAGCC	(Blaeser et al., 2003)
IL-7 Forward	GTGCCACATTAAAGACAAAGAAG	(Link et al., 2007)
IL-7 Reverse	GTTCATTATTCGGGCAATTACTATC	(Link et al., 2007)
LTα Forward	CCAGGACAGCCCATCCACT	(Shiu et al., 2015)
LTα Reverse	GTACCCAACAAGGTGAGCAGC	(Shiu et al., 2015)
LTβ Forward	ACCTCATAGGCGCTTGGATG	(Shiu et al., 2015)
LTβ Reverse	ACGCTTCTTCTTGGCTCGC	(Shiu et al., 2015)
16s rDNA Forward	ACTCCTACGGGAGGCAGCAGT	(Barman et al., 2008)
16s rDNA Reverse	ACCGCGGCTGCTGGC	(Barman et al., 2008)

Table 2.14 Sequences of primers used for quantitative PCR

2.16 Statistical Analysis

Statistical analyses were performed using GraphPad Prism software (version 7.0). Data were analyzed using the unpaired students t test. For multiple analyses, ANOVA was used and where significance was found, the Tukey-Kramer multiple comparisons test was used for two-way, and the Bonferroni test was used for one-way ANOVA, for identifying differences between groups. When $P < 0.05$, the statistical difference was considered significant.

Chapter 3: Role of CD45 in extramedullary erythroid development in spleen

3.1 Introduction and Rationale

While bone marrow is known as the primary site of erythropoiesis, extramedullary erythropoiesis occurs in sites such as the spleen, to augment the production of erythrocytes during oxidative stress (Hara and Ogawa, 1976; Socolovsky, 2007). Other physical and immunological stresses such as pregnancy, long-term tumor burden and bacterial infection modeled by both endotoxin injection and Salmonella infection, too, have been reported to increase extramedullary erythropoiesis in spleen (Fowler and Nash, 1968; Jackson et al., 2010; Zhao et al., 2018). In addition, both human and mouse neonates have high rates of splenic erythropoiesis (Elahi et al., 2013; Yan et al., 2018) to accommodate the increasing demands for oxygen elicited by the rapid growth of the body (Finne and Halvorsen, 1972).

Erythroid populations are $CD71^{+}TER119^{+}$ populations including the Pro E and downstream progenitor populations, Ery A and Ery B, and are present in both humans and mice (Elahi et al., 2013; Hermansen, 2001). These populations and the mature RBC, referred to as EryC, can be distinguished based on size and differential expression of the cell surface markers, CD71 and TER119 (Chen et al., 2009). In addition to generating mature RBCs, these erythroid progenitors have been shown to possess immunosuppressive properties (Elahi, 2019). The maturation of the committed erythroid progenitors into mature erythrocytes is regulated by EPO, which drives proliferation and survival of the erythroid progenitor cells (Bouscary et al., 2003; Socolovsky et al., 2001). RPMs also regulate the erythroid development by recycling iron and clearing senescent RBCs through phagocytosis (Schroit et al., 1985). Tissue-resident to the

spleen, RPMs are characterized by the high surface expression of F4/80 and low expression of CD11b (Kohyama et al., 2009).

CD45 is a receptor tyrosine phosphatase expressed on all nucleated hematopoietic cells, which excludes mature RBC (Scheid and Triglia, 1979). However, the precise stage at which erythroid cells lose CD45 expression is unclear. CD45 modulates Lyn and JAK kinase activities (reviewed in (Saunders and Johnson, 2010)) and all have been implicated in EPO signaling (Gillinder et al., 2017; Saunders and Johnson, 2010; Witthuhn et al., 1993). Irie-Sasaki *et al.* showed that CD45 can act as a JAK phosphatase in IL-3 signaling and can negatively regulate EPO-dependent hematopoiesis *in vitro* (Irie-Sasaki et al., 2001). Furthermore, another study which used human $CD34^+$ cells from umbilical cord and a CD45 antibody, NU-L_{PAN}, showed that binding CD45 interrupted EPO induced proliferation, as well as erythroid differentiation to mature erythrocytes (Harashima et al., 2002). Thus, CD45 is implicated in the regulation of erythroid development, yet its impact on specific erythroid progenitors and erythropoiesis *in vivo* remains to be investigated.

In this study, I address the role of CD45 in erythroid maturation mainly in extramedullary erythropoiesis using CD45KO and CD45RAGKO mouse models. To better understand the role of CD45 in this process, I investigated both CD45 expression levels and the effect of CD45 deficiency along the different stages of erythroid maturation.

3.2 Results

3.2.1 CD45-deficient mice have an increased number of erythrocyte progenitors in the spleen

Comparing WT and CD45KO adult mice, as well as RAGKO and CD45RAGKO mice, we observed that the CD45-deficient mice had larger spleen than their CD45-positive counterparts (Fig 3.1A). To confirm this was true, the weight of the spleens from WT, CD45KO, RAGKO and CD45RAGKO were compared and it revealed a significant increase in the weight of the spleens from the CD45-deficient mice (Figure 3.1B). Analysis of the splenocytes revealed significantly more erythroid progenitors in the CD45-deficient mice compared to WT mice, identified by CD71 and TER119 (Figure 3.1C). CD45RAGKO had the greatest accumulation of erythroid progenitors, a ten-fold increase in numbers compared to the RAGKO splenocytes, whereas a five-fold increase was observed in CD45KO splenocytes compared to the WT. As the highest frequency and number of erythroid cells were observed from the CD45RAGKO mice, I decided to use RAGKO and CD45RAGKO to study the role of CD45 in regulating erythropoiesis.

To investigate where CD45 was having its effect, its expression on the specific erythroid populations was first examined by flow cytometry. $CD71^{+}TER119^{+}$ progenitors include the Pro E, Ery A and Ery B populations, whereas the mature RBC lose CD71, and earlier progenitors such as megakaryocyte–erythroid progenitor (MEP) and CFU-E lack TER119 (Figure 3.2A). As shown in figure 3.2B, the expression level of CD45 was high on the TER119- population isolated from the spleen, and 10-fold lower on the Pro E population. CD45 levels gradually diminished further as the cells matured to the EryA population and then to the Ery B population,

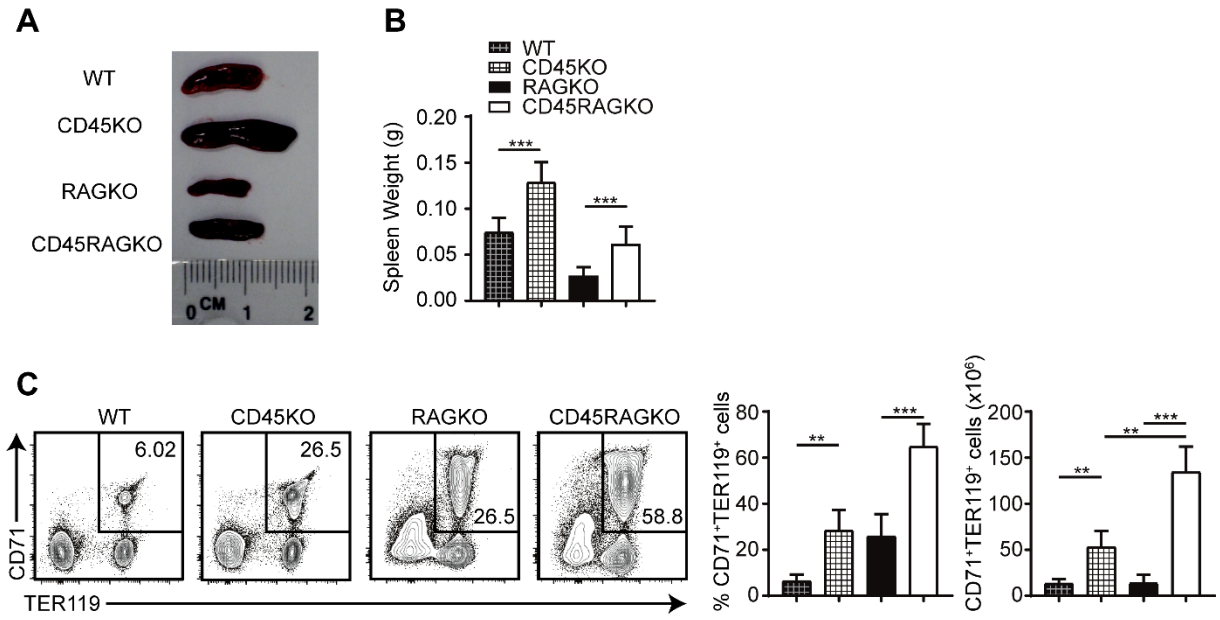

Figure 3.1 CD45-deficient mice have splenomegaly with increased number of erythroid progenitor cells

(A) Representative pictures of spleens from WT, CD45KO, RAGKO, CD45RAGKO mice at steady state. (B) Graph showing weight of spleens, n= 6-16. (C) Representative flow cytometric analysis (left) showing CD71+TER119+ gating from the splenocytes which have been pre-gated for size and live cells. Graphs (right) show pooled data of the frequency and number of CD71+TER119+ erythroid progenitor cells from 2 experiments, n=4-6.

where expression was very low, and finally, as cell matured into the Ery C population, CD45 expression was undetectable (Figure 3.2C). Comparison of these erythroid progenitor populations in the RAGKO and CD45RAGKO mice revealed a significant increase in the percentage and number of the Pro E, Ery A and Ery B populations (Figure 3.2C-D). However, the numbers of earlier progenitors (MEP) and later mature RBC (Ery C) were not significantly different.

3.2.2 CD45 RAGKO mice have more Pro E and Ery A progenitors in the bone marrow

To determine if this increase in erythroid progenitors was specific to the spleen, these progenitors were examined in the bone marrow of RAGKO and CD45RAGKO mice. CD45RAGKO had a greater number of isolated bone marrow cells (Figure 3.3A), as well as higher numbers of Pro E and Ery A populations, but not Ery B populations (Figure 3.3B-C). Numbers of Pro E and Ery A cells were increased 2 and 1.5-fold respectively in the CD45RAGKO bone marrow compared to the RAGKO. This increase was comparable for the Pro E population in the spleen but was not as large as the 5-fold increase for the splenic Ery A population or the 4-fold increase in the splenic Ery B population (Figure 3.2D).

As the CD45RAGKO had equal numbers of mature RBCs (Ery C) at both sites of hematopoiesis, despite the increased number of the progenitors, blood was analyzed to determine if the number of circulating mature erythrocytes was increased. The blood of CD45RAGKO mice had similar numbers of RBC and equivalent hematocrit and hemoglobin levels to that of the RAGKO mice (Figure 3.3D-F), indicating no accumulation of mature RBC in the circulation. In blood of CD45RAGKO mice, only the frequency of the Pro E population was increased (Figure 3.3G).

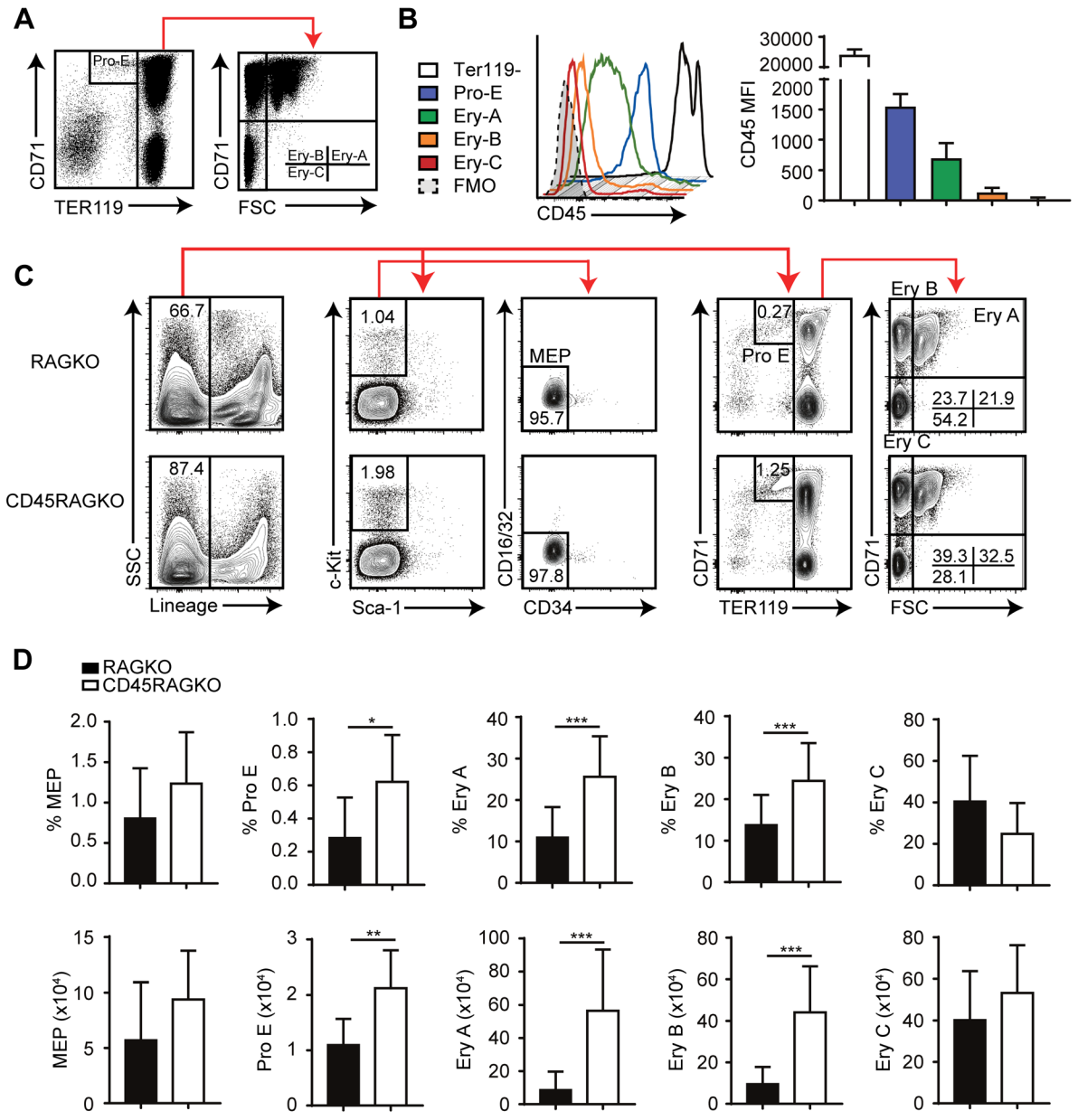

Figure 3.2 CD45RAGKO spleen has increased percentage and number of erythroid progenitors downstream of MEP but equal number of mature erythrocytes

(A) Representative flow cytometry showing the gating on the erythroid populations from Pro E to Ery C. Samples from RAGKO mice are pre-gated for size and live cells. (B) Histogram showing CD45 expression on the different populations of erythroid cells and TER119- cells from the spleen of RAGKO mice. Graphs of the average mean fluorescence intensity of CD45 expression from 2 experiments, n=5. (C) Representative flow cytometry showing the gating strategy used to analyze MEP, Pro E, Ery A, Ery B and Ery C populations in the spleen. Samples are pre-

gated for size and live cells. Lineage markers were CD11c, CD11b, MHCII and F4/80. (D) Graphs show pooled data of the frequency and cell number of MEP, Pro E, Ery A, Ery B and Ery C populations from 4 experiments, n=13-17.

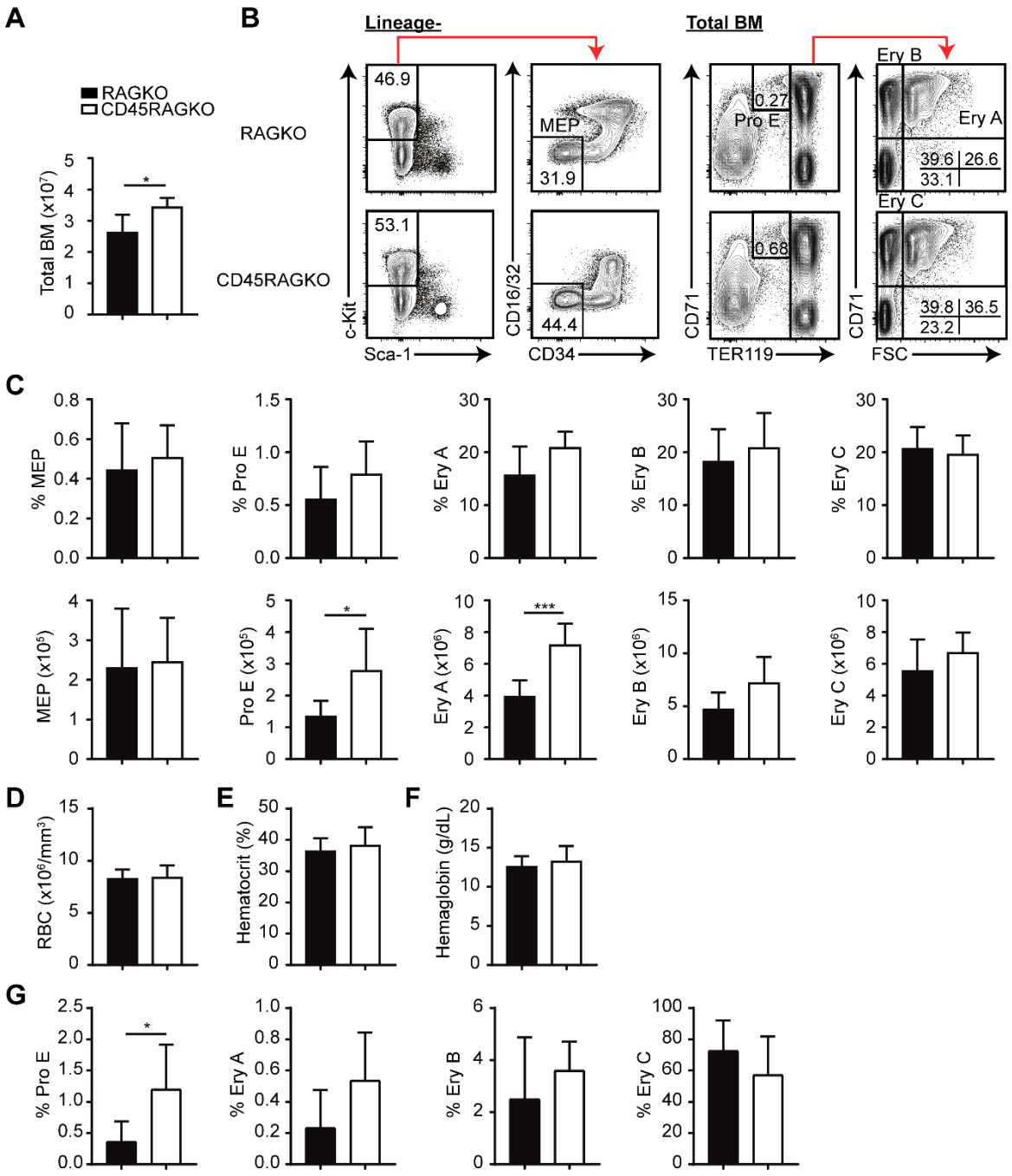

Figure 3.3 CD45RAGKO bone marrows has greater number of Pro E and Ery A progenitors while the number of circulating RBC is equal to the RAGKO

(A) Graph of number of total cells from the BM, n= 6. (B) Representative flow cytometry plots showing the gating strategy used to analyze MEP, Pro E, Ery A, Ery B and Ery C populations in the bone marrows after pre-gating for size and live cells. For MEP, lineage markers were used to exclude cells for analysis (Lineage$^-$) and were CD11c,

CD11b, MHCII and F4/80. (C) Graphs show pooled data of the frequency and cell number of MEP, Pro E, Ery A, Ery B and Ery C populations from 2 experiments, n=6. (D-F) Graph showing number of RBCs, hematocrit and hemoglobin in blood samples analyzed by hematology analyzer (scil Vet abc) pooled from 2 experiments, n=6-7 (G) Graphs show pooled data of the frequency of MEP, Pro E, Ery A, Ery B and Ery C populations in blood from 2 experiments, n=7.

3.2.3 CD45RAGKO mice retain the high level of erythroid progenitors observed in neonatal and juvenile mice

To begin to understand why the progenitor population was increased in CD45-deficient mice, I looked at younger mice where this population is more prevalent. At week 3, just after weaning, over 80% of the splenocytes were $CD71^{+}TER119^{+}$ erythroid progenitors, and similar numbers (approximately 200 million) were present in both RAGKO and CD45RAGKO spleens (Figure 3.4A-B). However, by 6 weeks of age, the percentage of $CD71^{+}TER119^{+}$ erythroid progenitors had dropped to 26 % of splenocytes (14 million cells) in the RAG mice, but to only 60% (140 million cells) in the CD45RAGKO mice. At 12 weeks, this significant difference in erythroid progenitors in the CD45RAGKO mice was maintained, indicating an inability to downregulate the erythroid progenitor pool. The cell number of $CD71^{-}TER119^{+}$ cells was equal between the RAGKO and CD45RAGKO mice in all the ages that were tested (Figure 3.4A-B).

3.2.4 Erythroid progenitors in the CD45RAGKO spleen are more proliferative and more apoptotic *in vivo*

One possible explanation for the increase in erythroid progenitors in CD45RAGKO spleen was an increase in proliferation: to investigate the proliferative state of these progenitors, mice were injected i.p. with EdU, a thymidine analogue, to identify cells that have undergone replication, and spleens were removed 2 h later for analysis. In the RAGKO, the most rapidly proliferating cells were the Ery A population with ~80% of the cells incorporating EdU in the 2 h period, followed by the Pro E population at ~40%, and the Ery B population at 20% (Figure 3.5A). Both the CD45RAGKO Pro E and Ery A populations showed an increased

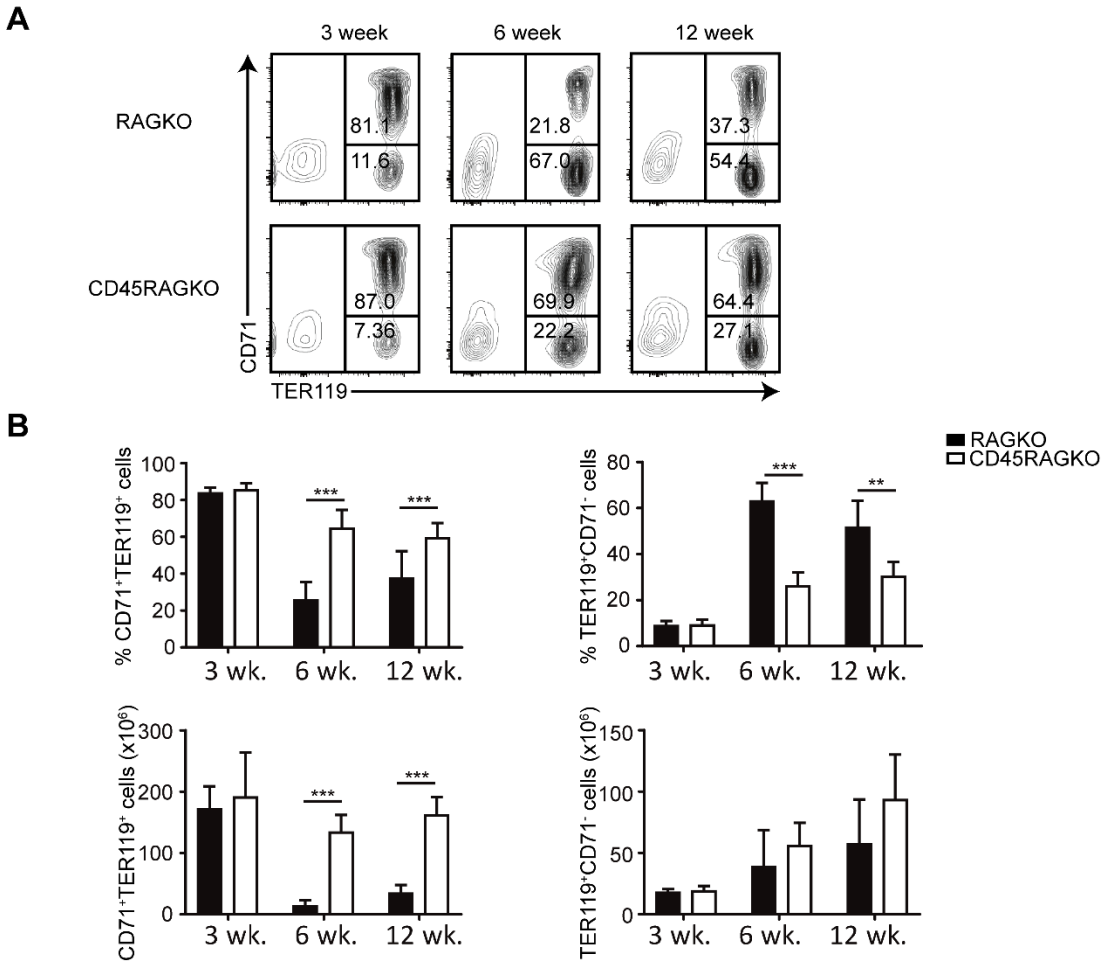

Figure 3.4 A high percentage and number of CD71$^+$TER119$^+$ cells are maintained in CD45RAGKO spleen over time

(A) Representative flow cytometry plots showing gating of the erythroid progenitors (CD71$^+$TER119$^+$) and mature erythrocyte (CD71$^-$TER119$^+$) populations from the spleens of mice at 3, 6, and 12 weeks of age. Samples are pre-gated for size and live cells. (B) Graphs show pooled data of the frequency and cell number from 2 sets of experiments for each age group, n=6-7.

proliferative rate compared to their RAGKO counterparts, whereas no significant difference in EdU incorporation was observed in the less proliferative Ery B population (Figure 3.5). These data indicate a higher proliferation rate in the CD45-deficient Pro E and Ery A populations.

To determine why increased proliferation in the $CD71^{+}TER119^{+}$ erythroid progenitors was not giving rise to an increased Ery C population, their apoptotic potential was examined by measuring caspase 3/7 activity using the FLICA660 reagent. The CD45RAGKO $CD71^{+}TER119^{+}$ population was significantly more apoptotic than the same population from the RAGKO spleen (Figure 3.6A). Fas and FasL expression on $CD71^{+}TER119^{+}$ cells was also compared since the homeostatic pool size of the erythroid progenitors in the bone marrow is regulated by their expression (De Maria et al., 1999). Fas and FasL expression were low on these progenitors and no difference in the percentage of Fas or FasL expressing cells was observed. However, on the few cells that were positive for FasL, their expression was higher on the CD45RAGKO progenitors (Figure 3.6B). In addition, the CD45RAGKO $CD71^{+}TER119^{+}$ progenitor cells had lower expression of the cell survival signaling molecule, Bcl-2, compared to the RAGKO erythroid cells (Figure 3.6C).

3.2.5 CD45RAGKO mice have increased RPMs and EPO levels in the spleen and their erythroid progenitors are hypersensitive to EPO

To investigate how the $CD71^{+}Ter119^{+}$ erythroid progenitors (ProE, Ery A and Ery B) were able to expand and contract in the absence of CD45, I focused on EPO and EPO signaling. The measurement of EPO levels in the spleen, plasma and kidney (a major source of EPO) revealed similar levels of EPO in the plasma and kidney, but a significant increase in EPO in the spleen of CD45RAGKO mice compared to RAGKO mice (Figure 3.7A-B). This increase was

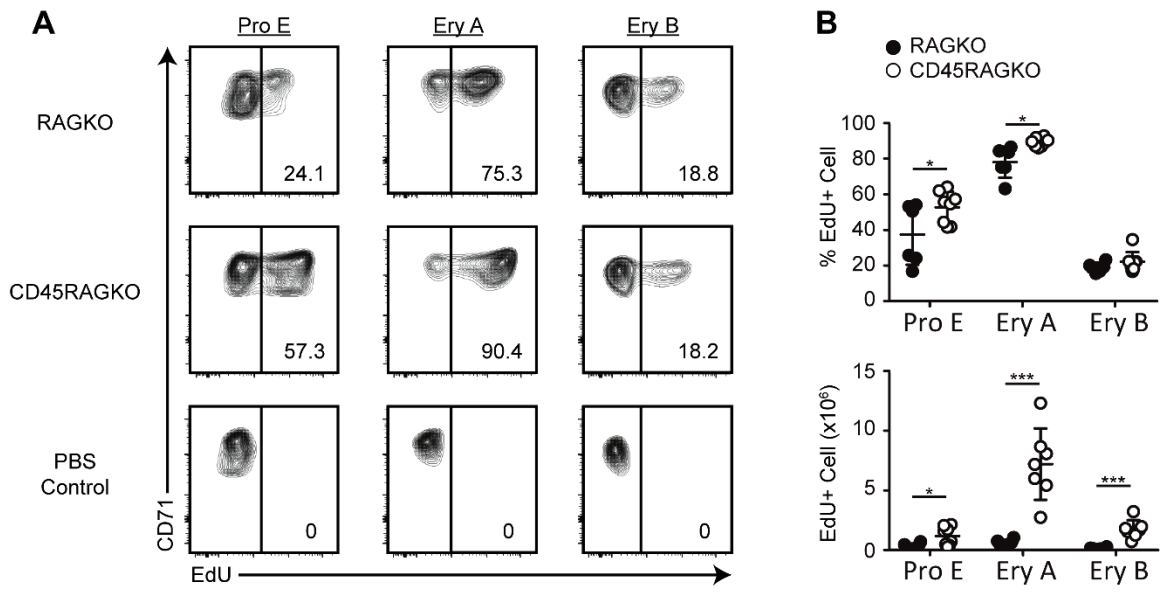

Figure 3.5 Splenic CD45RAGKO Pro E and Ery A populations show increased proliferation

EdU was injected i.p. into mice 2 h prior to spleen harvest. Splenic cells were isolated and labeled for surface markers and the ClickIT reaction was performed to detect EdU uptake. (A) Representative flow cytometry plots of EdU uptake by Pro E, Ery A and Ery B populations. (B) Graphs show pooled data of the frequency and cell number of cells that have taken up Edu from 2 experiments, n=6-8.

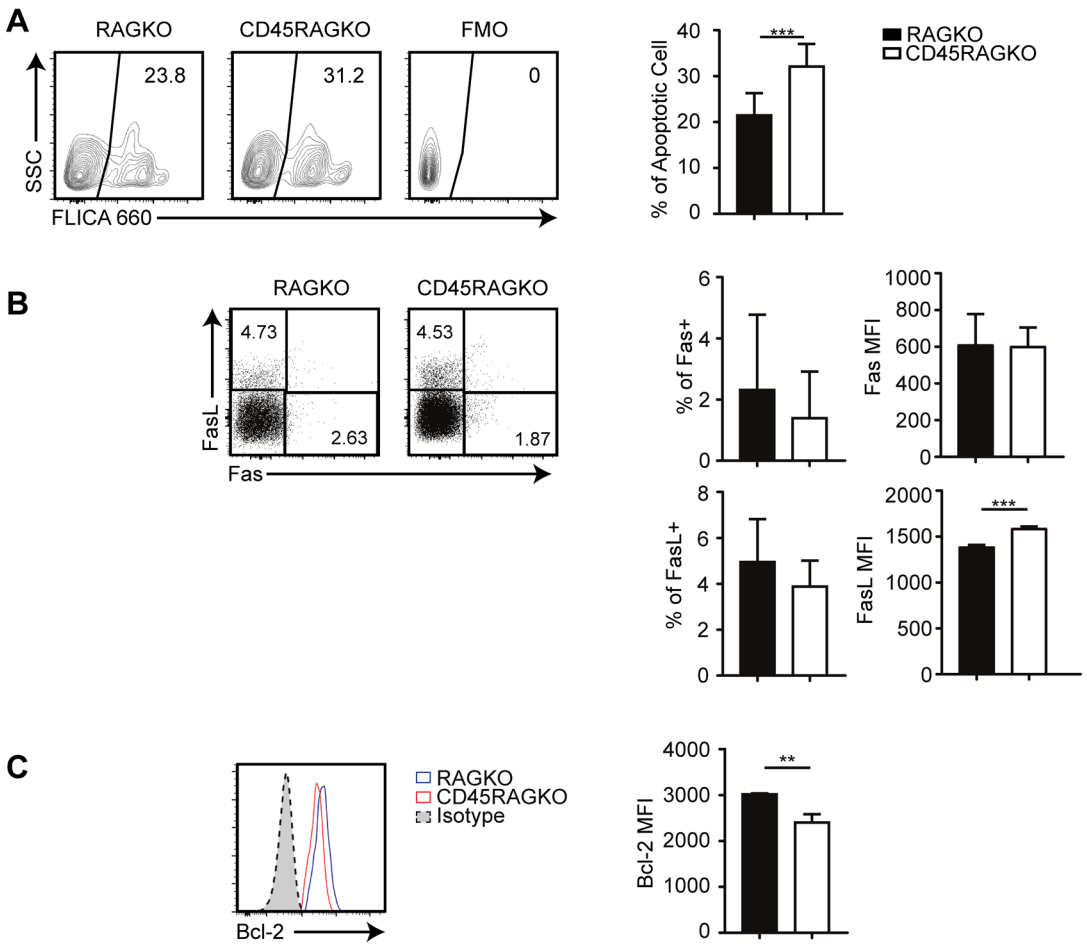

Figure 3.6 Splenic CD45RAGKO CD71$^+$TER119$^+$ erythroid progenitors are more apoptotic

(A) Splenocytes were labeled with FLICA660 and Caspase-3/7 activity from CD71$^+$TER119$^+$ cells was measured by flow cytometry. Cells were pre-gated for size and live cells, then gated on the CD71$^+$TER119$^+$ population. Cells which were not treated with FLICA660 reagent were used as a negative control for gating. Graph shows data pooled from 2 experiments, n=8. (B) Flow cytometry plots and graphs of FasL and Fas expression on CD71$^+$TER119$^+$ cells. Graph of frequency shows pooled data and graph of MFI shows representative (n=4) from 2 experiments, total n=7-8. (C) Representative histogram comparing Bcl-2 expression on CD71$^+$TER119$^+$ cells from the spleens of the indicated mouse strains. Graph shows representative data from 2 experiments, n=6-7.

observed both when the total level of EPO in the spleen and the level of EPO per mg of spleen were compared (Figure 3.7C). This provides one explanation for the expansion of the erythroid progenitors in the CD45-deficient spleens. To try and understand how CD45 could impact EPO production in the spleen, RPM were examined since they have been reported to produce EPO upon exposure to high S1P in blood (Bode et al., 2010; Luo et al., 2016). These RPMs represented about 10% of the splenic population in both RAG and CD45RAGKO mice, however, due to its larger size, there were approximately three-fold more RPMs in the CD45RAGKO spleen (Figure 3.7D). This meant that despite a slightly lower percentage of EPO producing RPMs in the CD45RAGKO assessed by intracellular staining (40% compared to 50% for RAGKO RPM), the total number of EPO positive CD45RAGKO RPM was significantly higher (Figure 3.7E), providing an explanation for the increased EPO levels in the spleen.

Next, the response to EPO by the erythroid progenitors was examined. There were no significant differences in the percentage of erythroid progenitors expressing the EPO receptor, or in the levels of EPO receptor expression within the erythroid progenitor populations, between CD45RAGKO and RAGKO spleens (Figure 3.8A-B). EPO receptor levels were the highest in the Ery A population, consistent with this population being the most proliferative. To determine whether there were differences in EPO signaling from the receptor, splenic erythroid cells were isolated from RAGKO and CD45RAGKO mice and starved for 3 h in fresh RPMI without EPO prior to *in vitro* stimulation with EPO, then STAT5 phosphorylation was monitored over 2 hrs. pSTAT5 was higher in the CD45RAGKO Ery A population compared to the RAGKO Ery A population, at both the 30 min and 1 h time points (Figure 3.8C-D). The level of pSTAT5 expression compared by MFI normalized to the unstimulated controls was higher in the CD45RAGKO Ery A cells than the RAGKO Ery A cells after 30 min of EPO stimulation,

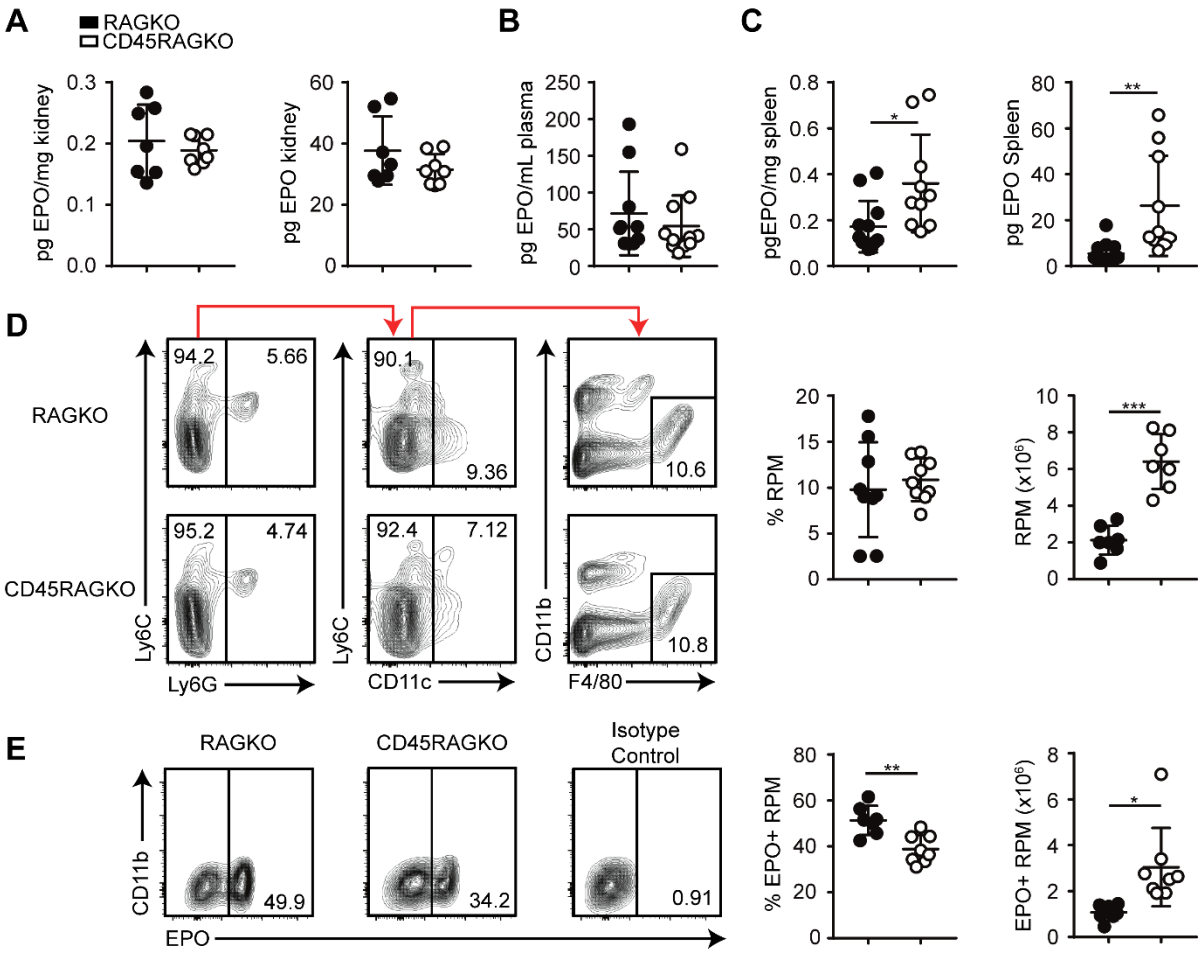

Figure 3.7 CD45RAGKO mice has increased EPO and RPMs in the spleen

Kidneys and spleens were homogenized for protein extraction and EPO was measured by ELISA. (A) Graphs show EPO/mg of kidney and total amount of EPO. Data pooled from 2 experiments, n=7-8. (B) Plasma from blood was analyzed for EPO using ELISA. Graph pooled data of EPO concentration in plasma from 3 experiments, n=10-13. (C) Graphs show amount of EPO/mg spleen and total EPO in spleens, measured by ELISA. Data pooled from 3 experiments, n=11-12. (D) Representative gating strategy used for flow cytometric analysis of RPMs in the collagenase-digested spleens of RAGKO and CD45RAGKO mice after pre-gating for size and live cells. Graphs (right) showing frequency and number of RPMs in spleens. Data was pooled from 2 experiments, n= 7-9. (E) Representative staining of EPO in the RPMs after 4hr incubation with brefeldin A. Graphs show frequency and number of EPO+ RPMs in spleens. Data was pooled from 2 experiments, n= 7-9.

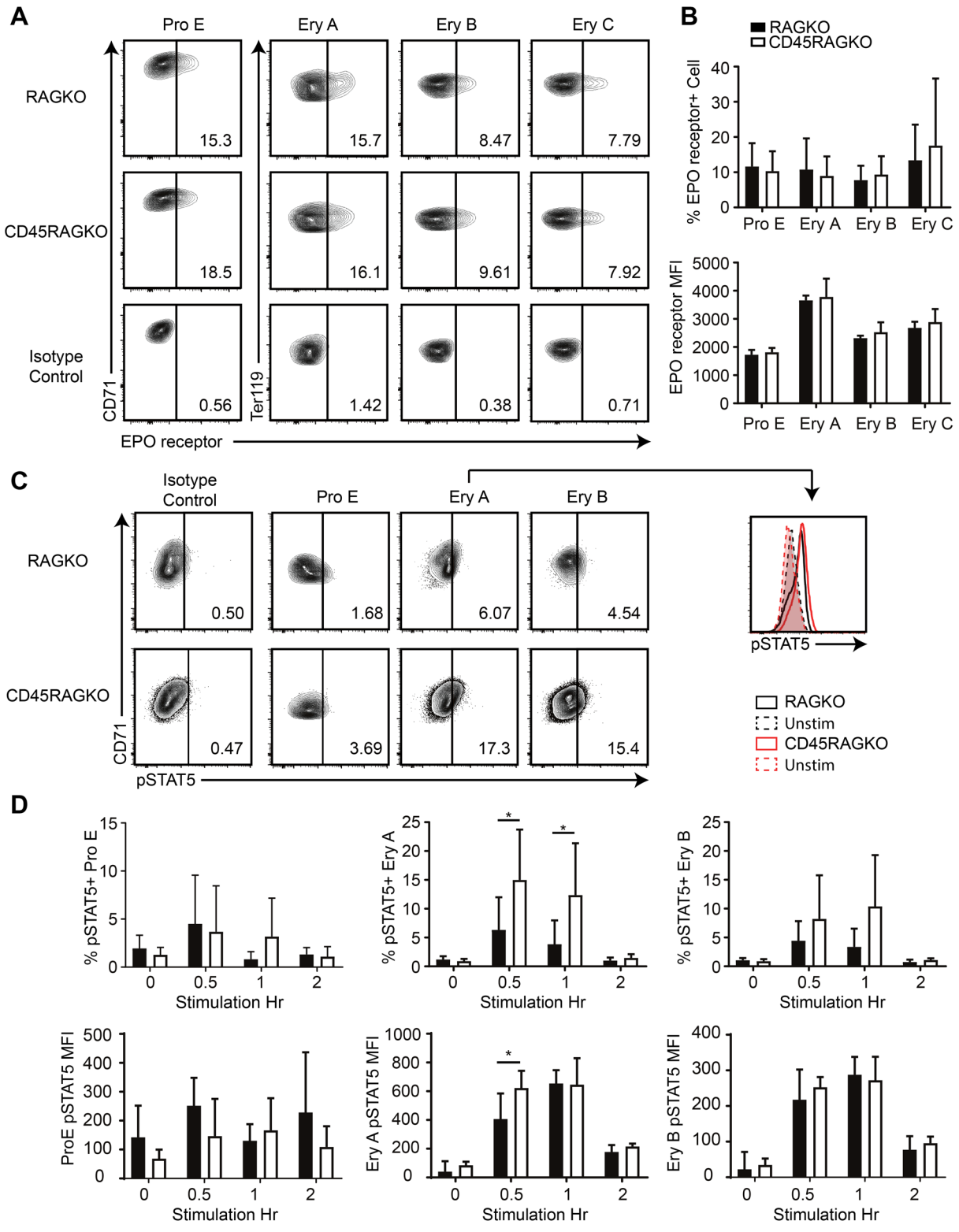

Figure 3.8 The CD45RAGKO Ery A population is hyper-responsive to EPO stimulation

(A) Representative flow cytometry plots of EPO-R expression on ProE, Ery A, Ery B and Ery C populations. (B) Graphs show pooled data of frequency and MFI of EPO-R expression on ProE, Ery A, Ery B and Ery C populations from 2 experiments, n=7-8. (C) Splenocytes were harvested and starved in unsupplemented RPMI for 2hr at 37°C followed by stimulation with 100 pg/mL EPO for various times before pSTAT5 measurement by intracellular staining and flow cytometry. For each of Pro E, Ery A and Ery B populations, gating was determined by analyzing isotype control sample. Flow cytometry plots of the Isotype control shown are representative of Ery A population. Historam shows the level of pSTAT5 expression in Ery A populations after 30 min of EPO stimulation compared to unstimulated controls. (D) Top graphs show data pooled from 2 experiments, n=7-8. Bottom graphs show representative data from one of the two experiments, n=4.

indicating a hypersensitive response to EPO in the CD45-deficient Ery A population.

3.3 Discussion

Here, I have provided *in vivo* evidence for a role for CD45 in the regulation of erythroid progenitors, especially the Pro E to Ery B stages, with the biggest effect observed in the Ery A population ($CD71^{+}TER119^{+}$, high FSC). In the absence of CD45, mature CD45RAGKO mice failed to downregulate erythroid progenitor cell numbers in the spleen from neonatal levels, resulting in the accumulation of Pro E, Ery A and Ery B populations without any overt signs of anemia. Further investigation revealed an effect of CD45 on regulating RPM numbers and EPO levels in the spleen, as well as the negative regulation of EPO signaling in the EryA progenitors, which together, explain the accumulation of the $CD71^{+}TER119^{+}$ erythroid progenitors *in vivo.*

While the absence of CD45 expression on mature RBC was known (Scheid and Triglia, 1979), exactly when CD45 was downregulated during erythroid development was unknown. The results presented here demonstrate that the Pro E population express a lower level of CD45 compared to other $CD45^{+}$ $TER119^{-}$ cells in the spleen. CD45 expression was further reduced in the Ery A population compared to the Pro E population and reduced further in the Ery B population and absent from the Ery C population. The loss of CD45 affected the ProE, Ery A and EryB populations, which expressed decreasingly low levels of CD45, however, the biggest impact was observed on the highly proliferative Ery A population.

Increased numbers of Pro E and Ery A populations were also observed in the bone marrow of CD45RAGKO mice, whereas the number of the earlier MEP progenitors was unchanged in both the spleen and bone marrow. This suggests that the effect of CD45 is occurring downstream of the MEP progenitors. The MEP progenitors are KIT^{+} and proliferate in

response to SCF, which signals via the PI3K/AKT pathway (Sanchez et al., 2006; Wang et al., 2008), and this signaling pathway may be less affected by the loss of CD45. The downstream erythroid progenitors depend on EPO for their proliferation (Bouscary et al., 2003) and this is where the impact of CD45 was observed. Pro E, Ery A and Ery B populations expressed the EPO receptor, with the highest level of expression observed on the Ery A population. Accordingly, the Ery A population was the most proliferative *in vivo* and their proliferation was enhanced in the CD45RAGKO mice.

A greater effect of CD45 was observed on the erythroid progenitors in the spleen than the bone marrow. This may be due to the increased EPO levels in the CD45RAGKO spleen, attributed to the increased number of RPM present in the CD45RAGKO spleen. EPO levels were equal in the plasma and kidney between CD45RAG and RAGKO mice, suggesting that circulating levels were similar. However, I have not specifically measured EPO levels in the bone marrow, as EPO mRNA has been reported to be undetectable in the bone marrow, even after exposure to hypoxia (Tan et al., 1991). Since comparable number of RBCs, and comparable levels of hematocrit and hemoglobin were observed in the blood of CD45RAG and RAGKO mice, hypoxia or anemia, which increase extramedullary erythropoiesis, are unlikely to be contributing factors to the CD45RAGKO phenotype.

Unlike the RAGKO mice which downregulated the high number of erythroid progenitor cells present in neonatal and juvenile mice as they matured, CD45RAGKO mice consistently produced high levels of $CD71^{+}TER119^{+}$ erythroid progenitors from 3 weeks through to 12 weeks, suggesting an inability to downregulate the erythroid progenitor pool as the mice mature into adults. A higher number of reticulocytes is also observed in human neonates during the first 3 months after birth compared to adults (Kling et al., 1996). However, what downregulates the

number of reticulocytes as infants mature is unclear. A rat study showed a drastic reduction in the concentration of EPO during the first 3 weeks after birth with a corresponding reduction in EPO transcription from the kidney (Eckardt et al., 1992), suggesting that changes in erythropoiesis during development may be regulated by the abundance of EPO. High numbers of these $CD71^{+}TER119^{+}$ progenitor cells in neonates are associated with immunosuppressive activity both *in vitro* and *in vivo* in animal infection models (Elahi, 2019). Although beyond the scope of this study, it will be of interest to determine if this large progenitor population in the CD45-deficient mice is also immunosuppressive.

The reason for the increased number of RPMs in the CD45RAGKO spleen is not known but may just reflect the overall increase in cell numbers from the larger spleen. Alternatively, increased numbers may arise in response to the increase in apoptotic erythroblasts, as I showed that the $CD71^{+}TER119^{+}$ population was not only more proliferative in the CD45RAG spleen, but also more apoptotic. The phagocytosis of RBC, and heme in particular, by monocytes activates the expression of SPI-C, a signature transcription factor for RPMs that drives the maturation of monocytes into RPMs (Haldar et al., 2014; Kohyama et al., 2009). Therefore, it is possible that the increased number of apoptotic erythroid progenitor cells in the CD45RAGKO spleen may lead to an increased number of RPMs, thereby creating a feedback loop between the erythroid cells and the RPMs. The detection of intracellular EPO in the RPMs identified RPMs as a source of EPO in the spleen, consistent with their role in erythroid maturation (Rhodes et al., 2016). Macrophages are known to produce EPO in response to S1P released by dying cells, which activates hypoxia-induced factor-1α and induces EPO as well as EPO receptor expression (Luo et al., 2016). RPMs may also produce EPO in response to continual exposure to S1P, which is stored in RBC and prevalent in the blood (Hanel et al., 2007).

The Pro E, Ery A and Ery B populations all expressed the EPO receptor and proliferated *in vivo* (Ery A > Pro E > Ery B), consistent with EPO providing proliferation and survival signals for erythroid progenitors (Bouscary et al., 2003; Socolovsky et al., 2001). Greater *in vivo* proliferation of the Pro E and Ery A populations in the CD45RAGKO spleen was attributed to, at least in part, an increased sensitivity to EPO as demonstrated *in vitro* by increased pSTAT5 signaling, despite expressing equal levels of the EPO receptor. This *in vivo* demonstration of CD45 negatively regulating EPO signaling and proliferation supports an earlier study showing that CD45 negatively regulates EPO-dependent hematopoiesis *in vitro,* where CD45 was identified as a JAK phosphatase (Irie-Sasaki et al., 2001). However, CD45 can also regulate the Src family kinase, Lyn (Saunders and Johnson, 2010), which along with JAK2 (Witthuhn et al., 1993), regulates EPO signaling and proliferation (Slavova-Azmanova et al., 2014). Erythropoiesis was affected in both LynKO (Ingley et al., 2005; Slavova-Azmanova et al., 2014) and $Lyn^{up/up}$ mice (Slavova-Azmanova et al., 2013), with both mice showing more complex phenotypes than the CD45-deficient mice. The LynKO $CD71^{+}TER119^{+}$ erythroid progenitors showed increased pSTAT5 in response to EPO stimulation, with increased apoptotic activity (Slavova-Azmanova et al., 2014), but the mice only showed an accumulation of erythroid progenitor cells in the spleen at around 16 week of age (Harder et al., 2004). Unlike CD45RAGKO mice, the $Lyn^{up/up}$ mice showed signs of anemia with reduced hematocrit and circulating RBCs, and the $CD71^{+}$ erythroid cells isolated from the spleen did not show increased pSTAT5 in response to EPO signaling. CD45 may therefore modulate EPO signaling and STAT5 phosphorylation by affecting both Lyn and JAK kinase activities.

Chapter 4: Immunosuppressive Activity of Erythroid Cells in T cell Colitis

4.1 Introduction and Rationale

IBD arises when tolerance is lost towards innocuous antigens derived from microbes, food and self, leading to a chronic inflammatory condition that causes severe damage to the intestinal tissues. This can lead to further infiltration of microbes into host tissues and exacerbation of the inflammatory response, ultimately manifesting as hemorrhage, rectal bleeding, weight loss and in some cases, death. IBD is not only restricted to the intestine, but also leads to systemic inflammation and may cause complications such as cachexia and anemia (Cronin and Shanahan, 2005; Danese and Fiocchi, 2011; Peyrin-Biroulet et al., 2016).

To investigate the role of CD45 in inflammation, our lab has previously studied the role of CD45 in an acute model of colitis using DSS and found that CD45 had opposing functions on T cells and myeloid cells (Samarakoon et al., 2016). CD45 on T cells plays an inhibitory role in colitis development by negatively regulating T cell homing to the gut and inflammatory cytokine production by the T cells in the colon, whereas CD45 on innate immune cells contributed to pathogenesis by promoting GM-CSF and retinoic acid production, which enhance inflammation and T cell homing to the gut (Samarakoon et al., 2016).

Here, I investigate the role of CD45 in a chronic model of inflammation by using T cell transfer colitis in RAGKO and CD45RAGKO mice induced by transfer of WT T cells. This model was chosen since it allowed me to focus on the role of CD45 on nonlymphoid cells. Also, as described in chapter 3, I have found that CD45 deficiency results in an increased number of $CD71^{+}TER119^{+}$ cells, which have been reported to be immunosuppressive. Therefore, I wanted to investigate whether the increased $CD71^{+}TER119^{+}$ population impacts the inflammatory

response in CD45-deficient mice using a model where inflammation in the intestinal and extraintestinal sites can be compared separately.

The T cell transfer model of colitis involves the transfer of $CD25^{-}CD45RB^{high}CD4^{+}$ T cells, which are enriched for naïve T cells and depleted of T_{Reg}, into lymphopenic mice such as RAGKO (Powrie et al., 1993). In the lymphopenic environment and in the absence of T_{Reg}, the transferred T cells proliferate and become activated and colitogenic in response to microbial antigens (Feng et al., 2010). As the development of IBD progresses, leukocyte infiltration leads to severe inflammation, ulceration, loss of architecture of the intestine, along with signs of weakness, dehydration and wasting. The most prominent T cell response is Th1 and Th17 with the production of inflammatory cytokines such as IFNγ, TNFα, IL-17 and IL-23. Normally, T_{Reg} cells would prevent colitis through their immunosuppressive activity, such as production of anti-inflammatory cytokines, IL-10 and TGFβ (Groux et al., 1997; O'Connor et al., 2009; Powrie et al., 1994). In addition to the role of T cells, intestinal myeloid cells, including dendritic cells (DCs) and macrophages, and their cytokines have also been implicated in regulating and perpetuating inflammation (Ahern et al., 2008; Coombes and Powrie, 2008). In inflammation, macrophages produce various pro-inflammatory mediators such as TNFα, IL-6, and IL-1β (Rivollier et al., 2012), which can propagate T cell responses.

Here, I aim to study the impact of CD45 deficiency on T cell transfer colitis to investigate a role of CD45 on myeloid cells regulating intestinal and extraintestinal inflammatory responses in colitis. Also, I wanted to assess if the accumulation of $CD71^{+}TER119^{+}$ cells in the CD45-deficient RAGKO creates an immunosuppressive environment. Therefore, I further aim to study the impact of increased erythroid progenitors on the outcome of T cell transfer colitis.

4.2 Results

4.2.1 CD45RAGKO have delayed weight loss in response to T cell transfer colitis despite having comparable intestinal inflammation

CD45 regulates proinflammatory cytokine production by *in vitro* derived DCs in a TLR dependent manner (Cross et al., 2008), and its presence on innate immune cells promotes pathology in an acute model of colitis induced by DSS (Samarakoon et al., 2016). Here, the impact of CD45 on myeloid cells in a chronic model of colitis was assessed using the T cell transfer model, where the T cells are CD45-sufficient. Wild-type $CD45^{+}CD4^{+}CD25^{-}CD45RB^{high}$ T cells were isolated and injected into RAGKO and CD45RAGKO mice housed in a specific pathogen-free animal unit that was positive for *Helicobacter*.

Upon the induction of T cell colitis, CD45RAGKO mice showed no weight loss compared to the RAGKO mice over the time points of the experiment (Figure 4.1A). The microbial status of mice in particular animal units can accelerate disease and the presence *Helicobacter hepaticus* in RAGKO mice has been well described to accelerate weight loss in response to colitis (Kullberg et al., 2003; Kullberg et al., 2002). During the course of this study, colitis was induced in RAGKO and CD45RAGKO mice from two other animal units, one of which was complete specific pathogen free (Figure 4.1B-C). In all three units, although the onset of weight loss varied between units, there was always less weight loss in the CD45RAGKO mice compared to the RAGKO mice. When the mice were monitored over a longer time course in one unit (Figure 4.1B), the CD45RAGKO mice did eventually start to lose weight. Together, a consistent difference in the onset and weight loss was observed from CD45RAGKO mice compared to RAGKO mice after the induction of T cell-induced colitis, and this was not dependent on the presence or absence of *Helicobacter*.

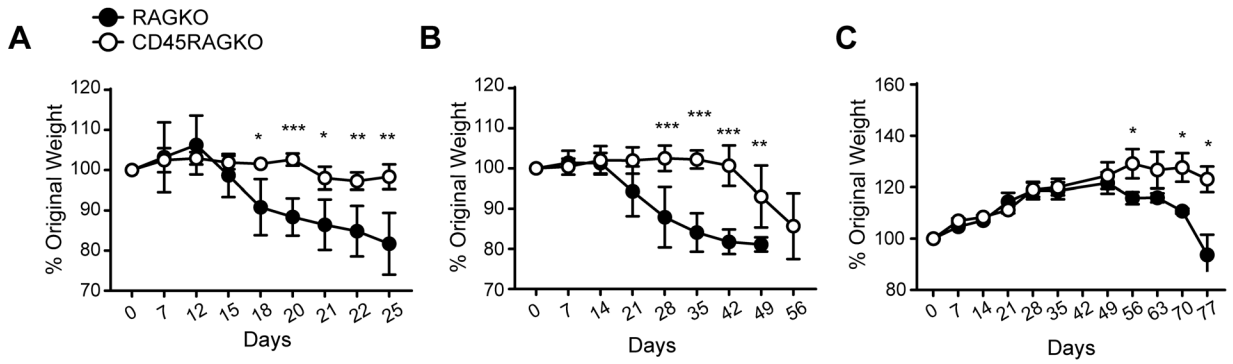

Figure 4.1 CD45RAGKO mice have delayed weight loss from the induction of T cell transfer colitis

T cell transfer colitis was induced by injecting 4×10^5 $CD4^+CD25^-CD45RB^{high}$ T cells from C57Bl/6 mice interperitoneally into RAGKO and CD45RAGKO mice. Weight change after the induction of colitis is shown. The mice were weighed every 3-7 days and representative data from at least 2 experiments is shown. (A) UBC Modified Barrier Facility, where the facility is SPF except for *Helicobacter pylori*, n=4. (B) UBC Wesbrook Animal Unit, where the facility is SPF except for *Helicobacter pylori* and *Spironucleus,* n=6-7. (C) Containment Level 1 of the UBC Centre for Disease Modeling Mice, SPF facility where the mice were rederived and free of *H. pylori* and *Spironucleus,* n=5-6.

In mouse models of colitis, weight loss is commonly used as an indicator of intestinal inflammation and therefore a decrease in gut inflammation in the CD45RAGKO mice compared to RAGKO mice was expected. However, at the endpoint for the RAGKO mice, the severity of intestinal inflammation in the CD45RAGKO was comparable to the RAGKO mice, as assessed by colon histology, intestinal weight/length and leukocyte infiltration (Figure 4.2A-D). Although the percentage of T cells was slightly lower in the CD45RAGKO colon, T cell numbers were not significantly different (Figure 4.2E). CD45 deficiency did not affect the percentage or number of IFNγ or IL-17A expressing T cells in the intestine, nor did it alter the number of Foxp3+ T regulatory cells (Figure 4.2F). There was also no significant difference in total TNFα produced from colon explants (Figure 4.2G). In addition, isolation of cells from the lamina propria and stimulation with PMA and ionomycin for 4-6 h in the presence with brefeldin A did not lead to any differences in TNFα production (Figure 4.2H). These results demonstrate that overall, CD45RAGKO mice have comparable intestinal inflammation to RAGKO mice, despite exhibiting differences in weight loss.

4.2.2 CD45RAGKO spleens do not have less inflammatory IFNγ and IL-17A expressing T cells

After observing comparable intestinal inflammation between the RAGKO and CD45RAGKO mice, we hypothesized that the lack of weight loss observed from the CD45RAGKO mice may be due to a lower systemic inflammatory response with less inflammatory T cells in the spleen and periphery. CD45-deficient mice were previously observed to have larger spleens, partly attributed to increased erythroid progenitors, and a comparison of total splenocytes also showed this to be the case following induction of colitis (Figure 4.3A).

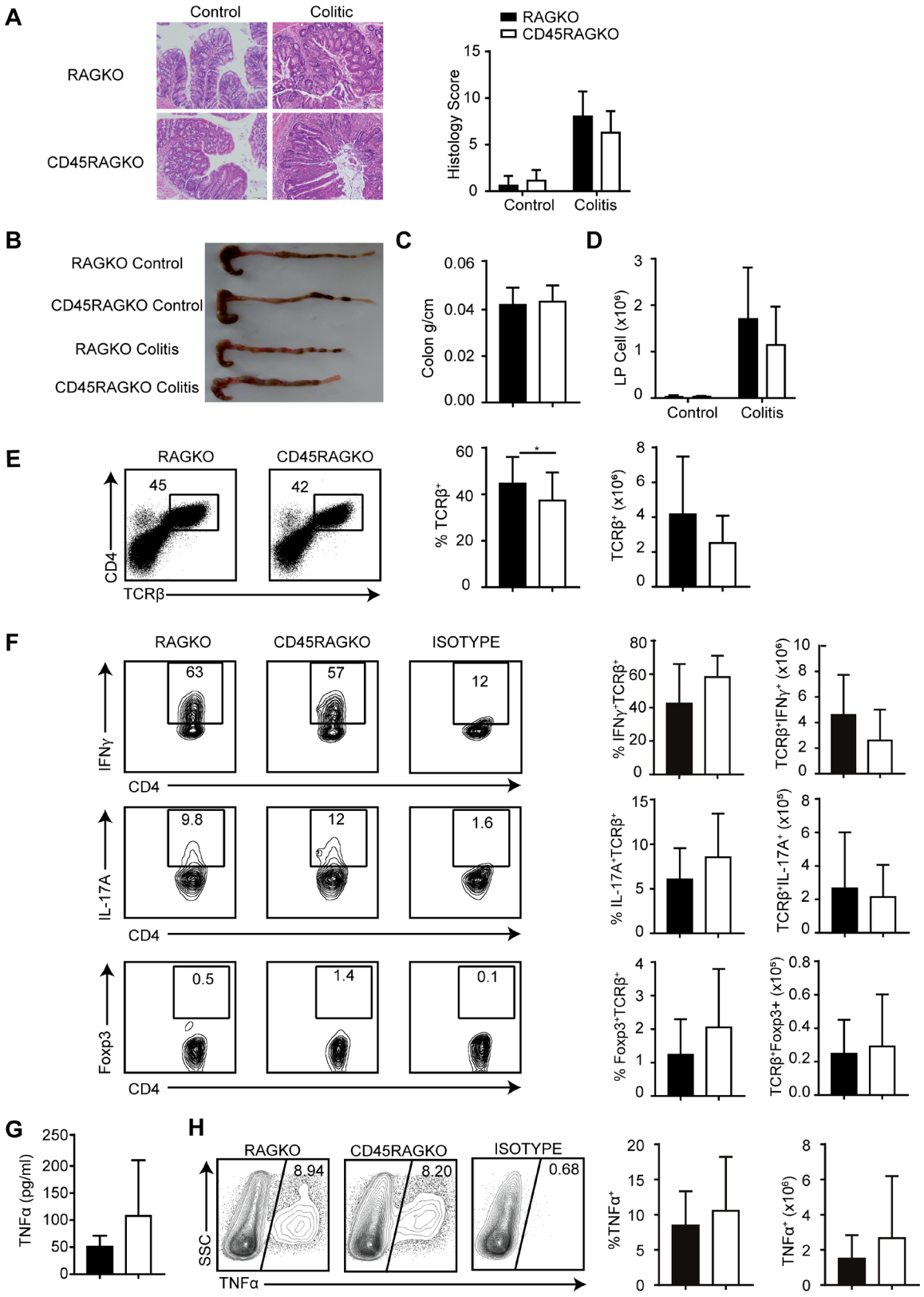
A
Control
Colitic
RAGKO
CD45RAGKO
RAGKO
CD45RAGKO
Histology Score
Control
Colitis
B
RAGKO Control
CD45RAGKO Control
RAGKO Colitis
CD45RAGKO Colitis
C
Colon g/cm
D
LP Cell (x10⁶)
Control
Colitis
E
RAGKO
CD45RAGKO
45
42
CD4
TCRβ
% TCRβ⁺
TCRβ⁺ (x10⁶)
F
RAGKO
CD45RAGKO
ISOTYPE
63
57
12
IFNγ
CD4
9.8
12
1.6
IL-17A
CD4
0.5
1.4
0.1
Foxp3
CD4
% IFNγ⁺TCRβ⁺
TCRβ⁺IFNγ⁺ (x10⁶)
% IL-17A⁺TCRβ⁺
TCRβ⁺IL-17A⁺ (x10⁵)
% Foxp3⁺TCRβ⁺
TCRβ⁺Foxp3+ (x10⁵)
G
TNFα (pg/ml)
H
RAGKO
CD45RAGKO
ISOTYPE
8.94
8.20
0.68
SSC
TNFα
%TNFα⁺
TNFα⁺ (x10⁶)

Figure 4.2 CD45RAGKO mice have comparable intestinal inflammation

(A) Representative rectal colon cross-sections of control and colitis RAGKO and CD45RAGKO mice at the RAGKO endpoint stained with hematoxylin and eosin. The histology scores prior to and post colitis at the RAGKO endpoint of RAGKO and CD45RAGKO mice, n=10-17. Data was pooled from at least 3 independent experiments. (B) Representative pictures of the large intestine of control and colitis mice at the RAGKO endpoint. (C) Colon weight/length of RAGKO and CD45RAGKO mice at the RAGKO endpoint, as described in Material and Methods. The data was pooled from at least 2 experiments, n=5-12. (D) Total cell numbers in the colon prior to and after induction of colitis at the RAGKO endpoint. Data was pooled from at least 3 experiments, n=10-27. (E) Representative flow cytometry plots showing the gating for $TCR\beta^{+}CD4^{+}$ cells in the colon of mice post colitis induction at the RAGKO endpoint after pre-gating for size and live cells. Graphs show T cell frequency and cell number post colitis at the RAGKO endpoint. Data was collected from 2 experiments, n=17-33. (F) Representative flow pots of IFNγ, IL-17A and Foxp3 expression in the $TCR\beta^{+}CD4^{+}$ population after induction of colitis. Data was pre-gated for size and live cells post T cell transfer colitis. Graphs show frequency and number of $IFN\gamma^{+}$, $IL\text{-}17A^{+}$, $Foxp3^{+}$ T cells in the colon at the RAGKO endpoint. Data are pooled from at least 2 experiments, n=5-18. (G) Weighed colons were cultured overnight in complete media at 37°C and supernatants from culture were analyzed to assess production of TNFα. Graphs represent pooled data from 2 experiments, n=5-6. (H) Flow cytometry plots showing TNFα expression by the cells isolated from LP harvested from RAGKO and CD45RAGKO after colitis. Samples are pre-gated for size and live cells. Bar graphs show frequency and number of $TNF\alpha^{+}$ cells from 3 experiments, n= 11-14.

After inducing T cell colitis, CD45RAGKO mice had a significant decrease in the frequency of T cells in the spleen compared to RAGKO mice, however since CD45RAGKO spleens are bigger, the total number of T cell was not different between the RAGKO and CD45RAGKO mice (Figure 4.3B). There was also no difference in the percentage of $Foxp3^+$ T cells between the RAGKO and CD45RAGKO spleens. (Figure 4.3C). The Th1 inflammatory response was assessed by intracellular staining of splenic T cells after 4-6 h of stimulation with PMA and ionomycin and with brefeldin A and there was no difference in the frequency or number of IFNγ expressing T cells (Figure 4.3C). The frequency of Th17 cells was present at a lower percentage compared to the Th1 cells and there was an increased percentage of IL-17A producing T cells from the CD45RAGKO spleen, but no difference in cell numbers (Figure 4.3C). Overall, there was no major reduction in effector T cells in the spleens of CD45RAGKO mice.

To further investigate reduced systemic inflammation as a possible reason for the reduced weight loss, the level of the proinflammatory cytokine, TNFα, was measured in mice at the RAGKO colitis endpoint. A significant reduction in TNFα was observed in the serum of CD45RAGKO mice (Figure 4.4A) and the percentage of TNFα expressing cells was significantly lower in the CD45RAGKO spleen, assessed *ex vivo* by intracellular staining after collagenase digestion and stimulation with PMA and ionomycin with brefeldin A for 4-6 h (Figure 4.4B). However, this did not translate into greater cell numbers, and overnight culture of spleen explants did not result in significantly more TNFα production from the CD45RAGKO spleen (Figure 4.4C). Examination of the specific cell populations making TNFα revealed a decreased percentage of TNFα producing neutrophils ($Ly6G^+$) and macrophages ($Ly6G^-$ $CD11b^+Ly6c^-$ and $Ly6G^-F4/80^+CD11b^-$) in the CD45RAGKO spleen (Figure 4.4D-E). However, TNFα expression by the splenic T cells was not detectable by intracellular staining and flow

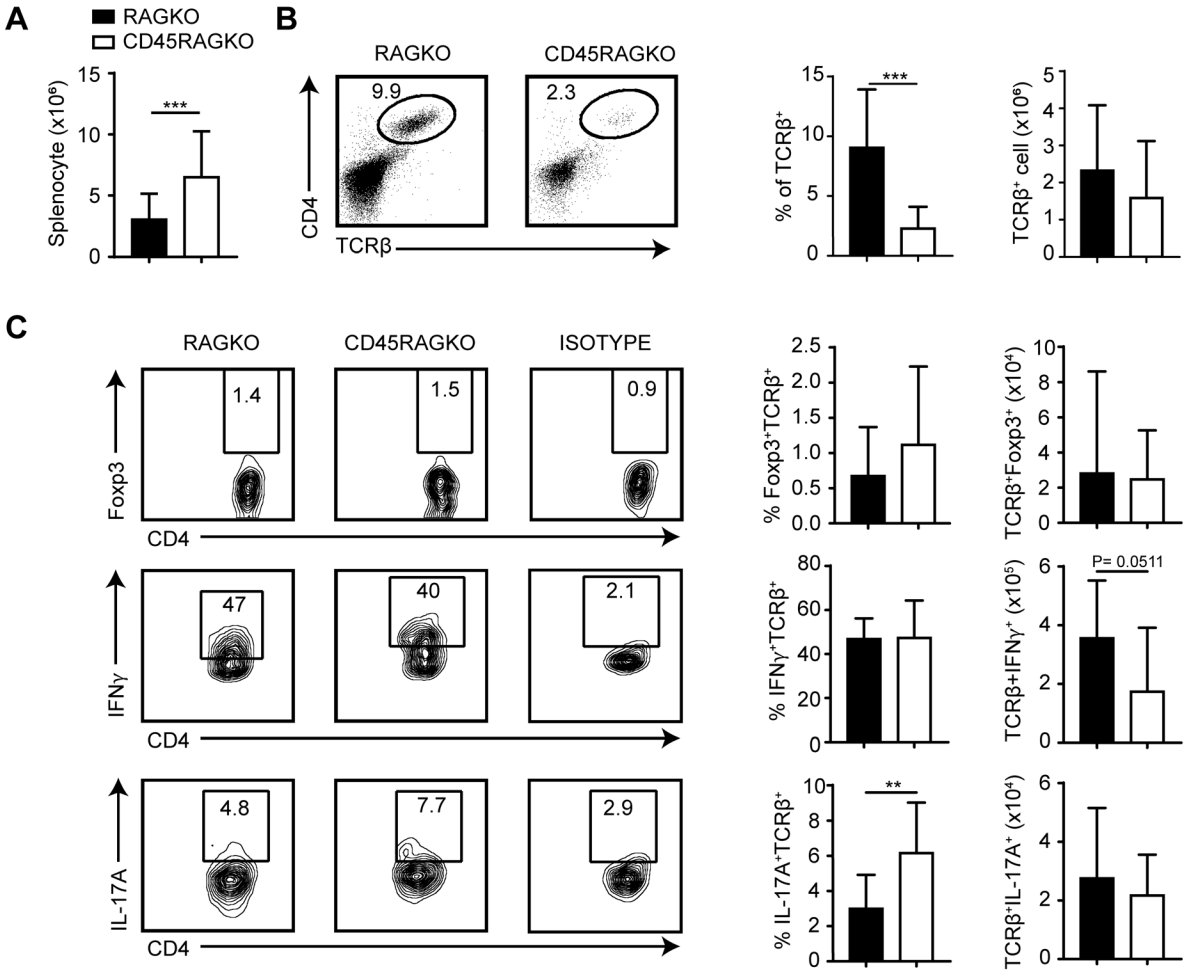

Figure 4.3 CD45RAGKO mice have reduced systemic T cells

(A) The total number of splenocytes in RAGKO and CD45RAGKO mice prior to and post colitis induction at the RAGKO endpoint. Data was averaged over 4 experiments, n=12-38. (B) Representative flow cytometry plots showing gating for TCRβ$^+$ cells in the spleen after pre-gating for size and live cells. Graphs show pooled data of the frequency and number of TCRβ$^+$ cells from 4 experiments, n=12-36. (C) Representative staining of Foxp3$^+$, IFNγ$^+$ and IL-17A$^+$ cells after pre-gating for size, live cells and CD4$^+$TCRβ$^+$ cells in the spleens from RAGKO and CD45RAGKO mice at the RAGKO endpoint post colitis. Graphs show pooled data of the frequency and number of Foxp3$^+$, IFNγ$^+$ and IL-17A$^+$ CD4$^+$TCRβ$^+$ cells in the spleen from at least 3 experiments, n=10-11.

cytometric analysis even after stimulation with PMA and ionomycin with brefeldin A, suggesting that the splenic T cells do not contribute to systemic TNFα level (Figure 4.4F). This shows that the lack of CD45 results in lower circulating levels of TNFα in the serum, and that there was a lower percentage of myeloid cells producing TNFα, in particular neutrophils and macrophages, in the CD45RAGKO spleen after T cell induced colitis. Since TNFα has been linked to systemic inflammation and cachexia, this raised the possibility that the differences in TNFα expression by the myeloid cells may contribute to the reduced systemic weight loss observed in the CD45RAGKO mice after T cell induced colitis.

4.2.3 CD45RAGKO erythroid progenitor cells attenuate weight loss and reduce TNFα production by F4/80^{+}CD11b^{-} cells

To further investigate why CD45RAGKO mice showed reduced wasting disease and cachexia compared to the RAGKO mice, a role for the increased number of erythroid progenitors present in CD45RAGKO spleen was considered. CD71^{+}TER119^{+} erythroid progenitors can have an immunosuppressive role (Elahi, 2019) and here, the percentage and number of CD71^{+}TER119^{+} erythroid progenitors in the CD45RAGKO spleen remained high after the induction of colitis compared to the RAGKO spleen (Figure 4.5A). To determine if these cells contributed to the reduced systemic inflammation and weight loss observed in the CD45RAGKO mice, CD71^{+}TER119^{+} cells were isolated from the CD45RAGKO spleen with the average purity of CD71^{+}TER119^{+} cells above 90% (Figure 4.5B), and were adoptively transferred into RAGKO mice. These cells (3×10^{6}) were injected (i.v.) every 3-5 days beginning a day before the induction of colitis and weight loss was monitored throughout disease progression. Interestingly, the transfer of cells into the

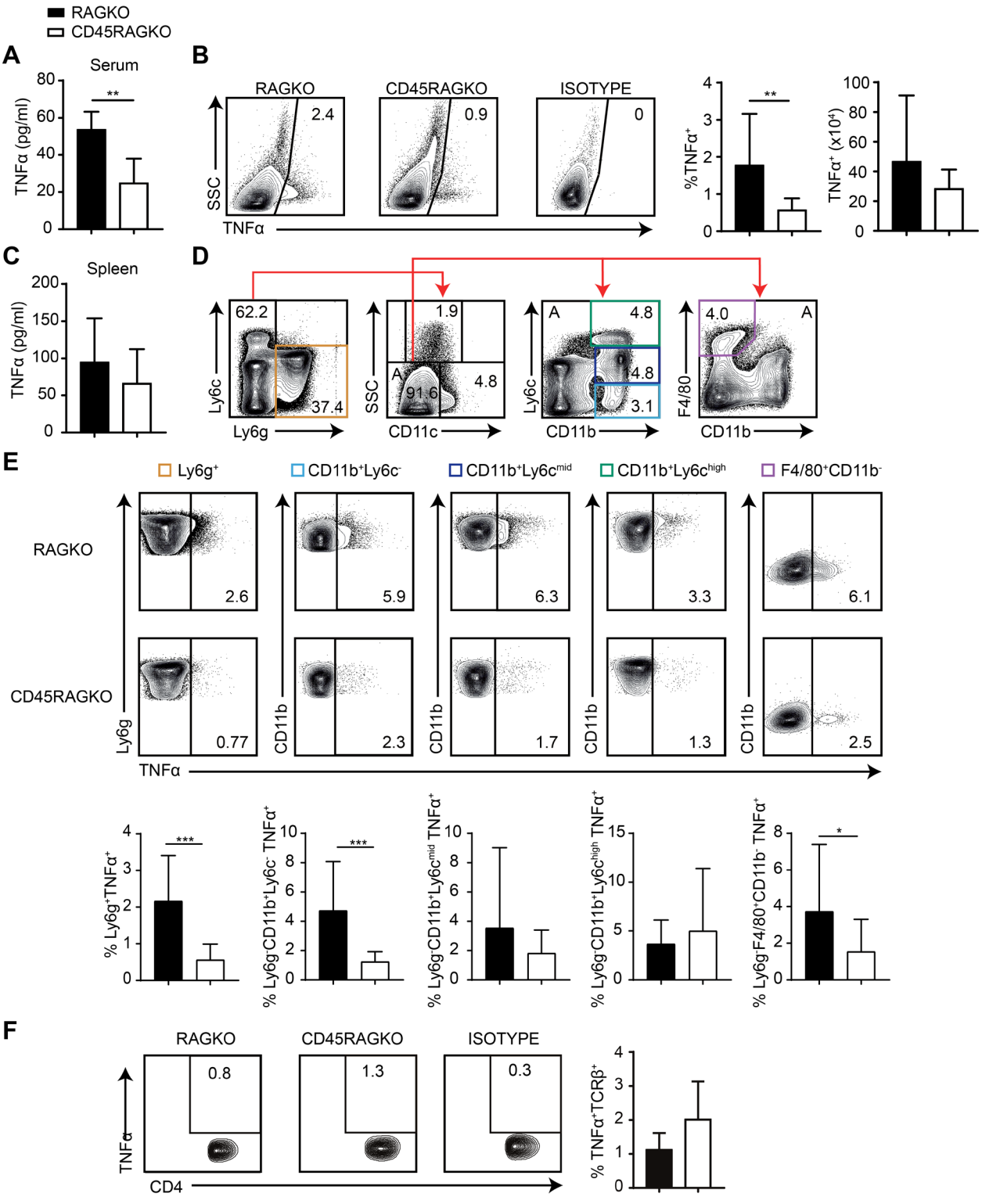
RAGKO
CD45RAGKO
A
Serum
TNFα (pg/ml)
**
B
RAGKO
CD45RAGKO
ISOTYPE
2.4
0.9
0
SSC
TNFα
%TNFα+
TNFα+ (x10⁴)
C
Spleen
D
62.2
37.4
Ly6c
Ly6g
1.9
91.6
4.8
SSC
CD11c
4.8
4.8
3.1
CD11b
4.0
F4/80
E
Ly6g+
CD11b+Ly6c-
CD11b+Ly6cmid
CD11b+Ly6chigh
F4/80+CD11b-
RAGKO
CD45RAGKO
2.6
5.9
6.3
3.3
6.1
0.77
2.3
1.7
1.3
2.5
Ly6g
CD11b
TNFα
% Ly6g+TNFα+
% Ly6g-CD11b+Ly6c- TNFα+
% Ly6g-CD11b+Ly6cmid TNFα+
% Ly6g-CD11b+Ly6chigh TNFα+
% Ly6g-F4/80+CD11b- TNFα+
***
*
F
RAGKO
CD45RAGKO
ISOTYPE
0.8
1.3
0.3
TNFα
CD4
% TNFα+TCRβ+

Figure 4.4 CD45RAGKO mice have reduced systemic production of TNFα

(A) Serum TNFα from RAGKO and CD45RAGKO mice at the RAGKO endpoint, averaged over 2 experiments, n=6. (B) Representative intracellular flow cytometry of total $TNF\alpha^+$ cells in the collagenase-digested spleens of RAGKO and CD45RAGKO mice after 4-6 h of PMA and ionomycin stimulation with brefeldin A at the RAGKO endpoint post colitis after pre-gating on size and live cells. Graphs show frequency and number of $TNF\alpha^+$ cells after pooling data from 2 experiments, n=8. (C) Weighed spleens were cultured overnight in complete media at 37°C and supernatants from culture were analyzed to assess production of TNFα. Graphs show pooled data from 2 experiments, n=5-6. (D) Representative gating strategy used for flow cytometric analysis of different myeloid types in the collagenase-digested spleens of RAGKO and CD45RAGKO for intracellular detection of TNFα expressions after 4 h of PMA and ionomycin stimulation with brefeldin A post colitis after pre-gating for size and live cells. (E) Representative intracellular flow cytometry plots and graph of TNFα expression in the different myeloid subsets in the spleens of RAGKO and CD45RAGKO mice at RAGKO endpoint post colitis. Representative flow plots have been pre-gated for singlets, size and live cells. Graphs are of pooled data from 2 experiments, n=8. (F) Representative flow cytometry plot showing TNFα expression in $CD4^+$ T cells harvested from RAGKO and CD45RAGKO mice at RAGKO endpoint post colitis. Graph show representative data from 2 independent experiments. n=3

RAGKO mice significantly reduced their weight loss after the induction of colitis (Figure 4.5C). The RAGKO mice that received the $CD71^{+}TER119^{+}$ cells had reduced weight loss compared to the RAGKO mice which received PBS alone, although they still lost more weight than the CD45RAGKO mice.

To determine if the adoptive transfer of $CD71^{+}TER119^{+}$ erythroid progenitors impacted TNFα production in the spleen, myeloid cells were isolated from the spleens of RAGKO mice that received CD45RAGKO erythroid progenitors at the RAGKO experimental endpoint. The isolated cells were then stimulated with PMA and ionomycin *ex vivo*. Examination of the specific myeloid subsets in the spleen by flow cytometry showed a drop in TNFα production for the neutrophils and $Ly6C^{-}$ macrophage population, however, this was not significant (Figure 4.5C). In contrast, the drop in TNFα production in the splenic RPM population ($F4/80^{+}CD11b^{-}$) was significant and was reduced to the levels observed in the CD45RAGKO mice (Figure 4.5D). As in the CD45RAGKO spleen, the TNFα levels produced by the monocytes were not affected by these cells. Furthermore, the percentage of TNFα producing myeloid cells in the intestine did not change with the injection of these erythroid cells (Figure 4.6). This showed that the adoptive transfer of $CD71^{+}$ $TER119^{+}$ erythroid progenitors is sufficient to reduce the TNFα response by the splenic macrophages *in vivo*.

4.2.4 Erythroid cells from CD45RAGKO spleen directly reduce TNFα production from $F4/80^{+}CD11b^{-}$ macrophages *in vitro*

To determine if the erythroid progenitor cells directly affected TNFα production by the splenic macrophages, myeloid cells were isolated from RAGKO spleens at steady state and cocultured or not with total $TER119^{+}$ erythroid cells isolated from the CD45RAGKO spleen, which included

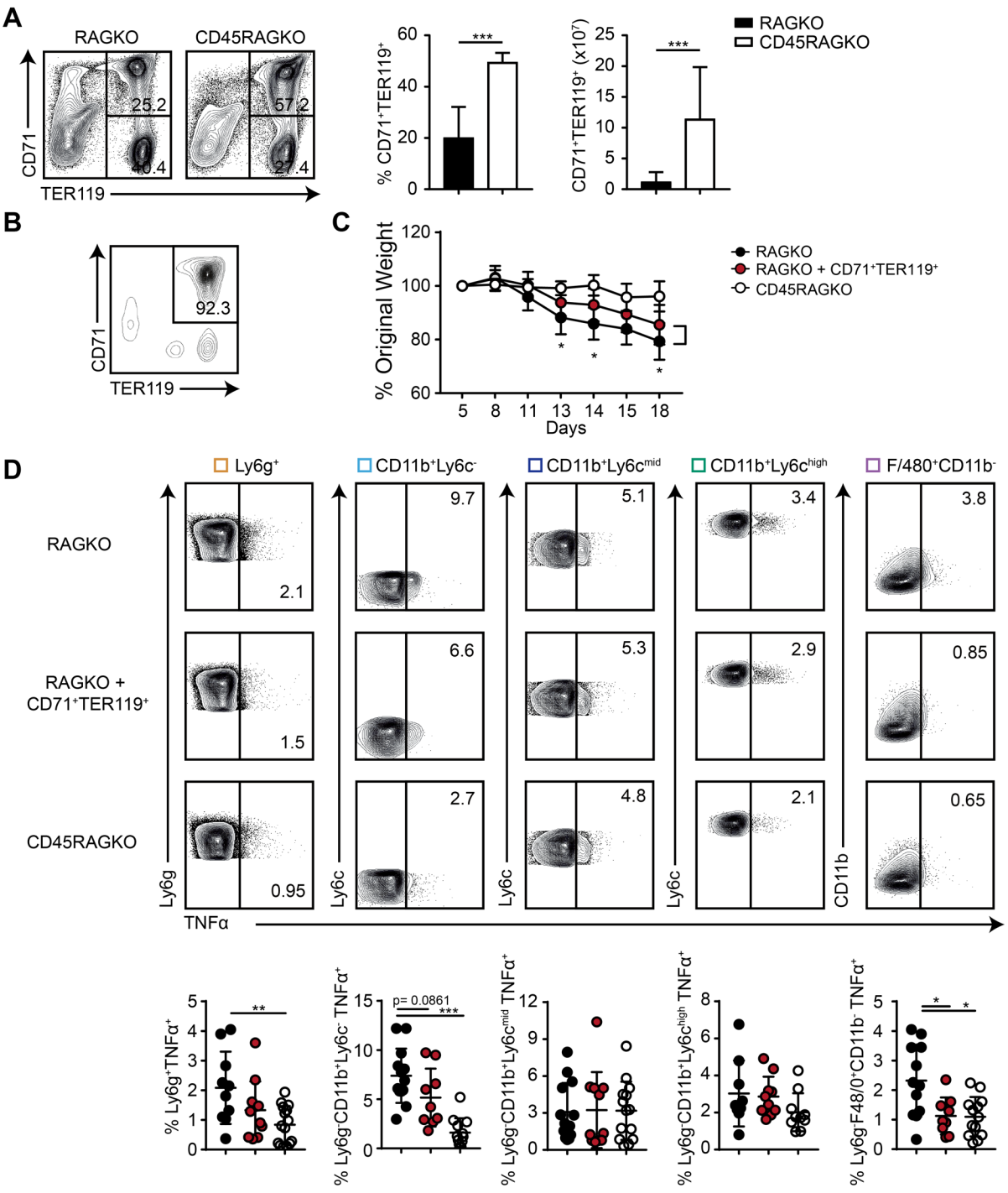

Figure 4.5 CD45RAGKO mice have increased numbers of CD71$^+$TER119$^+$ erythroid cells in the spleens, and these cells have immunosuppressive properties

(A) Representative gating strategies used for analysis of erythroid progenitors (CD71$^+$TER119$^+$) and mature erythroid cells (CD71$^+$TER119$^-$) in the spleen after colitis and after pre-gating for size and live cells. Bar graphs

show the frequency and the number of erythroid progenitors and mature erythrocytes pooled from 2 experiments, n=6-7. $CD71^{+}TER119^{+}$ cells isolated from control CD45RAGKO spleen was injected i.v. into the RAGKO mice a day prior to the induction of colitis and every 3-5 days after induction throughout the development of colitis. (B) A representative flow plot showing the purity of $CD71^{+}TER119^{+}$ cells isolated from the control CD45RAGKO spleens using magnetic isolation methods described in chapter 2. (C) Weight change after the induction of colitis. The mice were weighed every 3-5 days and representative data (n=5) from at least 3 experiments are shown, total n=13-16. Statistical significance shown on graph is of the weights between the RAGKO which received $CD71^{+}TER119^{+}$ cells compared to PBS control. (D) Representative staining of TNFα expression in different myeloid subsets in the spleens of RAGKO which received $CD71^{+}TER119^{+}$ cells compared to control RAGKO and CD45RAGKO mice at control RAGKO endpoint post colitis. Samples have been pre-gated for singlets, size and live cells. Graphs show pooled data of the frequency and cell numbers of the $TNF\alpha^{+}$ myeloid subsets from 2 experiments, n=9-13.

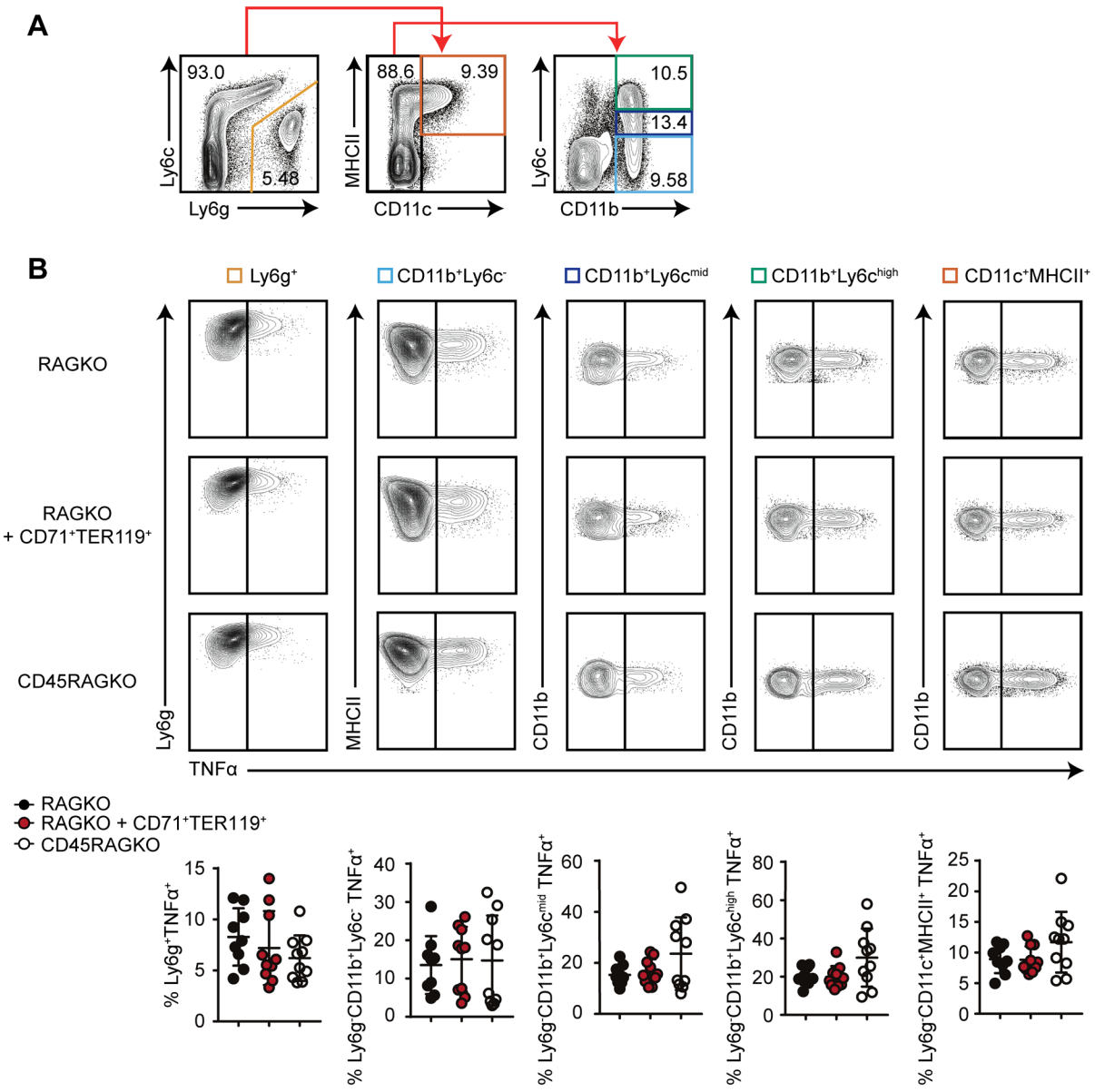

Figure 4.6 Production of TNFα by the myeloid cells in the RAGKO LP does not change with the injection of CD71^{+}TER119^{+} cells

(A) Representative flow cytometry plots showing gating strategy used for the analysis of different myeloid populations in the LP of RAGKO and CD45RAGKO. (B) Representative intracellular staining for TNFα in the different myeloid subsets after pre-gating for singlets, size and live cells in the LP of RAGKO and CD45RAGKO mice at RAGKO endpoint post colitis. Graphs show pooled data of the frequency and cell numbers of the TNFα^{+} myeloid subsets from 2 experiments, n=8.

both $CD71^{+}TER119^{+}$ and $CD71^{-}TER119^{+}$ cells, or with just $CD71^{+}TER119^{+}$ enriched cells. The myeloid cells were activated by LPS for 15 h with brefeldin A, and TNFα levels were measured by intracellular staining. Analysis of the $Ly6C^{high}$ monocyte subset and the $F4/80^{+}$ splenic macrophage subset showed a specific effect of the erythroid cells on the $F4/80^{+}$ macrophages but no effect on the monocytes. The TNFα expressing $F4/80^{+}$ splenic macrophage population was significantly reduced by half from 15.1% to 7.8% $TNFα^{+}$ cells with a ratio of 1:5 myeloid:erythroid cell (Figure 4.7). Adding the entire $TER119^{+}$ erythroid cell populations at a 1:10 ratio also reduced the percentage of TNFα expressing $F4/80^{+}$ macrophages to 9.5% TNFα, but these were less effective than the enriched population. These results directly demonstrate the ability of $CD71^{+}TER119^{+}$ enriched cells to reduce the percentage of LPS induced, TNFα expressing splenic macrophages.

4.2.5 RBC-phagocytic $F4/80^{+}CD11b^{-}$ RPMs produce less TNFα than nonphagocytic $F4/80^{+}CD11b^{-}$ cells

To further understand how erythroid progenitor cells suppress TNFα expression by the $F4/80^{+}CD11b^{-}$ macrophages, arginase-2 expression was examined in the erythroid progenitors, as this is one possible mechanism that has been described previously (Delyea et al., 2018; Elahi et al., 2013). Both RAGKO and CD45RAGKO $CD71^{+}TER119^{+}$ erythroid cells expressed arginase-2 at steady state (Figure 4.8A), providing one potential explanation for their suppressive effect. However, why this would affect the $F4/80^{+}CD11b^{-}$ macrophages and not the monocyte population, is not clear. Since the $F4/80^{+}CD11b^{-}$ splenic macrophage population make up the RPM population which are responsible for the phagocytosis of senescent erythrocytes, it was

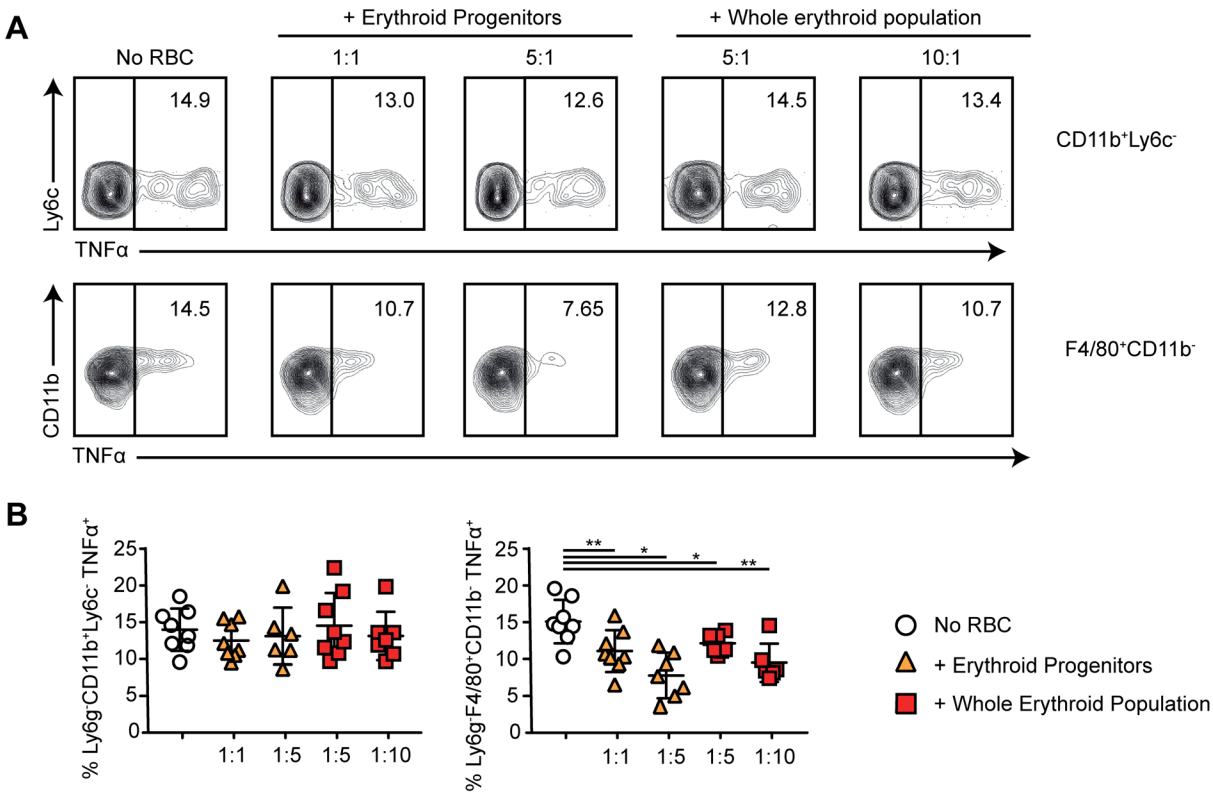

Figure 4.7 CD71^{+}TER119^{+} erythroid cells can directly reduce TNFα expression from splenic F4/80^{+}CD11b^{-} macrophages in coculture

Co-culture of 5 × 10^5 myeloid cells harvested from control RAGKO spleens with 5 × 10^5 or 4.5 × 10^6 CD71^{+}TER119^{+} cell from the CD45RAGKO mice or with 4.5 × 10^6 or 45 × 10^6 total erythroid cells including the CD71^{-}TER119^{+} cells in the 24 well plate. Cells were activated with 10ng/mL LPS for overnight with brefeldin A added concurrently and the cells were assessed for TNFα expression by intracellular staining and flow cytometry. (A) Representative intracellular staining for TNFα after pre-gating for live and size and then Ly6g^{-}CD11b^{+}Ly6c^{low} and then for Ly6g^{-}F4/80^{+}CD11b^{-} cell populations. (B) Graphs of the frequency of TNFα^{+} cells within the Ly6g^{-}CD11b^{+}Ly6c^{low} and Ly6g^{-}F4/80^{+}CD11b^{-} populations from the RAGKO that have been cocultured with varying numbers of erythroid cells from the CD45RAGKO spleens or cultured alone. Data were pooled from 2 experiments, n= 8.

possible that erythroid cells reduce the percentage of TNFα producing F4/80^{+}CD11b^{-} cells in a phagocytosis-dependent manner. To test this idea, the erythroid cells were labeled with amine-reactive pH sensitive dye, pHrodo. The dye gains fluorescent activity when in a low pH environment such as the phagosome, thus enabling the detection of cells which have phagocytosed the labeled erythroid cells. First, I confirmed that F4/80^{+}CD11b^{-} cells phagocytose erythroid cells, including both CD71^{+} and CD71^{-} cells, and a time course indicated that 50% of the RPMs had taken up RBC by 4 h (Figure 4.8B-C). Splenic myeloid cells from the RAGKO mice were treated with LPS and brefeldin A and cocultured with pHrodo labeled erythroid cells. After 4 hrs, the cells were sorted based on pHrodo fluorescence, and then analyzed for TNFα expression by flow cytometry and intracellular staining. More than 60% of the cells found in the pHrodo positive gate were F4/80^{+}CD11b^{-} cells, while fewer than 1% of the cells were F4/80^{+}CD11b^{-} cells in the pHrodo negative fraction, suggesting that F4/80^{+}CD11b^{-} cells readily phagocytosed the erythroid cells. Comparison of TNFα expression by the F4/80^{+}CD11b^{-} cells that were pHrodo+ compared to those that were pHrodo^{-}, revealed a significant reduction in the percentage of TNFα positive cells (Figure 6D-F). Very few of the cells (less than 1%) that phagocytosed the erythroid cells produced TNFα whereas significantly more cells produced TNFα was produced by RPMs that had not phagocytosed the erythroid cells.

Combined, these results suggest that erythroid cells downregulate TNFα production by F4/80^{+}CD11b^{-} macrophages and this interaction is associated with phagocytosis.

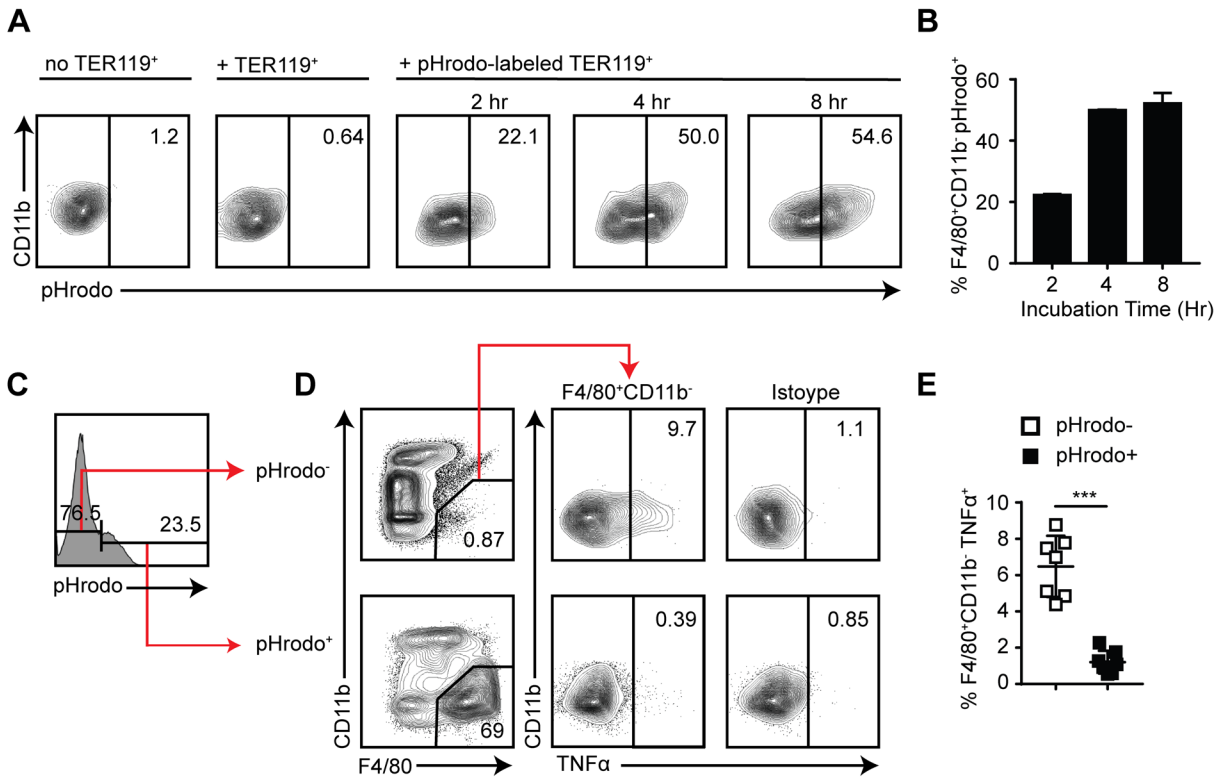

Figure 4.8 Erythroid cells suppress TNFα production from the F4/80^{+}CD11b^{-} cells in a phagocytosis dependent way

(A) Representative histogram of arginase-2 expression from the Ter119^{+}CD71^{+} cells isolated from the RAGKO and CD45RAGKO spleens in steady state. From 2 experiments. 5 × 10^{5} myeloid cells harvested from control RAGKO spleens were cultured in 24 well plates with 45 × 10^{6} total erythroid cells which were labeled with 20 µM pHrodo at 37°C for 30 min. Detection of erythrophagocytosis across different period was detected on F4/80^{+}CD11b^{-} cells through flow cytometric analysis. (B) Representative flow cytometric analysis after varying time of coculture. (C) bar graph showing data from n=2 (D) The culture was stimulated with 10 ng/ml of LPS for 4 hrs, then the cells were enriched for myeloid cells by running the cells down the magnetic columns. Cells were then sorted for pHrodo+ fraction and pHrodo- fractions. (E) Representative ICS staining and graphs of TNFα expression by F4/80^{+}CD11b^{-} cells present in pHrodo^{+} and pHrodo^{-} fractions. (F) Bar graph of pooled data of F4/80^{+}CD11b^{-} cells producing TNFα in pHrodo^{+} and pHrodo^{-} fractions from 2 experiments, n= 8.

4.3 Discussion

In this study, CD45RAGKO mice had equivalent intestinal inflammation to the RAGKO mice in the mouse model of T cell transfer colitis, which mimics several features of chronic IBD. This was based on gross observation of tissue, leukocyte infiltration and cytokine quantification in the colon. However, CD45RAGKO mice did not exhibit the associated weight loss commonly associated with systemic inflammation and cachexia, indicating a dissociation of systemic wasting disease with intestinal inflammation. This makes an important point that weight loss is not always a good predictor of intestinal inflammation in mouse models of colitis.

Further characterization of the systemic inflammatory response by studying the spleen revealed that the T cell response was comparable between CD45RAGKO and RAGKO mice, arising from similar numbers of injected T cells. However, differences were found in the innate immune response in the spleen, where the percentage of TNFα producing neutrophils and macrophages was lower in the CD45RAGKO mice. Notably, less TNFα was found systemically, in serum, but there was no reduction of TNFα producing myeloid cells in the intestine. This focused our attention to the spleen where CD45RAGKO mice had significantly more $CD71^{+}TER119^{+}$ erythroid cells, which have been described to be immunosuppressive in other models (Delyea et al., 2018; Elahi et al., 2013; Namdar et al., 2017). Through the adoptive transfer of these erythroid progenitors from the CD45RAGKO into RAGKO mice, I showed that these erythroid progenitors can attenuate the wasting syndrome and reduce the production of TNFα from splenic macrophage populations *in vivo*. I also showed that the erythroid progenitors can suppress TNFα expression from splenic RPMs *in vitro* in a phagocytosis dependent manner. Through this study, I define a novel interaction between erythroid cells and RPMs in the spleen

during colitis that can prolong the survival of the host by reducing systemic inflammation, notably by reducing TNFα which has a cachexic effect (Patel and Patel, 2017).

CD45 is a leukocyte specific protein tyrosine phosphatase and is known best as a negative and positive regulator of SFK in adaptive and innate immune cells and as a negative regulator of JAK-STAT mediated cytokine signaling (Hermiston et al., 2003; Saunders and Johnson, 2010). CD45 is expressed on early erythroid progenitors and its expression gradually decreases as the $CD71^{+}TER119^{+}$ erythroid progenitors mature into erythrocytes (Chapter 3). CD45-deficient bone marrow progenitors generate more erythroid colonies in response to EPO compared to control cells (Irie-Sasaki et al., 2001), and I showed that the $CD71^{+}TER119^{+}$ progenitors are greatly expanded in the spleens of CD45-deficient mice during homeostasis (Chapter 3). However, the functional consequence of this *in vivo* has not previously been examined. The results presented here show that the increased numbers of $CD71^{+}TER119^{+}$ erythroid progenitor cells are maintained after induction of colitis in the spleen of CD45RAGKO mice and show that these cells can impact systemic inflammation and weight loss induced in mouse models of colitis by reducing TNFα production by splenic RPM. Thus, I propose that the increased numbers of these cells in the spleen of CD45-deficient mice, which have been shown to be more apoptotic (Chapter 3), results in their increased phagocytosis by splenic RPM, which in turn dampens their ability to produce the proinflammatory cytokine, TNFα.

Increased $CD71^{+}TER119^{+}$ erythroid progenitors are found in immunosuppressive environments such as in neonates and tumor patients (Kling et al., 1996; Zhao et al., 2018). Several studies have shown their immunosuppressive activity using murine models of fetomaternal tolerance and *Salmonella* infection, and suggest arginase-2 by $CD71^{+}TER119^{+}$ cells is a driving force for erythroid immunosuppression (Delyea et al., 2018; Elahi et al., 2013). Zhao

et al. also reported accumulation of extramedullary erythroid progenitors in mice inoculated with Lewis lung cancer (LLC) cells (Zhao et al., 2018). When these mice were challenged with lymphocyte choriomeningitis virus (LCMV), the $CD71^{+}TER119^{+}$ cells in the tumor bearing mice suppressed the antiviral response and decreased their survival rate (Zhao et al., 2018). This group showed that $CD71^{+}TER119^{+}$ cells are immunosuppressive in a ROS dependent manner. Recently, Elahi's group reported that pregnant IBD patients have reduced $CD71^{+}$ erythroid cells compared to the healthy pregnant women, and this correlated with reduced T_{Reg} and increased proinflammatory cytokines (Dunsmore et al., 2018). This study provides *in vivo* and *in vitro* evidence for $CD71^{+}TER119^{+}$ erythroid progenitors to reduce TNFα producing RPMs in the spleen. Another group also reported an *in vitro* effect of $CD71^{+}$ enriched splenocytes (which includes the $CD71^{+}TER119^{+}$ progenitors) reducing TNFα expression by $CD11b^{+}$ cells, but saw no effect *in vivo* when these enriched splenocytes were adoptively transferred to a mouse model of sepsis (Wynn et al., 2015). Furthermore, despite the accumulation of $CD71^{+}TER119^{+}$ erythroid progenitors in the spleen of the CD45RAGKO mice, these mice are not protected from weight loss in a mouse model of DSS colitis (Samarakoon et al., 2016). Thus, the impact of these erythroid progenitors may depend on the disease model or severity of systemic inflammation.

RPMs are well known as spleen resident macrophages that phagocytose old and damaged erythrocytes and support development of erythroid progenitors into mature erythrocytes (Kurotaki et al., 2015). RPMs also constitutively express IL-10 and TGFβ that help induce Foxp3 expression in $CD4^{+}$ T cells to generate T_{Reg} (Dillon et al., 2006; Kurotaki et al., 2011). However, RPMs can also be proinflammatory in different environments and produce TNFα during endotoxemia(Inoue et al., 2014; Yadava et al., 1996). Here, using the mouse model of T-cell induced colitis, I showed that $F4/80^{+}CD11b^{-}$ RPMs in spleen also produce TNFα, thus

playing an inflammatory role in chronic colitis. These cells also responded to the erythroid cells in terms of reduced TNFα production *in vivo*. RPMs that have phagocytosed erythroid cells produced less TNFα compared to cells have not phagocytosed erythroid cells. This suggests that phagocytosis of erythroid cells may turn off the production of TNFα from the RPM, or there are distinct RPM populations with different functions. Akilesh *et al.* recently reported that chronic TLR7 and 9 signaling induces the differentiation of monocytes into what they called a specialized inflammatory hemophagocytes, iHPC, which are also F4/80^{+}CD11b^{-} and SPI-C^{+}, with high erythro-phagocytic activity (Akilesh et al., 2019). Based on RNA-sequencing and principal component analysis, these phagocytes were distinguishable from RPMs and Ly6C^{high} monocytes, suggesting heterogeneity after infection. Whether RPMs and iHPCs respond differently in terms of their ability to produce inflammatory cytokines such as TNFα, has not been addressed.

Overall, these results show a novel role for CD45 in regulating systemic inflammation and wasting disease in a mouse model of T cell induced colitis by regulating the number of erythroid progenitors and the production of TNFα by splenic myeloid cells. Erythroid progenitors play a role in reducing wasting disease and suppressing splenic macrophage TNFα production *in vivo*. I also found that F4/80^{+}CD11b^{-} RPMs that have phagocytosed erythroid cells produce less TNFα than those that have not. These findings highlight new avenues to explore in the development of novel therapeutics to treat cachexia associated with intestinal inflammation.

Chapter 5: Role of CD45 in Lymphopenia Induced Proliferation

5.1 Introduction and Rationale

In a healthy adult, the number of T cells in SLO is kept at constant level through a mechanism called homeostatic proliferation. When the T cell population density decreases, the availability of signals needed for T cell maintenance and proliferation increases for each individual cell and the T cells proliferate in the absence of their cognate antigens to fill up the niche (Takada and Jameson, 2009). The signals that are required for this include common-ɤ chain cytokines, such as IL-7 and IL-15, and in some circumstances of fast proliferation, TCR signals from the MHC (Martin et al., 2013; Takada and Jameson, 2009).

Previously, we have shown that CD45 on myeloid cells plays an important role in homeostatic proliferation modeled by LIP, where polyclonal T cells isolated from WT mice were injected into RAGKO and CD45RAGKO mice (Saunders et al., 2014). The absence of CD45 expression on non-lymphoid cells resulted in fewer transferred T cells recovered from CD45RAGKO spleens and pLNs at day 7 post-transfer compared to the T cells recovered from RAGKO mice. Based on the dilution of CFSE proliferation dye, T cells were divided into slow and fast proliferating fractions and the T cells recovered from CD45RAGKO mice had lower numbers of division in slow LIP and lower number of cells in fast LIP, indicating defects in signals that drive both slow and fast proliferation of T cells.

Slow proliferation in LIP is driven by common-ɤ chain cytokines (Min et al., 2005; von Freeden-Jeffry et al., 1995). Accordingly, CD45RAGKO mice have reduced levels of IL-7 protein in the spleen, and interestingly, stromal cells from CD45RAGKO spleen have lower levels of IL-7 mRNA (Saunders et al., 2014). As stromal cells do not express CD45, this result suggests that

CD45 on innate cells is involved in stromal cell function through a potential interaction between myeloid cells and stromal cells.

Fast proliferation in LIP is thought to be driven by MHC and antigen from self, dietary or commensal microbiota, which is different from the proliferation induced by classical T cell activation, as fast LIP occurs in the absence of strong antigenic and costimulatory signals (Martin et al., 2003; Zaft et al., 2005). We have previously shown that adoptive transfer of $CD45^+$ $CD11c^+$ cells from WT spleen at the time of LIP induction in CD45RAGKO mice partially increases fast LIP while transfer of $CD45^-$ $CD11c^+$ cells does not (Saunders et al., 2014). This observation may indicate that there are other ways by which CD45 regulates fast LIP or simply that the number of CD45+ CD11c+ cells injected was insufficient and further tests are required for clarification.

The presence of intestinal microbiota is strongly implicated in fast LIP as mice that are germ-free or treated with antibiotics cannot support fast LIP while slow LIP still occurs in the absence of microbiota (Feng et al., 2010; Kieper et al., 2005). CD45-deficient mice have been reported to have different intestinal microbial composition based on fingerprinting and principal component analysis of 16S rRNA genes of fecal bacteria from WT, CD45KO, RAGKO and CD45RAGKO mice (Dimitriu et al., 2013). However, whether this difference in microbial composition has an impact on the immune system has yet to be studied. Since the microbiota is already strongly implicated in fast LIP and $CD45^+CD11c^+$ adoptive transfer has a partial impact on increasing fast LIP in the CD45RAGKO mice, it raises the possibility that CD45 regulates fast LIP via its effect on the microbial composition of the intestine.

In this chapter, I aimed to further understand the regulation of LIP by CD45. One of my specific aims is to understand how fast LIP is regulated by CD45, by first testing to see if the partial increase in fast LIP by adoptive transfer of WT $CD11c^+$ cells can be further enhanced by

increasing the number of $CD11c^+$ cells injected. I also investigated whether the difference in microbiota composition in the intestine of the RAGKO and CD45RAGKO mice impacts their ability to support fast LIP. Next, I aimed to understand how the CD45RAGKO mice are less able to support slow LIP by studying the effect of CD45 deficiency on stromal cells, specifically the FRCs in the SLO, by looking at their maturation and function in a CD45-deficient environment.

5.2 Results

5.2.1 CD45 expression on $CD11c^+$ cells supports LIP

To see if the enhancement of fast LIP with the injection of $CD45^+CD11c^+$ cells is dose-dependent, I increased the number of $CD45^+CD11c^+$ cells injected to 10 million cells from 0.3-3 million cells injected in previous experiments. Even with the increased number of $CD11c^+$ cells transferred into the host mice, the increase in the number of T cells recovered from CD45RAGKO mice did not reach the level observed from the RAGKO mice by day 7 after the transfer (Figure 5.1A). This partial rescue effect by the transfer of $CD45^+CD11c^+$ cells was not accompanied by a significant increase in IL-7 levels (Figure 5.1B).

5.2.2 Depletion of microbiota with antibiotics removes the difference between the RAGKO and CD45RAGKO fast LIP

To test whether the altered microbial communities found in CD45RAGKO mice causes defective LIP either directly as a source of antigen or indirectly through altering IL-7 levels, an antibiotic cocktail which included Vancomycin, Metronidazole, Ampicillin and Neomycin was given in the drinking water for 2-3 weeks prior to LIP induction. I wanted to determine whether

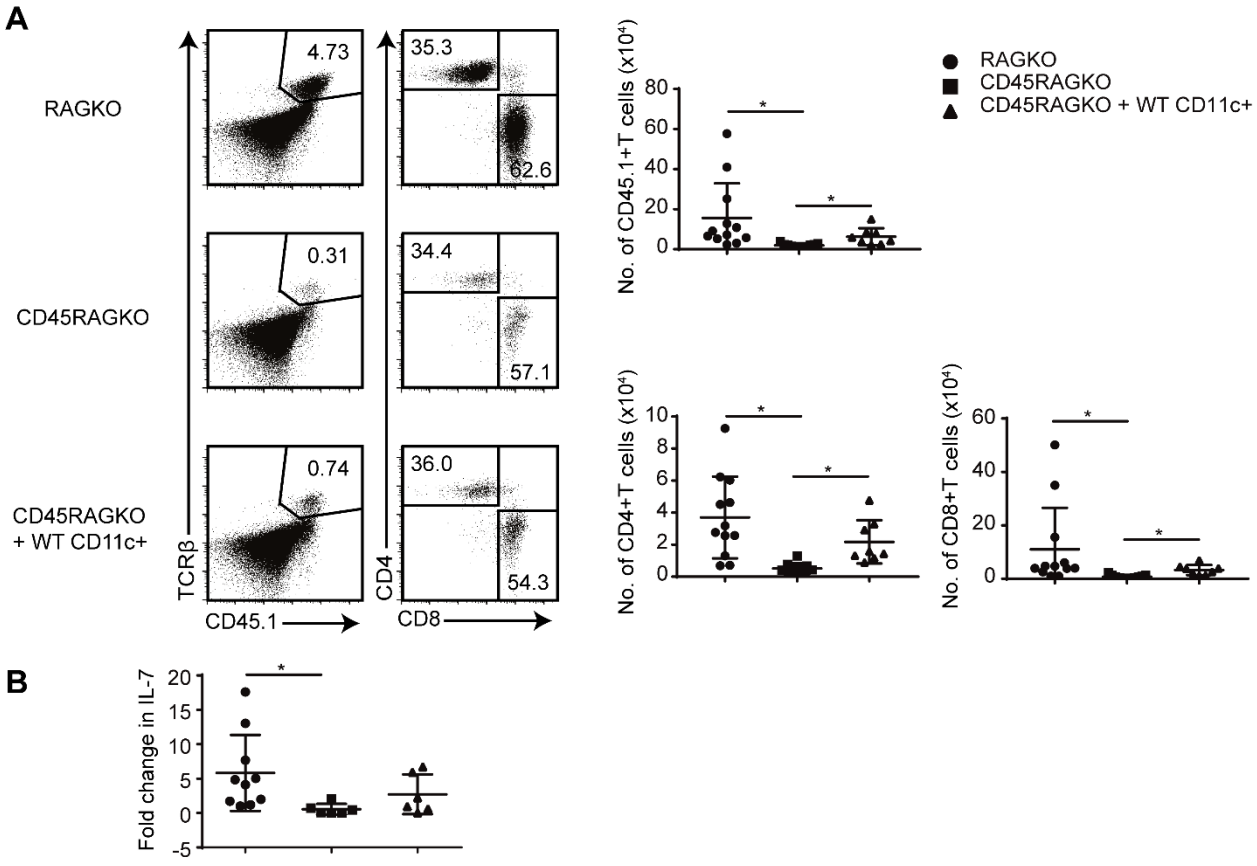

Figure 5.1 T cell LIP in the spleens of RAGKO and CD45RAGKO mice after adoptive transfer of CD11c$^+$

(A) WT CD11c$^+$ cells were isolated from mice which were injected with Flt3L-transfected B16 cells prior to harvest. 10×10^6 splenic CD11c$^+$MHCII$^+$ cells were isolated from Flt3L positive C57BL/6 mice and adoptively transferred (CD45RAGKO + WT CD11c$^+$), or not (CD45RAGKO), into CD45RAGKO hosts with 3×10^6 CFSE labeled T cells isolated from BoyJ mice. RAGKO refers to control where T cells alone were transferred into RAGKO hosts to induce LIP. On day 7 post T cell transfer, T cell LIP in the spleen was assessed by flow cytometry. Dot plots show the number of total T cells, CD4 T cells and CD8 T cells recovered. (B) CD45RAGKO mice received CD11c$^+$ cells as above, but without T cells, then spleens were harvested at day 7 to isolate mRNA. The graph shows IL-7 transcript levels normalized to GAPDH measured by qPCR, n = 6-10.

the depletion of intestinal microbiota would reduce fast LIP as well as reduce the difference in LIP between RAGKO and CD45RAGKO mice. At day 7 post-T cell transfer, total T cell recovery was dramatically reduced from both the RAGKO and CD45RAGKO pLNs, with a greater impact on the RAGKO mice with a 3-fold reduction in T cell number compared to a 2-fold reduction in the CD45RAGKO mice (Figure 5.2A-B). The CD4 and CD8 T cells were then gated based on the number of divisions they had undergone to differentiate between fast and slow LIP. T cells that have undergone 0-5 divisions were gated and defined as slow LIP and cells that had undergone 5+ divisions were gated and designated as fast LIP (Figure 5.2A).

The antibiotic treatment affected fast LIP in both CD4 and CD8 T cell populations, but slow LIP was not affected. (Figure 5.2C). Interestingly, the number of T cells that had undergone fast LIP was no longer different between RAGKO and CD45RAGKO mice after antibiotic treatment (Figure 5.2C). I confirmed that the antibiotics efficiently reduced the intestinal microbiota by checking that 16s rDNA in the fecal sample was reduced to below detectable levels after 21 days of the treatment (Figure 5.2D). The effect of antibiotics on LIP in the spleen was similar to that in the pLNs (Figure 5.3). The antibiotic treatment reduced the number of T cells recovered from RAGKO spleen by approximately 3-fold, whereas the recovery from CD45RAGKO spleen was less than 2-fold, resulting in comparable T cell recovery from RAGKO and CD45RAGKO spleens after the treatment (Figure 5.3A-B). Also, the antibiotics treatment did not change the number of CD4 and CD8 T cells that had undergone slow LIP, while the number of T cells that had undergone fast proliferation was significantly reduced from both the RAGKO and CD45RAGKO mice (Figure 5.3C). However, the number of CD4 T cells which had undergone fast LIP was still significantly lower in CD45RAGKO mice even after the antibiotic treatment (Figure 5.3C).

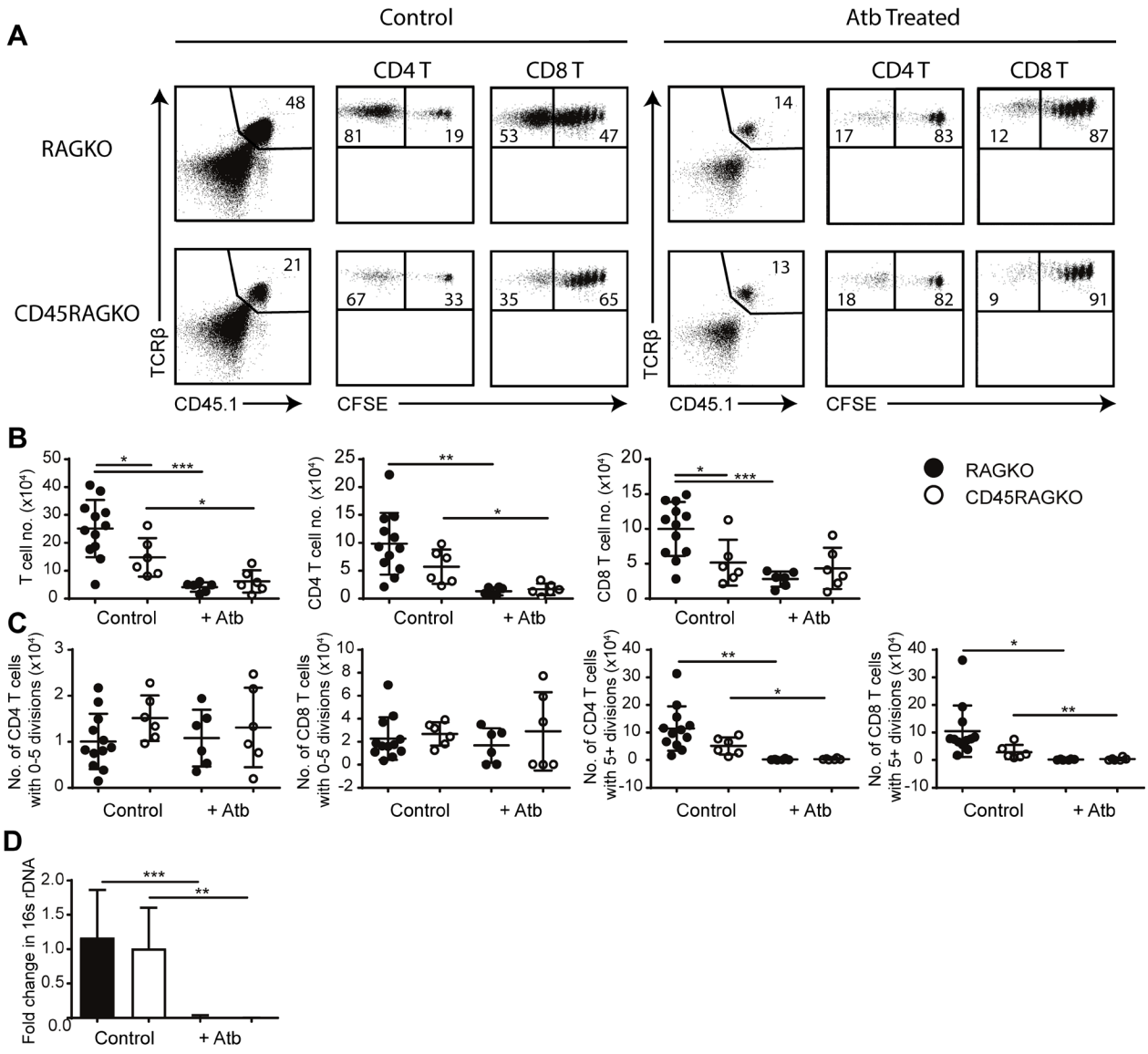

Figure 5.2 Microbiota depletion reduces fast LIP in both RAGKO and CD45RAGKO mice in the pLNs

(A) Representative flow cytometry plots showing proliferation of adoptively transferred CD45.1$^+$ T cells harvested from the pLNs of RAGKO and CD45RAGKO mice treated with either regular drinking water or antibiotic cocktail water ad libitum for two weeks prior to and one week during the experiment. (B) Numbers of total, CD4 and CD8 T cells recovered from the pLN. Data is pooled from 3 experiments, n=6-12. (C) Numbers of CD4 and CD8 T cell that have undergone slow and fast LIP. Data is pooled from 3 experiments, n=6-12. (C) Quantification of 16S rDNA in the fecal samples by qPCR analysis to check the efficacy of gut microbiota depletion using the antibiotic cocktails, n=4-12.

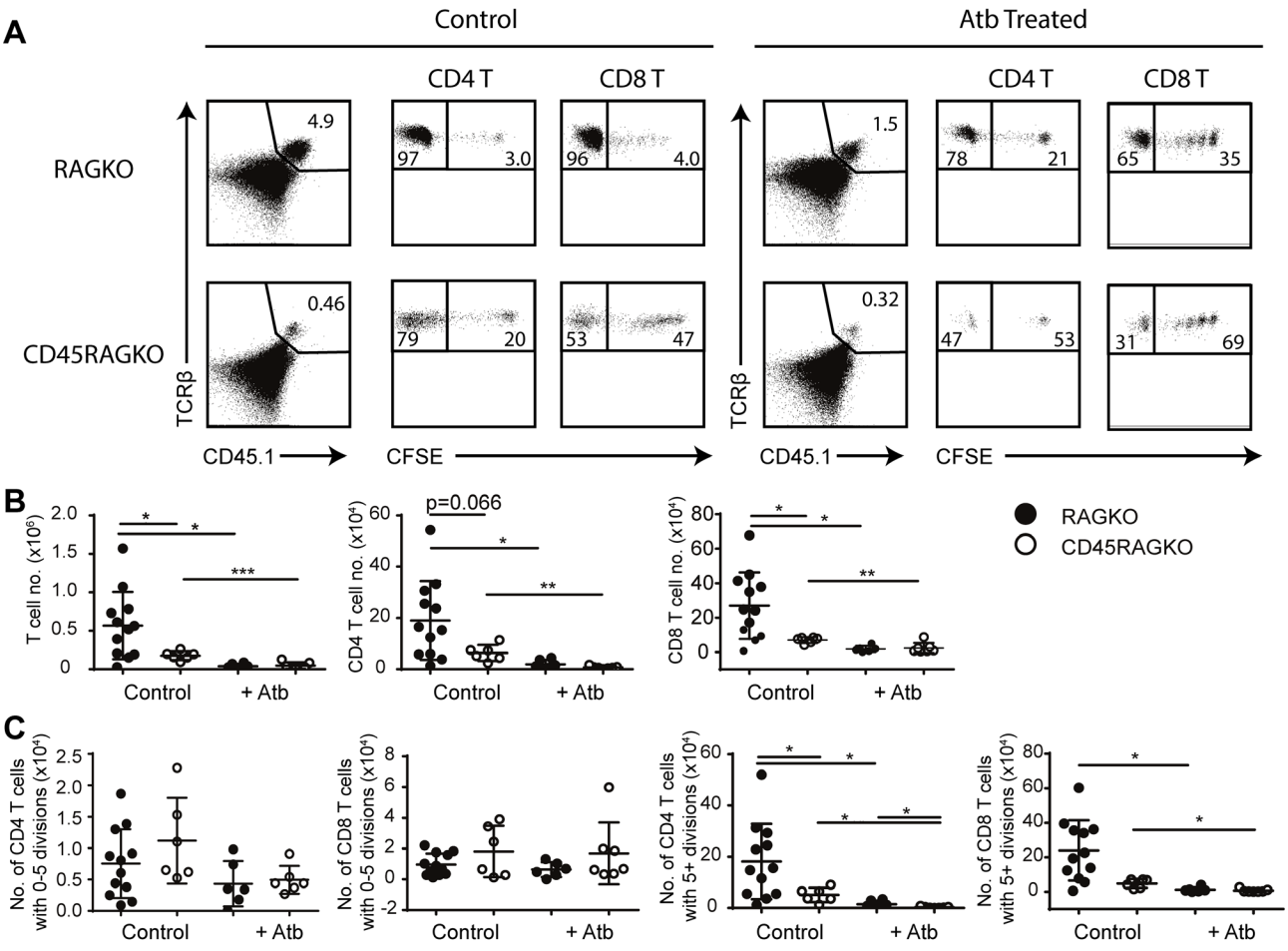

Figure 5.3 Microbiota depletion reduces fast LIP in both RAGKO and CD45RAGKO mice in the spleen

(A) Flow cytometry of the T cells harvested from the spleens of RAGKO and CD45RAGKO hosts treated with either regular drinking water or antibiotic cocktail water ad libitum for two weeks prior to and one week during the experiment. (B) Numbers of total, CD4 and CD8 T cell recovered from the spleen. Data is pooled from 3 experiments, n=6-12 mice. (C) Numbers of CD4 and CD8 T cell that have undergone slow LIP and fast LIP. Data is pooled from 3 experiments, n=6-12.

5.2.3 Microbiota from RAGKO mice skews LIP towards fast LIP in CD45RAGKO hosts

Since antibiotic treatment reduced the difference between the fast LIP of RAGKO and CD45RAGKO mice, I questioned whether the difference in the microbial community between the RAGKO and CD45RAGKO mice had an impact on their ability to drive fast LIP. To test this, fecal transfer was performed by placing fecal matter from RAGKO or CD45RAGKO donors into the clean experimental cages of RAGKO or CD45RAGKO mice biweekly starting immediately after weaning. After three weeks, LIP was induced by i.v. injection of WT T cells.

In RAGKO hosts, transferring CD45RAGKO fecal matter did not change the number of T cells recovered or the number of T cells that had undergone fast or slow LIP, both in spleen and pLN (Figure 5.4). In CD45RAGKO hosts, transferring RAGKO fecal matter did not affect LIP in the spleen (Figure 5.5A-B), however, in pLN, the frequency of T cells that had undergone fast LIP significantly increased in both the CD4 and CD8 T cells, even though it did not equal the levels seen in RAGKO mice with no fecal transfer (Figure 5.5 A, C). The increase in the fast LIP was reflected in the cell numbers, however the difference was not statistically significant. On the contrary, the number of cells that have undergone slow LIP were comparable between the mice that received fecal matter from RAGKO or CD45RAGKO mice. This result suggests that the microbiota in the RAGKO mice is better at inducing T cell expansion in the pLNs of CD45RAGKO mice.

5.2.4 CD45RAGKO spleen has increased number of immature FRC

Next, I investigated the effect of CD45 on slow LIP which is dependent on IL-7 production by the stromal cells. CD45RAGKO SLOs have been reported to have a lower concentration of IL-7 and the stromal cells had lowers IL-7 mRNA (Saunders et al., 2014). The

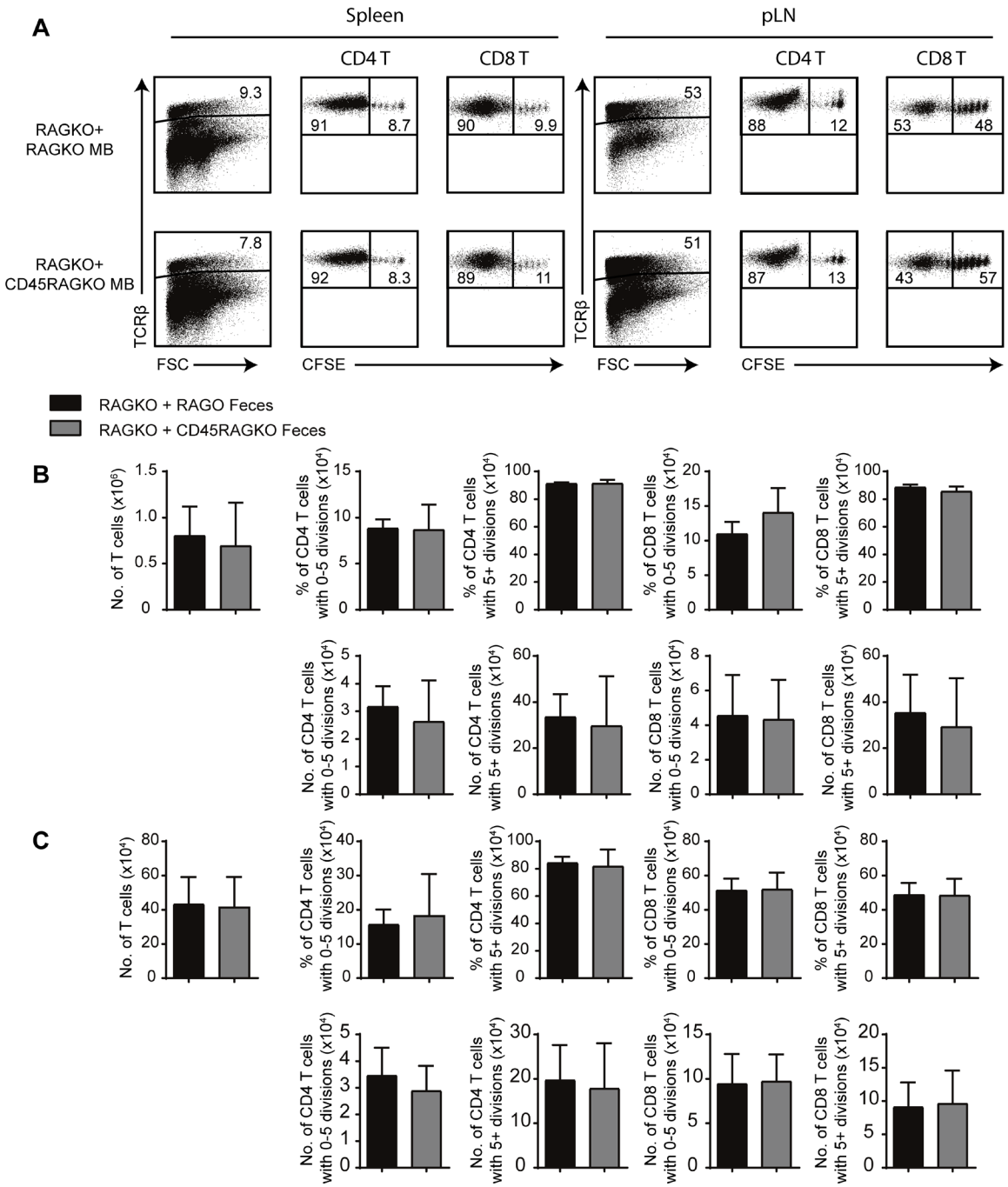

Figure 5.4 Microbiota from CD45RAGKO mice does not affect fast LIP in RAGKO hosts

(A) A flow cytometry data showing proliferation of adoptively transferred T cells recovered from spleen and pLNs of RAGKO mice on day 7 after induction of LIP. Fecal matter was transferred from either RAGKO or CD45RAGKO mice prior to the induction starting from weaning until the day of harvest. LIP was induced by

injecting 3×10^6 CFSE-labeled polyclonal T cells from wild-type mice by i.v. injection. MB stands for microbiota and indicates the donor of fecal matters. (B) Number of total T cells recovered from spleen and frequency and number of CD4 and CD8 T cells that underwent slow and fast proliferation. (C) Number of total T cells recovered from pLNs and frequency and number of CD4 and CD8 T cells that underwent slow and fast proliferations. (B-C) Data pooled from two experiments, n=8-9

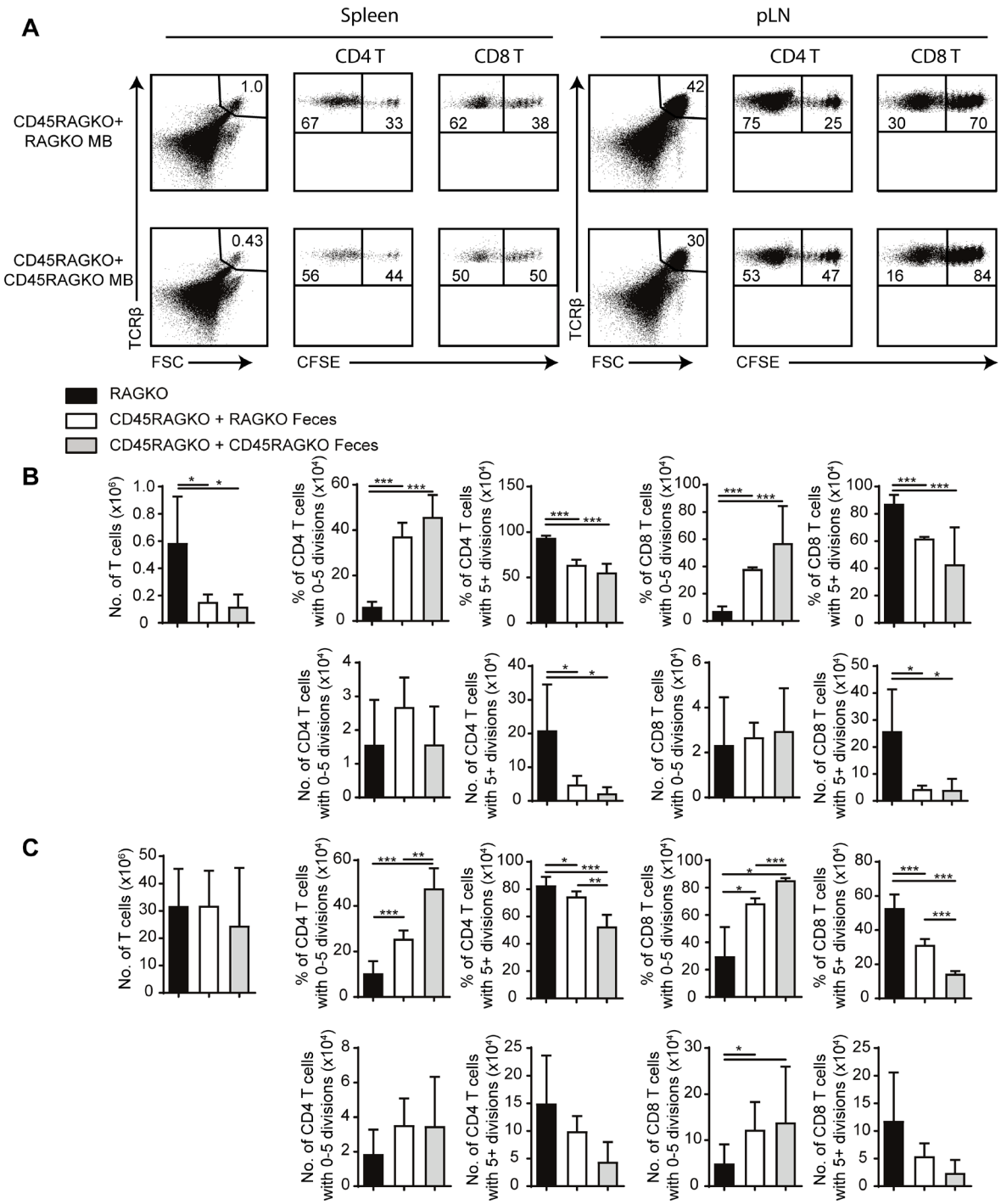

Figure 5.5 Microbiota from RAGKO mice skews the LIP towards fast LIP in CD45RAGKO pLNs

(A) Flow cytometry data showing proliferation of adoptively transferred T cells recovered from spleen and pLNs of CD45RAGKO mice on day 7 after induction of LIP. Fecal matter was transferred from either RAGKO or CD45RAGKO mice prior to the induction starting from weaning until the day of harvest. LIP was induced by

injecting 3×10^6 CFSE-labeled polyclonal T cells from wild-type mice by i.v. injection. MB stands for microbiota and indicates the donor of fecal matters. (B) Number of total T cells recovered from spleen and frequency and number of CD4 and CD8 T cells that underwent slow and fast proliferation. (C) Number of total T cells recovered from pLNs and frequency and number of CD4 and CD8 T cells that underwent slow and fast proliferations. (B-C) Data pooled from 3 experiments, n=8-12.

stromal cells gain IL-7 expression as they mature (Chai et al., 2013), therefore I tested to see if the defective IL-7 expression by the CD45RAGKO mice could be due to a disturbance in FRC maturation. One of the hall marks of FRC maturation is the step-wise increase in ICAM-1 and VCAM-1 expression, from low, mid to high (Chai et al., 2013); therefore, surface expression of these markers was compared on FRCs from RAGKO and CD45RAGKO spleens and pLNs. Due to the lack of CD45 expression in the CD45RAGKO mice, a lineage mix targeting common immune cell markers was used to gate out immune cells that are normally CD45 positive, before gating for $PDPN^{+}CD31^{-}$ FRCs (Figure 5.6A). Comparing RAGKO and CD45RAGKO mice, the number of FRCs in the CD45RAGKO spleen was equal to the number of FRCs in the RAGKO spleen despite the former having a lower frequency of these cells (Figure 5.6B) due to the CD45RAGKO spleens having a greater number of total cells (Figure 5.6C). However, a difference in the maturity of the FRCs was observed from the RAGKO and CD45RAGKO spleens by comparing the expression levels of ICAM-I, VCAM-1 and PDPN. Compared to the RAGKO FRCs, CD45RAGKO FRCs had an increased percentage and number of more immature ICAM-1^{low} VCAM-1^{low} and ICAM-1^{mid} VCAM-1^{mid} cells (Figure 5.6D), while the frequency of mature ICAM-1^{high} VCAM-1^{high} cells was lower in the FRC from the CD45RAGKO spleens, but with no difference in cell numbers (Figure 5.6D). Likewise, PDPN expression level was generally lower in CD45RAKO spleen (Figure 5.6E). Also, the level of PDPN expression was stratified from low, mid to high. CD45RAGKO FRCs were skewed towards low expression of PDPN and the number of $PDPN^{Low}$ FRCs were greater but the number of $PDPN^{mid}$ and $PDPN^{High}$ FRCs were comparable to the RAGKO (Figure 5.6F). These results indicate that the FRCs in the CD45RAGKO spleen are more immature compared to the RAGKO spleen.

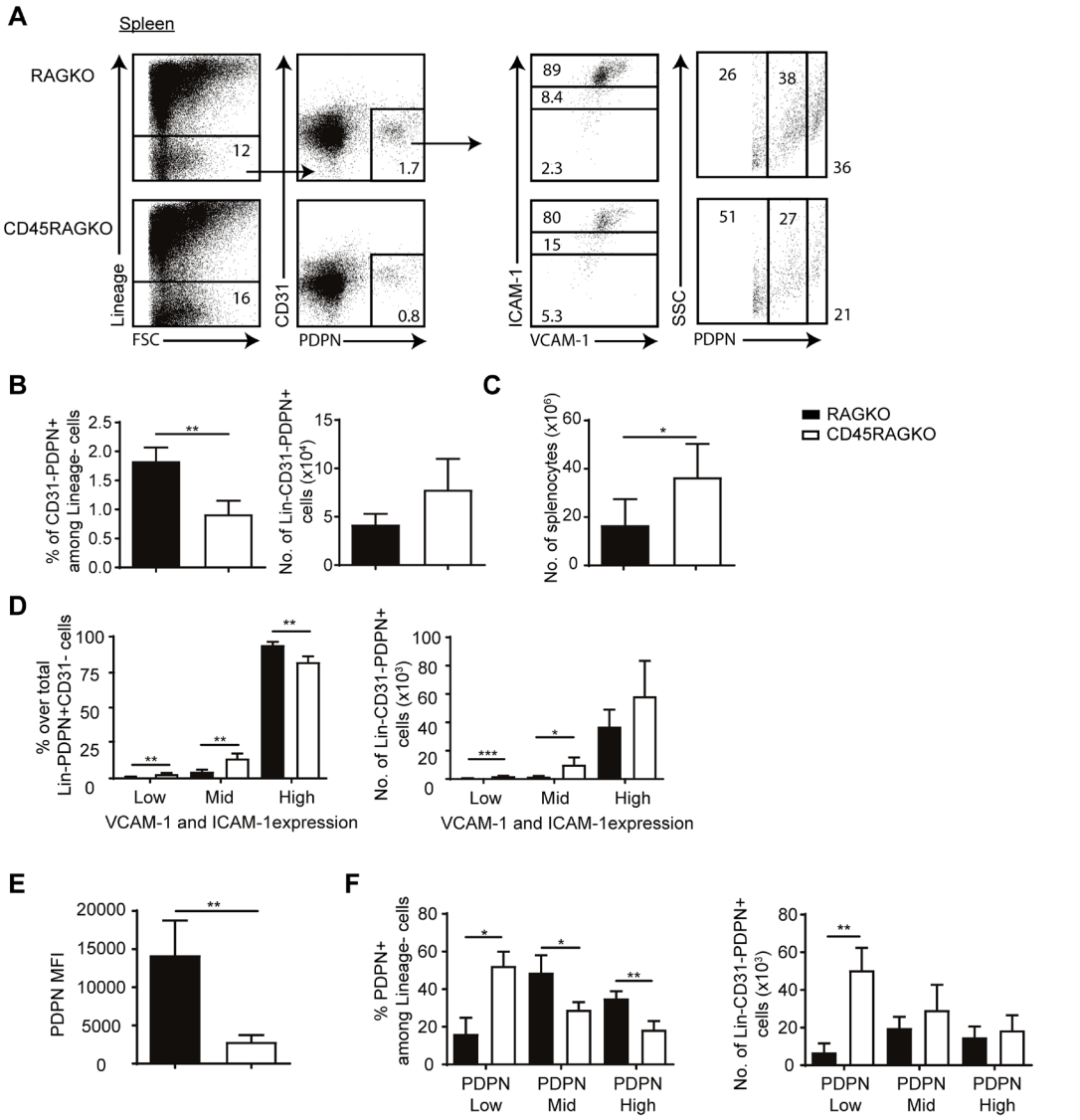

Figure 5.6 More immature FRCs are present in the CD45RAGKO spleen compared to the RAGKO spleen

(A) Representative flow cytometric analysis of RAGKO and CD45RAGKO splenocytes after enzymatic digestion to gate for the FRC (Lineage-PDPN+CD31-) population and to compare their surface expression of ICAM-1, VCAM-1 and PDPN. (B) Frequency and number of FRCs in spleen. (C) Number of splenocytes after enzymatic digestion and RBC lysis. (D) Frequency and number of FRCs that have low, mid, or high levels of ICAM-1 and VCAM-1 expression. (E) Expression level of PDPN on FRC. (F) Frequency and number of FRCs that have low, mid, or high levels of ICAM-1 and VCAM-1 expression. (F) Frequency and number of FRCs that have low, mid, or high levels of PDPN expression. (A-F) Data pooled from 2 experiments, n=6

In contrast to the spleen, the majority of the FRC in pLNs of CD45RAGKO mice had the mature phenotype (Figure 7A). CD45RAGKO pLNs had both a higher frequency and number of total FRCs at steady state, which was attributed to more mature FRCs, where the expression of ICAM-1, VCAM-1 and PDPN was similar to FRCs from the RAGKO mice (Figure 5.7 A-D).

5.2.5 CD45RAGKO spleen has a trend for low LTa ad LTb expression at the message level but no difference in LTβR expression

Since the defect in maturation has been observed from the FRCs in the CD45RAGKO spleen, I next questioned how CD45 could affect the maturation of stromal cells. LT, which is a complex of one α and two β subunits, is well defined as a key cytokine which mediates the interaction between immune cells and stromal cells and drives MSC proliferation and maturation into functional FRCs (Vondenhoff et al., 2009). Therefore, I hypothesized that CD45RAGKO mice could have defective LT production or LT signaling.

IL-7, LTa and LTb mRNA levels were measured from total spleen and pLNs. As expected, IL-7 mRNA was lower both in spleen and pLNs of CD45RAGKO mice, which helps to explain the reduced slow LIP in these mice (Figure 5.8A-B). CD45RAGKO spleen had equal amount of LTa transcripts, but had significantly lower amount of LTb compared to RAGKO. CD45RAGKO pLNs showed no significant difference in either LTa or LTb compared to RAGKO pLNs. While LTa and LTb levels should be also be assessed at the protein levels before drawing conclusions, the significant reduction in LTb levels observed in the CD45RAGKO spleen but not in pLNs may explain why the CD45RAGKO spleen has more immature FRCs compared to the RAGKO spleen.

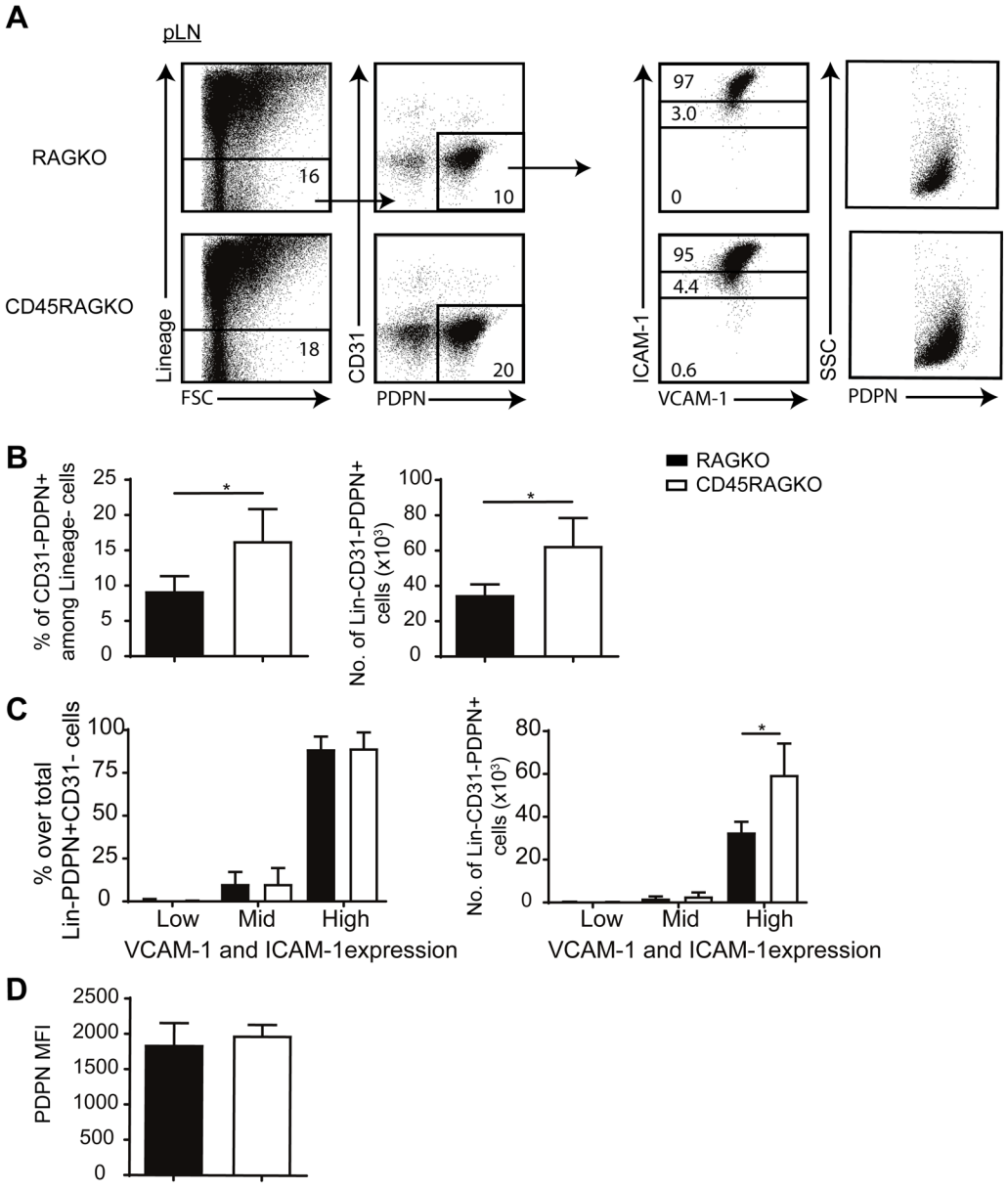

Figure 5.7 More mature FRCs in the CD45RAGKO pLN than the the RAGKO pLN

(A) Representative flow cytometric analysis of cells released from RAGKO and CD45RAGKO pLNs by enzymatic digestion and gated for the FRC (Lineage$^-$PDPN$^+$CD31$^-$) population and to compare their surface expression of ICAM-1, VCAM-1 and PDPN. (B) Frequency and number of FRCs in pLN. (C) Frequency and number of FRCs that have low, mid or high levels of ICAM-1 and VCAM-1 expression. (D) Expression level of PDPN on FRC. Data pooled from two experiments, n=5-6. (A-D) Data pooled from 2 experiments, n=6

Flow cytometric analysis showed LTβR expression by the FRC during steady state. Both the RAGKO and CD45RAGKO FRCs from spleen and pLNs expressed LTβR on the cell surface. However, no difference in the level of LTβR expression was observed between the FRCs from RAGKO and CD45RAGKO mice in spleen and pLNs (Figure 5.8C).

5.3 Discussion

Previous work showed that CD45 expression on myeloid cell is important for supporting both fast LIP and slow LIP, and that transfer of $CD45^+$ $CD11c^+$ cells into CD45RAGKO can partially increase fast LIP (Saunders et al., 2014). My work investigated additional factors that could contribute to the reduced T cell LIP observed in CD45RAGKO mice.

The fact that $CD45^+$ $CD11c^+$ cells could not fully restore fast LIP in CD45RAGKO mice suggested that CD45RAGKO mice have defects other than what can be accounted for by antigen presenting cells. Therefore, I looked at the microbiota which was suggested to be the source of antigens that drive fast LIP (Feng et al., 2010). Depletion of microbiota significantly reduced fast T cell LIP but not slow LIP in both RAGKO and CD45RAGKO mice. This data complements the work of others showing that fast LIP requires the microbiota (Feng et al., 2010; Kieper et al., 2005). The presence of microbiota has been shown to support IL-7 expression in the intestine (Vonarbourg et al., 2010). However, antibiotic treatment did not change the level of IL-7 transcript level in the SLO, which helps to explain why slow LIP was unaffected by the antibiotic treatment.

While the treatment of antibiotics significantly reduced the amount of 16s rDNA in the feces to levels undetectable by qPCR, it did not completely abolish the fast LIP. It is possible that the remaining fast LIP could be derived from a residual microbe or antigens still present

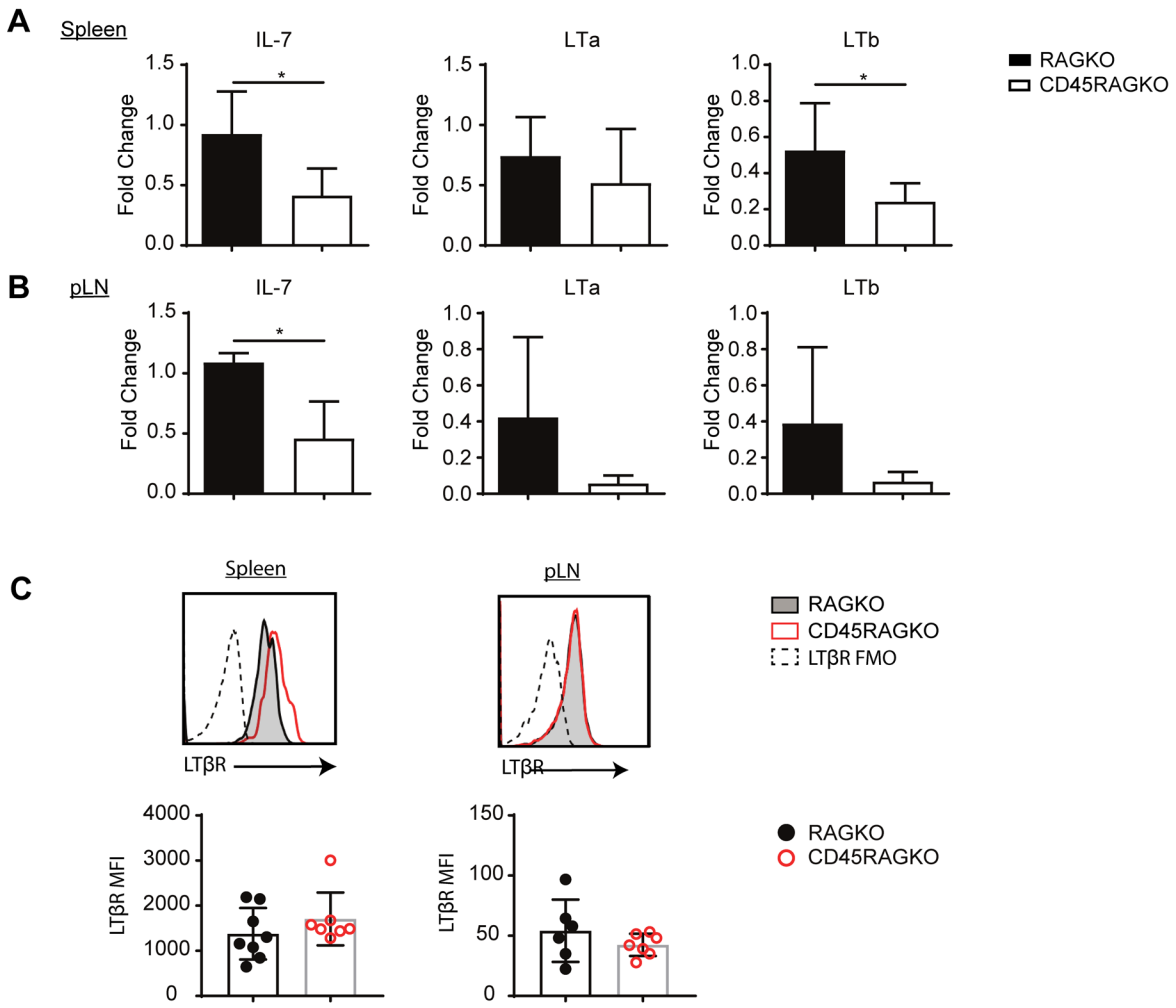

Figure 5.8 Expression levels of IL-7, LTa, LTb and LTβR in the spleen and pLN of CD45RAGKO and RAGKO mice

(A) Level of IL-7, LTa and LTb mRNA normalized to GAPDH measured from the whole spleen from RAGKO and CD45RAGKO mice. Data pooled from 2 experiments, n=6-7. (B) Level of IL-7, LTa and LTb mRNA normalized to GAPDH measured from whole pLNs from RAGKO and CD45RAGKO mice. Data pooled from 2 experiments, n=6. (C) Representative flow cytometric analysis of LTβR expression on FRCs isolated from spleen and pLNs. Graphs show data pooled from 2 experiments, n= 7-8.

after the antibiotic regimen. However, others who have studied LIP in germ free RAGKO mice also observed a reduced but not abolished fast LIP (Feng et al., 2010; Kieper et al., 2005), which suggests that there are signals which come from an antigen source other than the microbiota, such as self. Altogether, these findings imply that the microbiota helps to support the maintenance of the T cell population through LIP, and CD45 is implicated in these interactions, playing a role as a positive regulator.

The difference in fast LIP between the RAGKO and CD45RAGKO mice was removed by the antibiotics, suggesting that the different microbiota in the RAGKO and CD45RAGKO mice may be partially responsible for the comparatively inefficient LIP in CD45RAGKO mice. Transferring fecal matter from RAGKO cage into CD45RAGKO cages increased the frequency of the cells that have undergone fast LIP in the pLNs of CD45RAGKO mice, but the difference in cell number did not reach statistical significance. This result may suggest that microbiota in the RAGKO mice is better at inducing T cell expansion than that of CD45RAGKO mice. However, the increase did not fully restore the levels to that of the RAGKO mice, raising the possibility that other defects such as lack of CD45 on $CD11c^{+}$ cells, or incomplete fecal reconstitution could account for this difference. The microbiota was never analyzed after fecal transfer, so the percentage change is unknown. Another caveat of this experiment is that RAGKO and CD45RAGKO mice could have different stabilities of the pre-existing microbial community and thus have varying efficiency of assimilation of microbial community by fecal transfer. This was reported to be the case with WT and CD45KO mice, based on comparing the bacterial community detected from the feces of WT and CD45KO mice co-housed together compared to non-cohoused mice (Dimitriu et al., 2013). A better experiment would be to deplete

the microbiota using antibiotics prior to fecal transfer, or to do a fecal transfer into germ free mice and compare the LIP.

CD45RAGKO mice also have problems supporting slow LIP, which was attributed to defective IL-7 production by the stromal cells in the SLO (Saunders et al., 2014). In the spleen I found evidence for reduced FRC maturation indicated by the lower level of ICAM-1, VCAM-1 and PDPN expression on the cell surface, but this was not the case for FRCs in pLNs where the majority of FRCs were mature. This suggested that CD45 may be needed to promote maturation of FRCs in the spleen but not the pLNs, where more FRCs were present in the absence of CD45. However, it does not help to explain the defective IL-7 production by the FRCs in the CD45RAGKO SLOs, which may happen independently of maturation. Why the CD45RAGKO spleens have less mature FRC is unknown. It is possible that CD45RAGKO FRCs have an early developmental defect, which could be answered by comparing FRCs during fetal lymph-organogenesis, during which an ILC subset, LTi's, play an important role in the development of FRCs (Vondenhoff et al., 2009). Whether CD45 effects LTi cells is a topic for future investigation. It may be interesting to look at the function of CD45 in innate lymphoid cells, especially in the spleen, using a targeted deletion of CD45 on ILCs. So far, the only known impact of CD45 on ILC is in the reduced number of Rorγt^{+} ILCs in the lamina propria of CD45RAGKO mice in DSS-colitis (Samarakoon et al., 2016).

Compared to the RAGKO spleen and also to the CD45RAGKO pLNs, CD45RAGKO spleen had an increased number of immature FRCs, which had lower expression of ICAM-1, VCAM-1 and PDPN. PDPN expression by FRCs has been shown to induce efficient migration of DCs to and within the LNs through a direct engagement between PDPN on the FRCs and C-type lectin receptor, CLEC-2, on the DCs (Acton et al., 2012). In an earlier experiment, I

observed that the depletion of microbiota using antibiotics removed the difference between fast LIP occurring in the RAGKO and CD45RAGKO pLNs; however, the significant difference in the fast LIP of the CD4 T cell occurring in the spleen was retained. As the reduced level of PDPN expression on FRCs was observed in the CD45RAGKO spleen, it is possible that the CD45RAGKO spleen had an additional defect in the migration of DCs. Furthermore, in the LIP experiment where CD45RAGKO mice received fecal matter from either RAGKO or CD45RAGKO mice, the effect of fecal transfer was better demonstrated in the pLNs than in the spleen. This may suggest that the trafficking of antigens or the antigen presenting cells to the pLNs is more efficient than to the spleens, which may also be due to lower PDPN expression by the splenic FRCs in CD45RAGKO mice.

LT presentation by tissue resident ILCs in the SLO have been reported to induce IL-7 production by stromal cells during fetal development and post-infection tissue remodeling (Chai et al., 2013; Onder et al., 2012) . Therefore, I measured LTa and LTb mRNA levels from the spleen and pLNs to see if CD45RAGKO mice have lower levels of LTa and LTb than the RAGKO in the SLO. Although there was a trend for less LTa and LTb in the pLN, because of the low levels, I only detected a significant reduction in LTb from the spleen. Perhaps this needs to be looked at in fetal mice when the LN are developing and LTi cells are prevalent. Also, further assessment at the protein level is needed, especially on the isolated ILCs to see if the CD45RAGKO SLO do have lower LT levels. After LCMV infection, an increased level of IL-7 in the SLO induces LT expression by the LTi, which then activates stromal cells to upregulate IL-7 production, suggesting that IL-7 and LT mutually upregulate the expression of each other in a feed-forward manner (Onder et al., 2012). Since RAGKO mice have a higher level of IL-7 in

SLO due to their lack of T cells, it is possible that RAGKO mice have constitutively activated stromal cells with active LT and IL-7 signaling happening at steady state.

Recently, a term, virtual-memory T (T_{VM}) cells has appeared in immunological studies, referring to a population that have a $CD44^{high}CD62L^{low}$ phenotype similar to memory T cells, but are antigen-inexperienced (Kawabe et al., 2018; White et al., 2017). Found in both human and mouse, T_{VM} resemble T cells from homeostatic proliferation as they are only found in the periphery, outside of the thymus, and their frequency is low in young mice and increases with age (Akue et al., 2012). Furthermore, T_{VM} share many markers of T cells that have undergone homeostatic proliferation modeled by LIP (Haluszczak et al., 2009). T_{VM} are present in mice free of microbiota or food-derived antigens (Kim et al., 2016), but absent in mice that are deficient in IL-15 (White et al., 2016), which suggests that they are more similar to the T cells from slow LIP. Both $CD4^+$ and $CD8^+$ T_{VM} has been implicated in increased protection from type 1 immunity modeled by *Listeria monocytogenes* and *Toxoplasma gondii* infections, through their robust production of IFNγ in response to IL-12 and IL-18 stimulation (Kawabe et al., 2017; White et al., 2016).

CD45 is best understood as a regulator of signaling pathways within immunocytes, such as in TCR signaling pathways (Johnson et al., 2012). This work shows the involvement of CD45 in a broader sense, as we have seen the effect of CD45 extending beyond immune cells to microbiota and stromal cells, which in turn affects the ability of the host to drive fast LIP and slow LIP. LIP is reported to occur naturally in neonates with developing immune systems and in lymphocyte-deficient patients (Chomont et al., 2009; Min et al., 2003). Also, fast LIP in response to innate stimulation of microbiota has been described to a key process in inducing experimental

colitis in mice (Feng et al., 2010). This combined with recent research on T_{VM} cells in immune responses, understanding the role of CD45 in LIP may suggest new avenues for immunotherapy.

Chapter 6: Summary and Future Directions

6.1 Role of CD45 in Erythroid Development

It has previously been shown that CD45 is implicated in the negative regulation of erythropoiesis through culturing of bone marrow from mice and $CD34^+$ cells from human cord blood (Harashima et al., 2002; Irie-Sasaki et al., 2001). However, how CD45 impacts erythropoiesis *in vivo* was unknown. In this study, I found that CD45 negatively regulates late erythroid development, especially in extramedullary erythropoiesis in spleen, by regulating the EPO pathway.

The absence of CD45 resulted in higher numbers of Pro E, Ery A and Ery B populations with increased proliferative activity from Pro E and Ery A cells. Higher numbers of $CD71^+TER119^+$ cells in the spleen is normal in juvenile mice and these are reduced as the mice mature (Elahi et al., 2013). This occurred in the RAGKO mice, but the CD45RAGKO mice retained high numbers of the erythroid progenitors into adulthood. Despite the increased number of $CD71^+TER119^+$ cells in the CD45RAGKO spleen, the number of mature RBCs was equal to the RAGKO due to increased apoptotic activities in the $CD71^+TER119^+$ cells. CD45RAGKO mice had increased erythroid progenitors in the spleen due to increased EPO levels in the spleen and increased sensitivity to EPO signaling. The later was demonstrated by increased pSTAT5 in the Ery A population whose expression of EPO receptor was the highest among the Pro E, Ery A, Ery B and Ery C populations and the expression of CD45 was retained at a detectable level. The impact of CD45 on erythropoiesis was greater in the spleen than in the bone marrow. This was attributed to the increased concentration of EPO in the spleen due to the increased number of EPO producing RPM.

Monocytes can give rise to RPMs through the activation of SPI-C expression, which is triggered by the phagocytosis of heme through RBCs (Haldar et al., 2014). Since CD45RAGKO mice have more apoptotic $CD71^{+}TER119^{+}$ cells, it is possible that CD45RAGKO spleens have a higher number of RPMs at steady state due to increased phagocytosis of the erythroid cells by the monocytes. This can be tested by comparing the number of RPMs in the RAGKO and CD45RAGKO mice at 3 weeks of age when the number of $CD71^{+}TER119^{+}$ cells are still comparable and also by adoptively transferring $CD45.1^{+}$ monocytes into RAGKO mice with or without the erythroid cells isolated from CD45RAGKO mice. If the increased erythroid cells lead to increased RPMs, then RAGKO mice would have increased GFP^{+} or $CD45.1^{+}$ RPMs when they are co-transferred with RBCs.

Currently, how the reduction of erythroid progenitors is regulated during development is not well understood. One study in rats showed that EPO production is higher around birth and is reduced around 3 weeks after birth, suggesting that reduction of the erythroid progenitors during maturation of juvenile mice could be through reduced EPO production (Eckardt et al., 1992). Expression of EPO is regulated by the heterodimeric transcription factor HIF, where one of its subunits is HIFα whose stability is low under conditions of adequate oxygen supply due to ubiquitination and subsequent proteasomal degradation (Jaakkola et al., 2001). During hypoxia, however, its degradation is prevented to allow activation of EPO transcription (Jaakkola et al., 2001). From these findings, I hypothesize that mice younger than 3 weeks of age have mild hypoxia due to increased metabolic activities during fast growth, which increases the expression of EPO. I also hypothesize that adult CD45-deficient mice failed to downregulate the erythroid progenitors in the extramedullary pool by failing to downregulate EPO, potentially from a continued hypoxic environment in these mice. If true, then the RPMs from CD45RAGKO mice

would be predicted to have relatively equal levels of EPO and HIFα both in the neonates and the adults while the RAGKO mice would have higher levels in the spleens of neonates compared to adults.

This work extends the previous work done *in vitro* and further elucidates the role of CD45 in the regulation of splenic erythropoiesis through regulating the RPM population. CD45 can dephosphorylate Lyn and JAK, which are both implicated in EPO signaling(Ingley et al., 2005; Witthuhn et al., 1993). Harashima *et al.* have shown that a CD45 binding antibody specifically increases phosphorylation of Lyn over JAK (Harashima et al., 2002). Yet, both LynKO or $Lyn^{up/up}$ mice do not precisely phenocopy CD45KO mice (Slavova-Azmanova et al., 2014; Slavova-Azmanova et al., 2013), leaving the molecular mechanism of how CD45 negatively regulates the EPO signaling pathway still unclear. To solve this question, the phosphorylation status of Lyn at both the positive and negative regulatory tyrosine residues can be compared between the $CD45^{+/+}$ and $CD45^{-/-}$, EPO starved and EPO stimulated erythroid progenitors upon generation of effective antibodies that can target a specific tyrosine residue that is phosphorylated.

6.2 Role of CD45 in T cell colitis and identification of an immunosuppressive role of $CD71^{+}TER119^{+}$ erythroid progenitors *in vivo*

In this study, the increased erythroid progenitors present in the CD45RAGKO mice was shown to confer delayed wasting in a T cell transfer model of colitis. The role of CD45 expression on nonlymphoid cells in the pathogenesis of colitis was examined by inducing colitis in RAGKO and CD45RAGKO mice with T cells from WT mice. CD45RAGKO mice had delayed weight loss even though the intestinal inflammation was comparable. Between LP and

spleen, CD45RAGKO mice had an equivalent number of total T cells and $Foxp3^+$, $IFN\gamma^+$ an IL-$17A^+$ T cells. This suggests that CD45 deficiency in the nonlymphoid cells does not affect their ability to activate T cells in T cell colitis, which agrees with a previous observation of comparable activation of OT-I T cells by $CD45^{+/+}$ and $CD45^{-/-}$ $CD11c^+$ when loaded with OVA peptide (Saunders et al., 2014).

In contrast, the lack of CD45 reduced TNFα production by neutrophils, $Ly6c^-$ monocytes/macrophages, and RPMs in the spleen but not in the colon. CD45RAGKO spleen has an increased number of $CD71^+TER119^+$ erythroid progenitor cells which have an immunosuppressive property (Elahi, 2019). Adoptive transfer of $CD71^+TER119^+$ cells from CD45RAGKO mice into RAGKO mice attenuated the weight loss in RAGKO mice and reduced TNFα production by RPMs in the spleen, confirming that $CD71^+TER119^+$ cells in the CD45RAGKO spleen contribute to the lower TNFα response. However, this did not fully lower TNFα production to the level observed in the CD45RAGKO control mice. Also, the production of TNFα from other cells, such as neutrophils and $Ly6c^-$ monocytes/macrophages, was unaffected by the transfer of $CD71^+TER119^+$ cells, suggesting that these cells have intrinsic defects due to the lack of CD45 and that CD45 negatively regulates proinflammatory cytokine production or are affected by a different extrinsic mechanism.

Using an *in vitro* stimulation and coculturing system, RPMs were shown to downregulate TNFα expression in the presence of erythroid cells. Furthermore, RPMs were found to be highly phagocytic of RBCs compared to other myeloid cells in the spleen and the ones that had phagocytosed RBCs were negative for TNFα. It is possible that the phagocytosis of erythroid cells by RPMs turn off their TNFα expression and this could be evaluated by qPCR. But it is also possible that there is heterogeneity within the $F4/80^+CD11b^-$ population, where the ones that are

phagocytic are anti-inflammatory while the nonphagocytic ones are proinflammatory. An interesting hypothesis to test in the future is whether more recently monocyte-derived macrophages are more inflammatory, while the ones that are tissues resident or have adapted to the environment for a longer period are less inflammatory, and better at clearance of the oxidized RBCs through phagocytosis. One way to test this is through single-cell RNA sequencing and pathway analysis before and after stimulation and phagocytosis of RBCs by the RPMs and monocytes.

In the clinic, as many as one-third of IBD patients develop anemia mediated by excessive production of TNFα, IL-1 and IL-6, which can be treated with exogenous EPO (Gasche et al., 2004; Nairz et al., 2011). Studies have reported that EPO treatment not only alleviates the anemia but also intestinal and systemic inflammation due to an unprecedented role for EPO in triggering anti-inflammatory responses (Nairz et al., 2011). Here, my findings suggest that EPO may also elicit an anti-inflammatory response by increasing erythroid progenitor populations, which could further increase the anti-inflammatory RPM population.

6.3 Role of CD45 in Driving Homeostatic Proliferation of T cells

Here I showed that CD45 on nonlymphoid cells supports the homeostatic proliferation of T cells. In the first half, I showed that the expression of CD45 on $CD11c^+$ cells and the presence of intestinal microbiota both promote fast LIP. A trend for increased fast LIP was observed from CD45RAGKO mice when the microbiota from RAGKO was given through fecal transfer, however the difference was not statistically significant and was only observed in the pLNs and not the spleen. The caveats of this experiment may be an incomplete reconstitution of the microbiota and differences in the stability of the pre-existing microbial community, which could

impact the efficiency of assimilation of the microbial community by fecal transfer. In future experiments, a fecal transfer could be done after depleting the pre-existing community by antibiotic treatment. Alternatively, the fecal matter from RAGKO or CD45RAGKO mice could be transferred into GF RAGKO and CD45RAGKO hosts prior to inducing LIP.

I also showed that the maturation of stromal cells in the spleen as well as their IL-7 production at homeostasis were affected by the lack of CD45 expression on nonlymphoid cells. How CD45 is involved in the regulation of stromal cell maturation and number as well as IL-7 production is still unclear. Since the ILC subset called LTi has been described to play an important role in inducing stromal cell maturation during lymphorganogenesis at the fetal stage and restoration of LN after virus infections (Chai et al., 2013; Onder et al., 2012), it is possible that CD45 regulates stromal cell populations through LTi. The role of CD45 on ILCs has not been reported except for one publication that shows that CD45-deficient Rorγt^{+} ILCs have reduced production of IL-22 and GM-CSF in DSS-induced colitis (Samarakoon et al., 2016).

Erythroid progenitors have been shown to express arginase-2 and to suppress the proliferation of T cells (Elahi et al., 2013; Namdar et al., 2017). Since CD45RAGKO mice have increased number of erythroid progenitor cells at steady state, it is possible that both slow and fast LIP of T cells in the CD45RAGKO spleen have been affected by the increased number of CD71^{+}TER119^{+} cells. To test this, erythroid cells can be temporarily depleted, possibly through phenylhydrazine, to see if this could increase LIP in the RAGKO mice or in the CD45RAGKO mice. Also, L-arginine can be supplemented to the mice which received T cells or the T cells with erythroid progenitor cells to first see if the injection of erythroid cells reduces T cell LIP, and also to see if the supplementation of L-arginine can reverse the effect of the erythroid cells on LIP.

6.4 Concluding Remarks

Here, I have described that CD45 positively regulates erythroid development in extramedullary erythropoiesis, extra-intestinal inflammation in T cell transfer colitis and factors which support LIP, pointing to an effect of CD45 on cellular interactions. This work emphasizes how communication between cells plays an important role in our body.

My work on the basic role of immunological interactions mediated by CD45 suggests a novel approach to alleviating anemia and extra-intestinal inflammation associated with IBD through transfusion of immunosuppressive erythroid cells. Also, the appropriate size of the T cell repertoire is crucial to mount a proper adaptive immune response, however expansion of T cells that are reactive against innocuous targets such as self or commensal microbiota can elicit detrimental results such as IBD. A better understanding of how peripheral expansion of T cell is regulated is therefore important and my work shows that CD45 plays a role in this process.

References

Abraham, C., and Cho, J.H. (2009). Inflammatory Bowel Disease. N Engl J Med *361*, 2066-2078.

Acton, S.E., Astarita, J.L., Malhotra, D., Lukacs-Kornek, V., Franz, B., Hess, P.R., Jakus, Z., Kuligowski, M., Fletcher, A.L., Elpek, K.G.*, et al.* (2012). Podoplanin-rich stromal networks induce dendritic cell motility via activation of the C-type lectin receptor CLEC-2. Immunity *37*, 276-289.

Ahern, P.P., Izcue, A., Maloy, K.J., and Powrie, F. (2008). The interleukin-23 axis in intestinal inflammation. Immunol Rev *226*, 147-159.

Akilesh, H.M., Buechler, M.B., Duggan, J.M., Hahn, W.O., Matta, B., Sun, X., Gessay, G., Whalen, E., Mason, M., Presnell, S.R.*, et al.* (2019). Chronic TLR7 and TLR9 signaling drives anemia via differentiation of specialized hemophagocytes. Science *363*, eaao5213.

Akue, A.D., Lee, J.-Y., and Jameson, S.C. (2012). Derivation and Maintenance of Virtual Memory CD8 T Cells. J Immunol *188*, 2516-2523.

Argiles, J.M., Busquets, S., Stemmler, B., and Lopez-Soriano, F.J. (2015). Cachexia and sarcopenia: mechanisms and potential targets for intervention. Curr Opin Pharmacol *22*, 100-106.

Bachmann, S., Le Hir, M., and Eckardt, K.U. (1993). Co-localization of erythropoietin mRNA and ecto-5'-nucleotidase immunoreactivity in peritubular cells of rat renal cortex indicates that fibroblasts produce erythropoietin. J Histochem Cytochem *41*, 335-341.

Barman, M., Unold, D., Shifley, K., Amir, E., Hung, K., Bos, N., and Salzman, N. (2008). Enteric Salmonellosis Disrupts the Microbial Ecology of the Murine Gastrointestinal Tract. Infection and Immunity *76*, 907-915.

Berger, S.A., Mak, T.W., and Paige, C.J. (1994). Leukocyte common antigen (CD45) is required for immunoglobulin E-mediated degranulation of mast cells. J Exp Med *180*, 471-476.

Blaeser, F., Bryce, P.J., Ho, N., Raman, V., Dedeoglu, F., Donaldson, D.D., Geha, R.S., Oettgen, H.C., and Chatila, T.A. (2003). Targeted inactivation of the IL-4 receptor alpha chain I4R motif promotes allergic airway inflammation. J Exp Med *198*, 1189-1200.

Bode, C., Sensken, S.C., Peest, U., Beutel, G., Thol, F., Levkau, B., Li, Z., Bittman, R., Huang, T., Tolle, M.*, et al.* (2010). Erythrocytes serve as a reservoir for cellular and extracellular sphingosine 1-phosphate. J Cell Biochem *109*, 1232-1243.

Bossola, M., Muscaritoli, M., Costelli, P., Bellantone, R., Pacelli, F., Busquets, S., Argilès, J., Lopez-Soriano, F.J., Civello, I.M., Baccino, F.M.*, et al.* (2001). Increased muscle ubiquitin mRNA levels in gastric cancer patients. Am J Physiol Regul Integr Comp Physiol *280*, R1518-R1523.

Bouscary, D., Pene, F., Claessens, Y.E., Muller, O., Chretien, S., Fontenay-Roupie, M., Gisselbrecht, S., Mayeux, P., and Lacombe, C. (2003). Critical role for PI 3-kinase in the control of erythropoietin-induced erythroid progenitor proliferation. Blood *101*, 3436-3443.

Boxall, S., Stanton, T., Hirai, K., Ward, V., Yasui, T., Tahara, H., Tamori, A., Nishiguchi, S., Shiomi, S., Ishiko, O.*, et al.* (2004). Disease associations and altered immune function in CD45 138G variant carriers. Human Molecular Genetics *13*, 2377-2384.

Brown, W.R.A., Barclay, A.N., Sunderland, C.A., and Williams, A.F. (1981). Identification of a glycophorin-like molecule at the cell surface of rat thymocytes. Nature *289*, 456-460.

Byth, K.F., Conroy, L.A., Howlett, S., Smith, A.J., May, J., Alexander, D.R., and Holmes, N. (1996). CD45-null transgenic mice reveal a positive regulatory role for CD45 in early thymocyte development, in the selection of CD4+CD8+ thymocytes, and B cell maturation. J Exp Med *183*, 1707-1718.
Cerami, A., Ikeda, Y., Le Trang, N., Hotez, P.J., and Beutler, B. (1985). Weight loss associated with an endotoxin-induced mediator from peritoneal macrophages: The role of cachectin (tumor necrosis factor). Immunol Lett *11*, 173-177.
Chai, Q., Onder, L., Scandella, E., Gil-Cruz, C., Perez-Shibayama, C., Cupovic, J., Danuser, R., Sparwasser, T., Luther, S.A., Thiel, V.*, et al.* (2013). Maturation of lymph node fibroblastic reticular cells from myofibroblastic precursors is critical for antiviral immunity. Immunity *38*, 1013-1024.
Chang, V.T., Fernandes, R.A., Ganzinger, K.A., Lee, S.F., Siebold, C., McColl, J., Jonsson, P., Palayret, M., Harlos, K., Coles, C.H.*, et al.* (2016). Initiation of T cell signaling by CD45 segregation at 'close contacts'. Nat Immunol *17*, 574-582.
Chen, K., Liu, J., Heck, S., Chasis, J.A., An, X., and Mohandas, N. (2009). Resolving the distinct stages in erythroid differentiation based on dynamic changes in membrane protein expression during erythropoiesis. Proc. Natl. Acad. Sci. U.S.A. *106*, 17413-17418.
Chomont, N., El-Far, M., Ancuta, P., Trautmann, L., Procopio, F.A., Yassine-Diab, B., Boucher, G., Boulassel, M.R., Ghattas, G., Brenchley, J.M.*, et al.* (2009). HIV reservoir size and persistence are driven by T cell survival and homeostatic proliferation. Nat Med *15*, 893-900.
Christodoulou, D.K., and Tsianos, E.V. (2000). Anemia in inflammatory bowel disease - the role of recombinant human erythropoietin. European journal of internal medicine *11*, 222-227.
Coombes, J.L., and Powrie, F. (2008). Dendritic cells in intestinal immune regulation. Nat Rev Immunol *8*, 435-446.
Cronin, C.C., and Shanahan, F. (2005). Understanding symptoms and signs in inflammatory bowel disease. In Inflammatory Bowel Disease: From Bench to Bedside, S.R. Targan, F. Shanahan, and L.C. Karp, eds. (Boston, MA: Springer US), pp. 253-267.
Cross, J.L., Kott, K., Miletić, T., and Johnson, P. (2008). CD45 Regulates TLR-Induced Proinflammatory Cytokine and IFN-β Secretion in Dendritic Cells. J Immunol *180*, 8020-8029.
Danese, S., and Fiocchi, C. (2011). Ulcerative colitis. The New England journal of medicine *365*, 1713-1725.
De Maria, R., Testa, U., Luchetti, L., Zeuner, A., Stassi, G., Pelosi, E., Riccioni, R., Felli, N., Samoggia, P., and Peschle, C. (1999). Apoptotic Role of Fas/Fas Ligand System in the Regulation of Erythropoiesis. Blood *93*, 796-803.
Delyea, C., Bozorgmehr, N., Koleva, P., Dunsmore, G., Shahbaz, S., Huang, V., and Elahi, S. (2018). CD71+ Erythroid Suppressor Cells Promote Fetomaternal Tolerance through Arginase-2 and PDL-1. J Immunol *200*, 4044-4058.
Devemy, E., Billat, C., and Haye, B. (1997). Activation of Raf-1 and Mitogen-Activated Protein Kinases by Erythropoietin and Inositolphosphate-Glycan in Normal Erythroid Progenitor Cells: Involvement of Protein Kinase C. Cell. Signalling *9*, 41-46.
Dillon, S., Agrawal, S., Banerjee, K., Letterio, J., Denning, T.L., Oswald-Richter, K., Kasprowicz, D.J., Kellar, K., Pare, J., van Dyke, T.*, et al.* (2006). Yeast zymosan, a stimulus for TLR2 and dectin-1, induces regulatory antigen-presenting cells and immunological tolerance. J Clin Invest *116*, 916-928.

Dimitriu, P.A., Boyce, G., Samarakoon, A., Hartmann, M., Johnson, P., and Mohn, W.W. (2013). Temporal stability of the mouse gut microbiota in relation to innate and adaptive immunity. Environmental Microbiology Reports *5*, 200-210.
Drayton, D.L., Liao, S., Mounzer, R.H., and Ruddle, N.H. (2006). Lymphoid organ development: from ontogeny to neogenesis. Nature Immunology *7*, 344-353.
Dunsmore, G., Koleva, P., Ghobakhloo, N., Sutton, R.T., Ambrosio, L., Meng, X., Hotte, N., Nguyen, V., Madsen, K.L., Dieleman, L.A.*, et al.* (2018). Lower Abundance and Impaired Function of CD71+ Erythroid Cells in Inflammatory Bowel Disease Patients During Pregnancy. J Crohns Colitis.
Dzierzak, E., and Philipsen, S. (2013). Erythropoiesis: development and differentiation. Cold Spring Harbor perspectives in medicine *3*, a011601-a011601.
Eckardt, K.U., Ratcliffe, P.J., Tan, C.C., Bauer, C., and Kurtz, A. (1992). Age-dependent expression of the erythropoietin gene in rat liver and kidneys. J. Clin. Invest. *89*, 753-760.
Elahi, S. (2019). Neglected Cells: Immunomodulatory Roles of CD71+ Erythroid Cells. Trends Immunol *40*, 181-185.
Elahi, S., Ertelt, J.M., Kinder, J.M., Jiang, T.T., Zhang, X., Xin, L., Chaturvedi, V., Strong, B.S., Qualls, J.E., Steinbrecher, K.A.*, et al.* (2013). Immunosuppressive CD71+ erythroid cells compromise neonatal host defence against infection. Nature *504*, 158-162.
Ema, H., and Nakauchi, H. (2000). Expansion of hematopoietic stem cells in the developing liver of a mouse embryo. Blood *95*, 2284-2288.
Eri, R., McGuckin, M.A., and Wadley, R. (2012). T Cell Transfer Model of Colitis: A Great Tool to Assess the Contribution of T Cells in Chronic Intestinal Inflammation. In Leucocytes: Methods and Protocols, R.B. Ashman, ed. (Totowa, NJ: Humana Press), pp. 261-275.
Erslev, A.J., Caro, J., Kansu, E., and Silver, R. (1980). Renal and extrarenal erythropoietin production in anaemic rats. Br J Haematol *45*, 65-72.
Evans, W.J., Morley, J.E., Argiles, J., Bales, C., Baracos, V., Guttridge, D., Jatoi, A., Kalantar-Zadeh, K., Lochs, H., Mantovani, G.*, et al.* (2008). Cachexia: a new definition. Clin Nutr *27*, 793-799.
Fearon, K., Strasser, F., Anker, S.D., Bosaeus, I., Bruera, E., Fainsinger, R.L., Jatoi, A., Loprinzi, C., MacDonald, N., Mantovani, G.*, et al.* (2011). Definition and classification of cancer cachexia: an international consensus. Lancet Oncol *12*, 489-495.
Feng, T., Wang, L., Schoeb, T.R., Elson, C.O., and Cong, Y. (2010). Microbiota innate stimulation is a prerequisite for T cell spontaneous proliferation and induction of experimental colitis. J Exp Med *207*, 1321-1332.
Finne, P.H., and Halvorsen, S. (1972). Regulation of erythropoiesis in the fetus and newborn. Arch Dis Child *47*, 683-687.
Fiocchi, C. (1998). Inflammatory bowel disease: Etiology and pathogenesis. Gastroenterology *115*, 182-205.
Fisher, R.L. (1999). Wasting in Chronic Gastrointestinal Diseases. J Nutr *129*, 252S-255S.
Fletcher, A., Malhotra, D., Acton, S., Lukacs-Kornek, V., Bellemare-Pelletier, A., Curry, M., Armant, M., and Turley, S. (2011). Reproducible Isolation of Lymph Node Stromal Cells Reveals Site-Dependent Differences in Fibroblastic Reticular Cells. Front. Immunol. *2*.
Fowler, J.H., and Nash, D.J. (1968). Erythropoiesis in the spleen and bone marrow of the pregnant mouse. Dev Biol *18*, 331-353.

Franco, R.S. (2012). Measurement of red cell lifespan and aging. Transfus Med Hemother *39*, 302-307.
Friedrich, M., Pohin, M., and Powrie, F. (2019). Cytokine Networks in the Pathophysiology of Inflammatory Bowel Disease. Immunity *50*, 992-1006.
Gasche, C., Lomer, M.C., Cavill, I., and Weiss, G. (2004). Iron, anaemia, and inflammatory bowel diseases. Gut *53*, 1190-1197.
Ge, Q., Rao, V.P., Cho, B.K., Eisen, H.N., and Chen, J. (2001). Dependence of lymphopenia-induced T cell proliferation on the abundance of peptide/ MHC epitopes and strength of their interaction with T cell receptors. Proc. Natl. Acad. Sci. U.S.A. *98*, 1728-1733.
Gillinder, K.R., Tuckey, H., Bell, C.C., Magor, G.W., Huang, S., Ilsley, M.D., and Perkins, A.C. (2017). Direct targets of pSTAT5 signalling in erythropoiesis. PLOS ONE *12*, e0180922.
Grochowy, G., Hermiston, M.L., Kuhny, M., Weiss, A., and Huber, M. (2009). Requirement for CD45 in fine-tuning mast cell responses mediated by different ligand–receptor systems. Cell. Signalling *21*, 1277-1286.
Groux, H., O'Garra, A., Bigler, M., Rouleau, M., Antonenko, S., de Vries, J.E., and Roncarolo, M.G. (1997). A CD4+ T-cell subset inhibits antigen-specific T-cell responses and prevents colitis. Nature *389*, 737-742.
Haldar, M., Kohyama, M., So, Alex Y.-L., Kc, W., Wu, X., Briseño, Carlos G., Satpathy, Ansuman T., Kretzer, Nicole M., Arase, H., Rajasekaran, Namakkal S.*, et al.* (2014). Heme-Mediated SPI-C Induction Promotes Monocyte Differentiation into Iron-Recycling Macrophages. Cell *156*, 1223-1234.
Haluszczak, C., Akue, A.D., Hamilton, S.E., Johnson, L.D., Pujanauski, L., Teodorovic, L., Jameson, S.C., and Kedl, R.M. (2009). The antigen-specific CD8+ T cell repertoire in unimmunized mice includes memory phenotype cells bearing markers of homeostatic expansion. J Exp Med *206*, 435-448.
Hampe, J., Franke, A., Rosenstiel, P., Till, A., Teuber, M., Huse, K., Albrecht, M., Mayr, G., De La Vega, F.M., Briggs, J.*, et al.* (2007). A genome-wide association scan of nonsynonymous SNPs identifies a susceptibility variant for Crohn disease in ATG16L1. Nature genetics *39*, 207-211.
Hanel, P., Andreani, P., and Graler, M.H. (2007). Erythrocytes store and release sphingosine 1-phosphate in blood. FASEB J *21*, 1202-1209.
Hara, H., and Ogawa, M. (1976). Erythropoietic precursors in mice with phenylhydrazine-induced anemia. Am J Hematol *1*, 453-458.
Harashima, A., Suzuki, M., Okochi, A., Yamamoto, M., Matsuo, Y., Motoda, R., Yoshioka, T., and Orita, K. (2002). CD45 tyrosine phosphatase inhibits erythroid differentiation of umbilical cord blood CD34+ cells associated with selective inactivation of Lyn. Blood *100*, 4440-4445.
Harder, K.W., Quilici, C., Naik, E., Inglese, M., Kountouri, N., Turner, A., Zlatic, K., Tarlinton, D.M., and Hibbs, M.L. (2004). Perturbed myelo/erythropoiesis in Lyn-deficient mice is similar to that in mice lacking the inhibitory phosphatases SHP-1 and SHIP-1. Blood *104*, 3901-3910.
Hashimoto, D., Chow, A., Noizat, C., Teo, P., Beasley, M.B., Leboeuf, M., Becker, C.D., See, P., Price, J., Lucas, D.*, et al.* (2013). Tissue-resident macrophages self-maintain locally throughout adult life with minimal contribution from circulating monocytes. Immunity *38*, 792-804.
Hermansen, M.C. (2001). Nucleated red blood cells in the fetus and newborn. Archives of Disease in Childhood - Fetal and Neonatal Edition *84*, F211-F215.

Hermiston, M.L., Xu, Z., and Weiss, A. (2003). CD45: A Critical Regulator of Signaling Thresholds in Immune Cells. Annu Rev Immunol *21*, 107-137.
Hesslein, D.G.T., Palacios, E.H., Sun, J.C., Beilke, J.N., Watson, S.R., Weiss, A., and Lanier, L.L. (2011). Differential requirements for CD45 in NK-cell function reveal distinct roles for Syk-family kinases. Blood *117*, 3087-3095.
Hesslein, D.G.T., Takaki, R., Hermiston, M.L., Weiss, A., and Lanier, L.L. (2006). Dysregulation of signaling pathways in CD45-deficient NK cells leads to differentially regulated cytotoxicity and cytokine production. Proc. Natl. Acad. Sci. U.S.A. *103*, 7012-7017.
Ingley, E., and Klinken, S.P. (2006). Cross-regulation of JAK and Src kinases. Growth Factors *24*, 89-95.
Ingley, E., McCarthy, D.J., Pore, J.R., Sarna, M.K., Adenan, A.S., Wright, M.J., Erber, W., Tilbrook, P.A., and Klinken, S.P. (2005). Lyn deficiency reduces GATA-1, EKLF and STAT5, and induces extramedullary stress erythropoiesis. Oncogene *24*, 336-343.
Inoue, M., Arikawa, T., Chen, Y.-H., Moriwaki, Y., Price, M., Brown, M., Perfect, J.R., and Shinohara, M.L. (2014). T cells down-regulate macrophage TNF production by IRAK1-mediated IL-10 expression and control innate hyperinflammation. Proc. Natl. Acad. Sci. U.S.A. *111*, 5295-5300.
Irie-Sasaki, J., Sasaki, T., Matsumoto, W., Opavsky, A., Cheng, M., Welstead, G., Griffiths, E., Krawczyk, C., Richardson, C.D., Aitken, K.*, et al.* (2001). CD45 is a JAK phosphatase and negatively regulates cytokine receptor signalling. Nature *409*, 349-354.
Jaakkola, P., Mole, D.R., Tian, Y.M., Wilson, M.I., Gielbert, J., Gaskell, S.J., von Kriegsheim, A., Hebestreit, H.F., Mukherji, M., Schofield, C.J.*, et al.* (2001). Targeting of HIF-alpha to the von Hippel-Lindau ubiquitylation complex by O2-regulated prolyl hydroxylation. Science *292*, 468-472.
Jackson, A., Nanton, M.R., O'Donnell, H., Akue, A.D., and McSorley, S.J. (2010). Innate immune activation during Salmonella infection initiates extramedullary erythropoiesis and splenomegaly. J Immunol *185*, 6198-6204.
Jin, R., Wang, W., Yao, J.-Y., Zhou, Y.-B., Qian, X.-P., Zhang, J., Zhang, Y., and Chen, W.-F. (2008). Characterization of the In Vivo Dynamics of Medullary CD4⁺CD8[−] Thymocyte Development. J Immunol *180*, 2256-2263.
Johnson, P., Samarakoon, A., Saunders, A.E., and Harder, K.W. (2012). CD45 (PTPRC). In Encyclopedia of Signaling Molecules, S. Choi, ed. (New York, NY: Springer New York), pp. 328-334.
Kaplan, G.G., Bernstein, C.N., Coward, S., Bitton, A., Murthy, S.K., Nguyen, G.C., Lee, K., Cooke-Lauder, J., and Benchimol, E.I. (2018). The Impact of Inflammatory Bowel Disease in Canada 2018: Epidemiology. Journal of the Canadian Association of Gastroenterology *2*, S6-S16.
Kawabe, T., Jankovic, D., Kawabe, S., Huang, Y., Lee, P.-H., Yamane, H., Zhu, J., Sher, A., Germain, R.N., and Paul, W.E. (2017). Memory-phenotype CD4⁺ T cells spontaneously generated under steady-state conditions exert innate T_H1-like effector function. Science Immunology *2*, eaam9304.
Kawabe, T., Zhu, J., and Sher, A. (2018). Foreign antigen-independent memory-phenotype CD4+ T cells: a new player in innate immunity? Nat Rev Immunol *18*, 1.

Kazansky, A.V., and Rosen, J.M. (2001). Signal transducers and activators of transcription 5B potentiates v-Src-mediated transformation of NIH-3T3 cells. Cell growth & differentiation : the molecular biology journal of the American Association for Cancer Research *12*, 1-7.
Kieper, W.C., Troy, A., Burghardt, J.T., Ramsey, C., Lee, J.Y., Jiang, H.-Q., Dummer, W., Shen, H., Cebra, J.J., and Surh, C.D. (2005). Cutting Edge: Recent Immune Status Determines the Source of Antigens That Drive Homeostatic T Cell Expansion. J Immunol *174*, 3158-3163.
Kim, K.S., Hong, S.-W., Han, D., Yi, J., Jung, J., Yang, B.-G., Lee, J.Y., Lee, M., and Surh, C.D. (2016). Dietary antigens limit mucosal immunity by inducing regulatory T cells in the small intestine. Science *351*, 858-863.
Kishihara, K., Penninger, J., Wallace, V.A., Kundig, T.M., Kawai, K., Wakeham, A., Timms, E., Pfeffer, K., Ohashi, P.S., Thomas, M.L., and et al. (1993). Normal B lymphocyte development but impaired T cell maturation in CD45-exon6 protein tyrosine phosphatase-deficient mice. Cell *74*, 143-156.
Klei, T.R.L., Meinderts, S.M., van den Berg, T.K., and van Bruggen, R. (2017). From the Cradle to the Grave: The Role of Macrophages in Erythropoiesis and Erythrophagocytosis. Front. Immunol. *8*, 73-73.
Kling, P.J., Schmidt, R.L., Roberts, R.A., and Widness, J.A. (1996). Serum erythropoietin levels during infancy: Associations with erythropoiesis. J Pediatr *128*, 791-796.
Klingmuller, U., Wu, H., Hsiao, J.G., Toker, A., Duckworth, B.C., Cantley, L.C., and Lodish, H.F. (1997). Identification of a novel pathway important for proliferation and differentiation of primary erythroid progenitors. Proc Natl Acad Sci U S A *94*, 3016-3021.
Kohyama, M., Ise, W., Edelson, B.T., Wilker, P.R., Hildner, K., Mejia, C., Frazier, W.A., Murphy, T.L., and Murphy, K.M. (2009). Role for Spi-C in the development of red pulp macrophages and splenic iron homeostasis. Nature *457*, 318-321.
Kosmider, O., Buet, D., Gallais, I., Denis, N., and Moreau-Gachelin, F. (2009). Erythropoietin Down-Regulates Stem Cell Factor Receptor (Kit) Expression in the Leukemic Proerythroblast: Role of Lyn Kinase. PLOS ONE *4*, e5721.
Koulnis, M., Pop, R., Porpiglia, E., Shearstone, J.R., Hidalgo, D., and Socolovsky, M. (2011). Identification and analysis of mouse erythroid progenitors using the CD71/TER119 flow-cytometric assay. Journal of visualized experiments : JoVE, 2809.
Kozieradzki, I., Kündig, T., Kishihara, K., Ong, C.J., Chiu, D., Wallace, V.A., Kawai, K., Timms, E., Ionescu, J., Ohashi, P.*, et al.* (1997). T cell development in mice expressing splice variants of the protein tyrosine phosphatase CD45. J Immunol *158*, 3130-3139.
Kullberg, M.C., Andersen, J.F., Gorelick, P.L., Caspar, P., Suerbaum, S., Fox, J.G., Cheever, A.W., Jankovic, D., and Sher, A. (2003). Induction of colitis by a CD4+ T cell clone specific for a bacterial epitope. Proc Natl Acad Sci U S A *100*, 15830-15835.
Kullberg, M.C., Jankovic, D., Gorelick, P.L., Caspar, P., Letterio, J.J., Cheever, A.W., and Sher, A. (2002). Bacteria-triggered CD4(+) T regulatory cells suppress Helicobacter hepaticus-induced colitis. J Exp Med *196*, 505-515.
Kung, C., Pingel, J.T., Heikinheimo, M., Klemola, T., Varkila, K., Yoo, L.I., Vuopala, K., Poyhonen, M., Uhari, M., Rogers, M.*, et al.* (2000). Mutations in the tyrosine phosphatase CD45 gene in a child with severe combined immunodeficiency disease. Nat Med *6*, 343-345.
Kurotaki, D., Kon, S., Bae, K., Ito, K., Matsui, Y., Nakayama, Y., Kanayama, M., Kimura, C., Narita, Y., Nishimura, T.*, et al.* (2011). CSF-1–Dependent Red Pulp Macrophages Regulate CD4 T Cell Responses. J Immunol, 1001345.

Kurotaki, D., Uede, T., and Tamura, T. (2015). Functions and development of red pulp macrophages. Microbiol Immunol *59*, 55-62.
Lakatos, L., Pandur, T., David, G., Balogh, Z., Kuronya, P., Tollas, A., and Lakatos, P.L. (2003). [Extra-intestinal manifestation of IBD in Veszprem county (of Hungary): results of a 25-years follow-up study]. Orvosi hetilap *144*, 1965-1975.
Langhans, W., and Hrupka, B. (1999). Interleukins and tumor necrosis factor as inhibitors of food intake. Neuropeptides *33*, 415-424.
Lenz, D.C., Kurz, S.K., Lemmens, E., Schoenberger, S.P., Sprent, J., Oldstone, M.B.A., and Homann, D. (2004). IL-7 regulates basal homeostatic proliferation of antiviral CD4+T cell memory. Proc. Natl. Acad. Sci. U.S.A. *101*, 9357-9362.
Li, R., Wong, N., Jabali, M.D., and Johnson, P. (2001). CD44-initiated cell spreading induces Pyk2 phosphorylation, is mediated by Src family kinases, and is negatively regulated by CD45. J Biol Chem *276*, 28767-28773.
Link, A., Vogt, T.K., Favre, S., Britschgi, M.R., Acha-Orbea, H., Hinz, B., Cyster, J.G., and Luther, S.A. (2007). Fibroblastic reticular cells in lymph nodes regulate the homeostasis of naive T cells. Nat Immunol *8*, 1255-1265.
Llovera, M., Carbo, N., Garcia-Martinez, C., Costelli, P., Tessitore, L., Baccino, F.M., Agell, N., Bagby, G.J., Lopez-Soriano, F.J., and Argiles, J.M. (1996). Anti-TNF treatment reverts increased muscle ubiquitin gene expression in tumour-bearing rats. Biochem Biophys Res Commun *221*, 653-655.
Llovera, M., Garcia-Martinez, C., Lopez-Soriano, J., Carbo, N., Agell, N., Lopez-Soriano, F.J., and Argiles, J.M. (1998). Role of TNF receptor 1 in protein turnover during cancer cachexia using gene knockout mice. Mol Cell Endocrinol *142*, 183-189.
Luo, B., Gan, W., Liu, Z., Shen, Z., Wang, J., Shi, R., Liu, Y., Liu, Y., Jiang, M., Zhang, Z., and Wu, Y. (2016). Erythropoeitin Signaling in Macrophages Promotes Dying Cell Clearance and Immune Tolerance. Immunity *44*, 287-302.
Lutz, H.U. (2012). Naturally Occurring Anti-Band 3 Antibodies in Clearance of Senescent and Oxidatively Stressed Human Red Blood Cells. Transfusion Medicine and Hemotherapy *39*, 321-327.
Madu, A.J., and Ughasoro, M.D. (2017). Anaemia of Chronic Disease: An In-Depth Review. Med Princ Pract *26*, 1-9.
Manwani, D., and Bieker, J.J. (2008). Chapter 2 The Erythroblastic Island. In Current Topics in Developmental Biology (Academic Press), pp. 23-53.
Martin, B., Bourgeois, C., Dautigny, N., and Lucas, B. (2003). On the role of MHC class II molecules in the survival and lymphopenia-induced proliferation of peripheral CD4⁺ T cells. Proceedings of the National Academy of Sciences *100*, 6021-6026.
Martin, C.E., Frimpong-Boateng, K., Spasova, D.S., Stone, J.C., and Surh, C.D. (2013). Homeostatic proliferation of mature T cells. Methods in molecular biology (Clifton, N.J.) *979*, 81-106.
McCarroll, S.A., Huett, A., Kuballa, P., Chilewski, S.D., Landry, A., Goyette, P., Zody, M.C., Hall, J.L., Brant, S.R., Cho, J.H.*, et al.* (2008). Deletion polymorphism upstream of IRGM associated with altered IRGM expression and Crohn's disease. Nature genetics *40*, 1107-1112.
Medvinsky, A., and Dzierzak, E. (1996). Definitive hematopoiesis is autonomously initiated by the AGM region. Cell *86*, 897-906.

Mee, P.J., Turner, M., Basson, M.A., Costello, P.S., Zamoyska, R., and Tybulewicz, V.L. (1999). Greatly reduced efficiency of both positive and negative selection of thymocytes in CD45 tyrosine phosphatase-deficient mice. European journal of immunology *29*, 2923-2933.
Mendoza, J.L., Lana, R., Taxonera, C., Alba, C., Izquierdo, S., and Diaz-Rubio, M. (2005). [Extraintestinal manifestations in inflammatory bowel disease: differences between Crohn's disease and ulcerative colitis]. Medicina clinica *125*, 297-300.
Min, B., McHugh, R., Sempowski, G.D., Mackall, C., Foucras, G., and Paul, W.E. (2003). Neonates support lymphopenia-induced proliferation. Immunity *18*, 131-140.
Min, B., Yamane, H., Hu-Li, J., and Paul, W.E. (2005). Spontaneous and Homeostatic Proliferation of CD4 T Cells Are Regulated by Different Mechanisms. J Immunol *174*, 6039-6044.
Mirza, Z.K., Sastri, B., Lin, J.J., Amenta, P.S., and Das, K.M. (2006). Autoimmunity against human tropomyosin isoforms in ulcerative colitis: localization of specific human tropomyosin isoforms in the intestine and extraintestinal organs. Inflamm Bowel Dis *12*, 1036-1043.
Molenaar, R., Greuter, M., van der Marel, A.P., Roozendaal, R., Martin, S.F., Edele, F., Huehn, J., Forster, R., O'Toole, T., Jansen, W.*, et al.* (2009). Lymph node stromal cells support dendritic cell-induced gut-homing of T cells. Journal of immunology *183*, 6395-6402.
Moresi, V., Garcia-Alvarez, G., Pristera, A., Rizzuto, E., Albertini, M.C., Rocchi, M., Marazzi, G., Sassoon, D., Adamo, S., and Coletti, D. (2009). Modulation of caspase activity regulates skeletal muscle regeneration and function in response to vasopressin and tumor necrosis factor. PLoS One *4*, e5570.
Nairz, M., Schroll, A., Moschen, A.R., Sonnweber, T., Theurl, M., Theurl, I., Taub, N., Jamnig, C., Neurauter, D., Huber, L.A.*, et al.* (2011). Erythropoietin contrastingly affects bacterial infection and experimental colitis by inhibiting nuclear factor-kappaB-inducible immune pathways. Immunity *34*, 61-74.
Namdar, A., Koleva, P., Shahbaz, S., Strom, S., Gerdts, V., and Elahi, S. (2017). CD71+ erythroid suppressor cells impair adaptive immunity against Bordetella pertussis. Sci Rep *7*, 7728-7728.
Ng, S.C., Shi, H.Y., Hamidi, N., Underwood, F.E., Tang, W., Benchimol, E.I., Panaccione, R., Ghosh, S., Wu, J.C.Y., Chan, F.K.L.*, et al.* (2018). Worldwide incidence and prevalence of inflammatory bowel disease in the 21st century: a systematic review of population-based studies. Lancet *390*, 2769-2778.
O'Connor, W., Jr., Kamanaka, M., Booth, C.J., Town, T., Nakae, S., Iwakura, Y., Kolls, J.K., and Flavell, R.A. (2009). A protective function for interleukin 17A in T cell-mediated intestinal inflammation. Nat Immunol *10*, 603-609.
Ogura, Y., Bonen, D.K., Inohara, N., Nicolae, D.L., Chen, F.F., Ramos, R., Britton, H., Moran, T., Karaliuskas, R., Duerr, R.H.*, et al.* (2001). A frameshift mutation in NOD2 associated with susceptibility to Crohn's disease. Nature *411*, 603-606.
Onder, L., Narang, P., Scandella, E., Chai, Q., Iolyeva, M., Hoorweg, K., Halin, C., Richie, E., Kaye, P., Westermann, J.*, et al.* (2012). IL-7-producing stromal cells are critical for lymph node remodeling. Blood *120*, 4675-4683.
Palis, J., and Koniski, A. (2018). Functional Analysis of Erythroid Progenitors by Colony-Forming Assays. In Erythropoiesis: Methods and Protocols, J.A. Lloyd, ed. (New York, NY: Springer New York), pp. 117-132.

Park, C.-S., and Choi, Y.S. (2005). How do follicular dendritic cells interact intimately with B cells in the germinal centre? Immunology *114*, 2-10.
Patel, H.J., and Patel, B.M. (2017). TNF-α and cancer cachexia: Molecular insights and clinical implications. Life Sci. *170*, 56-63.
Paulson, R.F., Shi, L., and Wu, D.-C. (2011). Stress erythropoiesis: new signals and new stress progenitor cells. Curr Opin Hematol *18*, 139-145.
Peyrin-Biroulet, L., Panés, J., Sandborn, W.J., Vermeire, S., Danese, S., Feagan, B.G., Colombel, J.-F., Hanauer, S.B., and Rycroft, B. (2016). Defining Disease Severity in Inflammatory Bowel Diseases: Current and Future Directions. Clin Gastroenterol Hepatol *14*, 348-354.
Piercy, J., Petrova, S., Tchilian, E.Z., and Beverley, P.C. (2006). CD45 negatively regulates tumour necrosis factor and interleukin-6 production in dendritic cells. Immunology *118*, 250-256.
Powrie, F., Leach, M.W., Mauze, S., Caddle, L.B., and Coffman, R.L. (1993). Phenotypically distinct subsets of CD4+ T cells induce or protect from chronic intestinal inflammation in C. B-17 scid mice. Int Immunol *5*, 1461-1471.
Powrie, F., Leach, M.W., Mauze, S., Menon, S., Barcomb Caddle, L., and Coffman, R.L. (1994). Inhibition of Thl responses prevents inflammatory bowel disease in SCID mice reconstituted with CD45RB^{hi} CD4^{+} T cells. Immunity *1*, 553-562.
Qing, Y., and Stark, G.R. (2004). Alternative activation of STAT1 and STAT3 in response to interferon-gamma. J Biol Chem *279*, 41679-41685.
Rhodes, M.M., Koury, S.T., Kopsombut, P., Alford, C.E., Price, J.O., and Koury, M.J. (2016). Stress reticulocytes lose transferrin receptors by an extrinsic process involving spleen and macrophages. Am J Hematol *91*, 875-882.
Rivollier, A., He, J., Kole, A., Valatas, V., and Kelsall, B.L. (2012). Inflammation switches the differentiation program of Ly6Chi monocytes from antiinflammatory macrophages to inflammatory dendritic cells in the colon. J Exp Med *209*, 139-155.
Roozendaal, R., and Mebius, R.E. (2011). Stromal cell-immune cell interactions. Annu Rev Immunol *29*, 23-43.
Samarakoon, A., Shim, Y.A., Dosanjh, M., Crickmer, M., Labonté-Raymond, C., Arif, A.A., and Johnson, P. (2016). CD45 regulates GM-CSF, retinoic acid and T-cell homing in intestinal inflammation. Mucosal Immunol *9*, 1514.
Sanchez, M., Weissman, I.L., Pallavicini, M., Valeri, M., Guglielmelli, P., Vannucchi, A.M., Migliaccio, G., and Migliaccio, A.R. (2006). Differential Amplification of Murine Bipotent Megakaryocytic/Erythroid Progenitor and Precursor Cells During Recovery from Acute and Chronic Erythroid Stress. Stem Cells *24*, 337-348.
Saunders, A.E., and Johnson, P. (2010). Modulation of immune cell signalling by the leukocyte common tyrosine phosphatase, CD45. Cell. Signalling *22*, 339-348.
Saunders, A.E., Shim, Y.A., and Johnson, P. (2014). Innate Immune Cell CD45 Regulates Lymphopenia-Induced T Cell Proliferation. J Immunol *193*, 2831-2842.
Scheid, M.P., and Triglia, D. (1979). Further description of the Ly-5 system. Immunogenetics *9*, 423-433.
Schluns, K.S., Kieper, W.C., Jameson, S.C., and Lefrancois, L. (2000). Interleukin-7 mediates the homeostasis of naive and memory CD8 T cells in vivo. Nat Immunol *1*, 426-432.

Schroit, A.J., Madsen, J.W., and Tanaka, Y. (1985). In vivo recognition and clearance of red blood cells containing phosphatidylserine in their plasma membranes. J. Biol. Chem. *260*, 5131-5138.
Schwinzer, R., Witte, T., Hundrieser, J., Ehlers, S., Momot, T., Hunzelmann, N., Krieg, T., Schmidt, R.E., and Wonigeit, K. (2003). Enhanced frequency of a PTPRC (CD45) exon A mutation (77C-->G) in systemic sclerosis. Genes and immunity *4*, 168-169.
Shahbaz, S., Bozorgmehr, N., Koleva, P., Namdar, A., Jovel, J., Fava, R.A., and Elahi, S. (2018). CD71+VISTA+ erythroid cells promote the development and function of regulatory T cells through TGF-β. PLOS Biology *16*, e2006649.
Shenoi, H., Seavitt, J., Zheleznyak, A., Thomas, M.L., and Brown, E.J. (1999). Regulation of integrin-mediated T cell adhesion by the transmembrane protein tyrosine phosphatase CD45. J Immunol *162*, 7120-7127.
Shiu, J., Piazuelo, M.B., Ding, H., Czinn, S.J., Drakes, M.L., Banerjee, A., Basappa, N., Kobayashi, K.S., Fricke, W.F., and Blanchard, T.G. (2015). Gastric LTi cells promote lymphoid follicle formation but are limited by IRAK-M and do not alter microbial growth. Mucosal Immunol *8*, 1047-1059.
Slavova-Azmanova, N.S., Kucera, N., Louw, A., Satiaputra, J., Handoko, A., Singer, P., Stone, L., McCarthy, D.J., Klinken, S.P., Hibbs, M.L., and Ingley, E. (2014). Lyn kinase plays important roles in erythroid expansion, maturation and erythropoietin receptor signalling by regulating inhibitory signalling pathways that control survival. Biochem J *459*, 455-466.
Slavova-Azmanova, N.S., Kucera, N., Satiaputra, J., Stone, L., Magno, A., Maxwell, M.J., Quilici, C., Erber, W., Klinken, S.P., Hibbs, M.L., and Ingley, E. (2013). Gain-of-function Lyn induces anemia: appropriate Lyn activity is essential for normal erythropoiesis and Epo receptor signaling. Blood *122*, 262-271.
Snook, J.A., de Silva, H.J., and Jewell, D.P. (1989). The association of autoimmune disorders with inflammatory bowel disease. The Quarterly journal of medicine *72*, 835-840.
Socolovsky, M. (2007). Molecular insights into stress erythropoiesis. Curr Opin Hematol *14*, 215-224.
Socolovsky, M., Nam, H., Fleming, M.D., Haase, V.H., Brugnara, C., and Lodish, H.F. (2001). Ineffective erythropoiesis in Stat5a$^{-/-}$5b$^{-/-}$ mice due to decreased survival of early erythroblasts. Blood *98*, 3261-3273.
Spolski, R., Gromer, D., and Leonard, W. (2017). The gamma-chain family of cytokines: fine-tuning signals from IL-2 and IL-21 in the regulation of the immune response F1000Research *6*.
Stawarski, A., Iwanczak, B., Krzesiek, E., and Iwanczak, F. (2006). [Intestinal complications and extraintestinal manifestations in children with inflammatory bowel disease]. Polski merkuriusz lekarski : organ Polskiego Towarzystwa Lekarskiego *20*, 22-25.
Stijlemans, B., Cnops, J., Naniima, P., Vaast, A., Bockstal, V., De Baetselier, P., and Magez, S. (2015). Development of a pHrodo-based assay for the assessment of in vitro and in vivo erythrophagocytosis during experimental trypanosomosis. PLoS Negl Trop Dis *9*, e0003561.
Strober, W., and Fuss, I.J. (2011). Proinflammatory cytokines in the pathogenesis of inflammatory bowel diseases. Gastroenterology *140*, 1756-1767.
Takada, K., and Jameson, S.C. (2009). Naive T cell homeostasis: from awareness of space to a sense of place. Nat Rev Immunol *9*, 823-832.
Tan, C.C., Eckardt, K.-u., and Ratcliffe, P.J. (1991). Organ distribution of erythropoietin messenger RNA in normal and uremic rats. Kidney Int *40*, 69-76.

Tan, J.T., Dudl, E., LeRoy, E., Murray, R., Sprent, J., Weinberg, K.I., and Surh, C.D. (2001). IL-7 is critical for homeostatic proliferation and survival of naive T cells. Proc Natl Acad Sci U S A *98*, 8732-8737.
Tan, J.T., Ernst, B., Kieper, W.C., LeRoy, E., Sprent, J., and Surh, C.D. (2002). Interleukin (IL)-15 and IL-7 jointly regulate homeostatic proliferation of memory phenotype CD8+ cells but are not required for memory phenotype CD4+ cells. J Exp Med *195*, 1523-1532.
Tchilian, E.Z., Wallace, D.L., Wells, R.S., Flower, D.R., Morgan, G., and Beverley, P.C.L. (2001). A Deletion in the Gene Encoding the CD45 Antigen in a Patient with SCID. J Immunol *166*, 1308-1313.
Thomas, M.L. (1989). The Leukocyte Common Antigen Family. Annu Rev Immunol *7*, 339-369.
Toda, S., Segawa, K., and Nagata, S. (2014). MerTK-mediated engulfment of pyrenocytes by central macrophages in erythroblastic islands. Blood *123*, 3963-3971.
Tracey, K.J., Wei, H., Manogue, K.R., Fong, Y., Hesse, D.G., Nguyen, H.T., Kuo, G.C., Beutler, B., Cotran, R.S., and Cerami, A. (1988). Cachectin/tumor necrosis factor induces cachexia, anemia, and inflammation. J Exp Med *167*, 1211-1227.
Turkcapar, N., Toruner, M., Soykan, I., Aydintug, O.T., Cetinkaya, H., Duzgun, N., Ozden, A., and Duman, M. (2006). The prevalence of extraintestinal manifestations and HLA association in patients with inflammatory bowel disease. Rheumatology international *26*, 663-668.
Uddin, S., Kottegoda, S., Stigger, D., Platanias, L.C., and Wickrema, A. (2000). Activation of the Akt/FKHRL1 pathway mediates the antiapoptotic effects of erythropoietin in primary human erythroid progenitors. Biochem Biophys Res Commun *275*, 16-19.
van de Pavert, S.A., Olivier, B.J., Goverse, G., Vondenhoff, M.F., Greuter, M., Beke, P., Kusser, K., Höpken, U.E., Lipp, M., Niederreither, K.*, et al.* (2009). Chemokine CXCL13 is essential for lymph node initiation and is induced by retinoic acid and neuronal stimulation. Nature Immunology *10*, 1193-1199.
Varma, R., Campi, G., Yokosuka, T., Saito, T., and Dustin, M.L. (2006). T cell receptor-proximal signals are sustained in peripheral microclusters and terminated in the central supramolecular activation cluster. Immunity *25*, 117-127.
Vavricka, S.R., Schoepfer, A., Scharl, M., Lakatos, P.L., Navarini, A., and Rogler, G. (2015). Extraintestinal Manifestations of Inflammatory Bowel Disease. Inflamm Bowel Dis *21*, 1982-1992.
Vogel, A., Strassburg, C.P., and Manns, M.P. (2003). 77 C/G mutation in the tyrosine phosphatase CD45 gene and autoimmune hepatitis: evidence for a genetic link. Genes and immunity *4*, 79-81.
von Freeden-Jeffry, U., Vieira, P., Lucian, L.A., McNeil, T., Burdach, S.E., and Murray, R. (1995). Lymphopenia in interleukin (IL)-7 gene-deleted mice identifies IL-7 as a nonredundant cytokine. J Exp Med *181*, 1519-1526.
Vonarbourg, C., Mortha, A., Bui, V.L., Hernandez, P.P., Kiss, E.A., Hoyler, T., Flach, M., Bengsch, B., Thimme, R., Holscher, C.*, et al.* (2010). Regulated expression of nuclear receptor RORgt confers distinct functional fates to NK cell receptor-expressing RORgammat(+) innate lymphocytes. Immunity *33*, 736-751.
Vondenhoff, M.F., Greuter, M., Goverse, G., Elewaut, D., Dewint, P., Ware, C.F., Hoorweg, K., Kraal, G., and Mebius, R.E. (2009). LTβR Signaling Induces Cytokine Expression and Up-Regulates Lymphangiogenic Factors in Lymph Node Anlagen. J Immunol *182*, 5439-5445.

Walzel, H., Schulz, U., Neels, P., and Brock, J. (1999). Galectin-1, a natural ligand for the receptor-type protein tyrosine phosphatase CD45. Immunol Lett *67*, 193-202.
Wang, W., Horner, D.N., Chen, W.L.K., Zandstra, P.W., and Audet, J. (2008). Synergy between erythropoietin and stem cell factor during erythropoiesis can be quantitatively described without co-signaling effects. Biotechnol. Bioeng. *99*, 1261-1272.
White, A., Carragher, D., Parnell, S., Msaki, A., Perkins, N., Lane, P., Jenkinson, E., Anderson, G., and Caamaño, J.H. (2007). Lymphotoxin a-dependent and -independent signals regulate stromal organizer cell homeostasis during lymph node organogenesis. Blood *110*, 1950-1959.
White, J.T., Cross, E.W., Burchill, M.A., Danhorn, T., McCarter, M.D., Rosen, H.R., O'Connor, B., and Kedl, R.M. (2016). Virtual memory T cells develop and mediate bystander protective immunity in an IL-15-dependent manner. Nature Communications *7*, 11291.
White, J.T., Cross, E.W., and Kedl, R.M. (2017). Antigen-inexperienced memory CD8+ T cells: where they come from and why we need them. Nat Rev Immunol *17*, 391.
Witthuhn, B.A., Quelle, F.W., Silvennoinen, O., Yi, T., Tang, B., Miura, O., and Ihle, J.N. (1993). JAK2 associates with the erythropoietin receptor and is tyrosine phosphorylated and activated following stimulation with erythropoietin. Cell *74*, 227-236.
Wolber, F.M., Leonard, E., Michael, S., Orschell-Traycoff, C.M., Yoder, M.C., and Srour, E.F. (2002). Roles of spleen and liver in development of the murine hematopoietic system. Experimental hematology *30*, 1010-1019.
Wong, N.K., Lai, J.C., Birkenhead, D., Shaw, A.S., and Johnson, P. (2008). CD45 down-regulates Lck-mediated CD44 signaling and modulates actin rearrangement in T cells. J Immunol *181*, 7033-7043.
Wu, H., Liu, X., Jaenisch, R., and Lodish, H.F. (1995). Generation of committed erythroid BFU-E and CFU-E progenitors does not require erythropoietin or the erythropoietin receptor. Cell *83*, 59-67.
Wynn, J.L., Scumpia, P.O., Stocks, B.T., Romano-Keeler, J., Alrifai, M.W., Liu, J.-H., Kim, A.S., Alford, C.E., Matta, P., Weitkamp, J.-H., and Moore, D.J. (2015). Neonatal $CD71^{+}$ Erythroid Cells Do Not Modify Murine Sepsis Mortality. J Immunol *195*, 1064-1070.
Yadava, A., Kumar, S., Dvorak, J.A., Milon, G., and Miller, L.H. (1996). Trafficking of Plasmodium chabaudi adami-infected erythrocytes within the mouse spleen. Proc. Natl. Acad. Sci. U.S.A. *93*, 4595-4599.
Yan, H., Hale, J., Jaffray, J., Li, J., Wang, Y., Huang, Y., An, X., Hillyer, C., Wang, N., Kinet, S.*, et al.* (2018). Developmental differences between neonatal and adult human erythropoiesis. American Journal of Hematology *93*, 494-503.
Yang, Z.J., Koseki, M., Meguid, M.M., Gleason, J.R., and Debonis, D. (1994). Synergistic effect of rhTNF-alpha and rhIL-1 alpha in inducing anorexia in rats. Am J Physiol Regul Integr Comp Physiol *267*, R1056-R1064.
Zaft, T., Sapoznikov, A., Krauthgamer, R., Littman, D.R., and Jung, S. (2005). CD11chigh dendritic cell ablation impairs lymphopenia-driven proliferation of naive and memory CD8+ T cells. J Immunol *175*, 6428-6435.
Zhao, L., He, R., Long, H., Guo, B., Jia, Q., Qin, D., Liu, S.-Q., Wang, Z., Xiang, T., Zhang, J.*, et al.* (2018). Late-stage tumors induce anemia and immunosuppressive extramedullary erythroid progenitor cells. Nat Med *24*, 1536-1544.